

SS-H-2

HIGHWAY ACCIDENT REPORT

**COLLAPSE OF U. S. 35 HIGHWAY BRIDGE,
POINT PLEASANT, WEST VIRGINIA
DECEMBER 15, 1967**

Adopted: DECEMBER 16, 1970

**NATIONAL TRANSPORTATION SAFETY BOARD
Washington, D. C. 20591
REPORT NUMBER: NTSB-HAR-71-1**

	<u>PAGE</u>
I. FOREWORD	1
A. Photographs and Diagrams	4
II. SYNOPSIS	9
III. FACTS	10
A. Summary of Work Prior to October 1968 and Questions Which Remained Unresolved at That Time	10
1. Field Operations Completed as of October 1968	10
2. Laboratory Work Reported in Interim Report	11
3. Observed Facts and Witness Testimony Inadequately Explained at the Time of Interim Report	12
4. Logical Framework for the Conduct of the Investigation	13
B. Field Investigations Since September 1968	19
1. Further Examinations at Reassembly Site	19
a. Hanger connection at U13N	20
b. Cleavage fractures in hangers	20
c. Cleavage fracture in lower chord	20
d. Scars and deformations in Ohio tower	20
e. Presence of numerous cleavage fractures	21
2. Detailed Survey of the Extent of Corrosion on Eyebar Chain and Stiffening Trusses	22
3. Experimental Measurements on the St. Marys Bridge	23
a. Natural modes and frequencies	23
b. Dynamic response due to moving vehicle	23
c. Secondary effects in chain bent post and other members	23
d. Susceptibility of eyebar joints to rotation	24
e. Lateral distortions due to single lane loads	24
C. Laboratory Investigations Since September 1968	25
1. Laboratory Investigations at the National Bureau of Standards	25
a. Chemical and metallurgical examination of eyebar steel	25
b. Metallurgical and mechanical tests of eyebar steel	32
c. Fractographic and microprobe studies of fracture in eyebar No. 330	34
d. Chemical and mechanical tests of A7-24 steel	37
e. Examination of fracture in hanger U17N, part 12C	39
f. Examination of fracture in chord member L12-L13N	42
g. Rivet failures in joint U13N	42
h. Other NBS investigations	45

2. Studies at the Battelle Memorial Institute	45
a. Non-destructive search for eyebar flaws	46
b. Residual stress investigations	46
c. Fracture toughness of eyebar steel	47
d. Crack growth rates due to fatigue, hydrogen-stress cracking and stress-corrosion	54
e. Fractographic examination of freshly open crack	58
f. Fracture toughness of A7 steel	62
3. Investigations at U. S. Steel Applied Research Laboratory	64
a. Chemical and mechanical tests of eyebar steel	64
b. Slow bend test of eyebar steel	65
c. Depth of pitting in eyebar No. 33	65
d. Fractographic analysis of freshly opened crack	66
4. Laboratory Tests at Structures Laboratory, Fairbank Highway Research Station, Federal Highway Administration	68
a. Fatigue tests of eyebar steel	70
b. Scale model tests of eyebar joint C13N	70
5. Investigations of the Possibility of Fretting-Fatigue by Professor W. L. Starkey of Ohio State University	78
6. Static Tests of a Full-Scale Eyebar at Lehigh University	79
D. Status of Bridge Inspection and Maintenance	82

IV. ANALYSIS

A. The Properties of the Steels in the Point Pleasant Bridge	84
1. Chemical analysis of A7 steel of various laboratories compared	85
2. Mechanical tests of A7 steel of various laboratories compared.	85
3. Chemical analysis of eyebar steel	87
4. Mechanical tests of eyebar steel	87
5. Fatigue properties of eyebar steel	88
B. Actual Stress Levels in Various Components of the Structure as Compared to Primary Stress Analysis	89
1. Significance of secondary stresses	89
2. Stresses induced by wind excited oscillations	90
3. Stress concentrations in the eyebar head	91
C. The Mechanism of Collapse as Determined by the Process of Elimination	93
1. Elimination of causes other than fracture in eyebar No. 330	94
2. The fracture of eyebar No. 330	94
3. Mechanism of flaw growth to critical size	95
D. Compatibility of Established Mechanism of Failure with Observed Facts and Witness Testimony	100

	<u>PAGE</u>
1. Deformation of the structure just prior to collapse	100
2. Hypothesized sequence of collapse	101
3. Comparison with witness testimony	110
 E. Status of Bridge Design Practice in 1926	 114
1. Factors of safety	114
2. Special considerations for long span bridges	117
3. Treatment of stress concentration problems	119
 V. CONCLUSIONS	 121
A. With Respect to Sequence of Events in the Collapse of the Point Pleasant Bridge	 121
B. With Respect to the Elements which Contributed to the Failure	 122
C. With Respect to the Implications for the Safety of Other Bridges	 123
D. With Respect to Bridge Inspection and Maintenance	124
 VI. CAUSE	 126
 VII. RECOMMENDATIONS	 127
 VIII. REFERENCES	 129
 IX. TABLES 1-7, INCLUSIVE	 133
 X. APPENDICES	 After 142
Appendix A. Excerpts from report of E. G. Wiles on reassembly site work, specimen identification, and fracture catalog	 A1-17
Appendix B. Laboratory data on properties of eyebar steel and A7-2 steel from Point Pleasant Bridge	 B1-34

LIST OF FIGURES

<u>FIGURE NUMBER</u>	<u>LEGEND</u>	<u>PAGE NUMBER</u>
1	General View of Point Pleasant Bridge	4
2a	View of Bridge from Ohio End, with Locations of Typical Details to be shown in Figs. 2b - 2d	5
2b	Typical Detail of Truss to Chain Connection	6
2c	Typical Detail of Eyebars Chain and Hanger Connection	7
2d	Detail of Expansion Joint at Connection of Truss to Chain Bent Post	8
3	Logic Framework for Conduct of Investigation	14
4	Master Chart for Location of Laboratory Specimens	26
5a	Group "A" Specimens	27
5b	Group "B" Specimens	28
5c	Group "C" Specimens	29
5d	Group "D" Specimens	30
5e	Group "E" Specimens	31
6	Variation of Hardness through Thickness of Eyebars Materials (NBS Photo)	33
7	Small Semi-circular Crack (upper left of photo) which existed prior to Fracture in Eyebars No. 330 (NBS Photo)	33
8	Micro Structure of Eyebars Material (a) Outer Surface (b) Martensite at 0.2" depth (c) Interior	35
9	Location of Burr on Eyebars No. 33 (NBS Photo)	36
10	Detail of Burr on Eyebars No. 33 after Polishing and Etching (NBS Photo)	36

<u>FIGURE NUMBER</u>	<u>LEGEND</u>	<u>PAGE NUMBER</u>
11	Micro-Probe Evidence of Sulfur (a) Freshly exposed steel surface (b) Near lip of pre-existent crack	38
12	Cleavage Fracture in Hanger U17 - C17 N (a) Normal view showing paint in upper left and longitudinal crack in center (b) Oblique view showing evidence of torsion	41
13	Cleavage Fracture in Chord L12 - L13 N (a) Crack origin at rivet hole (b) Reflective specks in south channel	43
14	Rivet Fractures in Hanger Connection at U13 N	44
15	Eyebar with Gage Locations and Initial Cut Lines	48
16	Circumferential Stress Contours for Initial Cuts, Specimen B-17	49
17	Radial Stress Produced by Layer Removal, Specimen B-17	50
18	Fracture Toughness Test Arrangement for 0°F Temperature	51
19	Specimen Configuration with Strain-Gage Locations for Full-Scale Fracture Test	53
20a	Room-Temperature Fatigue-Crack-Propagation Rates for Eyebar Material	55
20b	Effect of Temperature and Environment on the Fatigue- Crack-Propagation Rates for Eyebar Material	56
21	Test Setup for Wedge-Force Loaded Specimens under Environmental Conditions	59
22	Microprobe Area Scans at Site A	61
23	The Effect of Strain Rate on the Three-Point Bend Properties of A-7 Steel Charpy V-Notch Specimens	63
24a	Appearance of Freshly Opened Crack in Eyebar Steel	67
24b	Fracture Regions in Freshly Opened Crack in Eyebar Steel	67
25	Appearance of Branch and Secondary Cracks Associated with Fracture in Eyebar No. 330	69

<u>FIGURE NUMBER</u>	<u>LEGEND</u>	<u>PAGE NUMBER</u>
26	Fatigue Properties of Eyebar Steel Based on Federal Highway Administration Tests	71
27	Details of Fatigue Specimen Employed in Federal Highway Administration Tests	72
28	General View of Model Test of Eyebar Chain Joint	74
29a	Model Eyebar Test A at Instant of Brittle Fracture in Lower Limb Model Eyebar No. 330	75
29b	Model Eyebar Test A at Instant of Final Separation of Model Eyebar No. 330	75
30a	Outboard Fragment of Eyebar No. 330, Test A Model	76
30b	Outboard Fragment of Eyebar No. 330, Prototype	76
31a	Results of Rotating Beam Fatigue Specimens Tested by W. L. Starkey	80
31b	Results of Fracturing Fatigue Specimens Tested by W. L. Starkey	81
32	Comparison of Charpy Impact Data for A7-24 Type Steel from Chain Bent Posts Obtained by Participating Laboratories	86
33	Relationship of Crack Propagation of Secondary Crack in Eyebar No. 330 to Grain Boundaries	97
34	Influence Lines for U5-U7, C11-C13	99
35	Fractures and Other Structural Damage on Towers	102
36	Summary of Experience of Survivors as Related to Sequence of Collapse	112

NATIONAL TRANSPORTATION SAFETY BOARD
WASHINGTON, D. C. 20591
HIGHWAY ACCIDENT REPORT

Adopted: December 16, 1970

COLLAPSE OF U. S. 35 HIGHWAY BRIDGE
POINT PLEASANT, WEST VIRGINIA
DECEMBER 15, 1967

I. FOREWORD

This final report by the National Transportation Safety Board supplements the interim report issued October 4, 1968, entitled "Collapse of U. S. 35 Highway Bridge, Point Pleasant, West Virginia, December 15, 1967," File SS-H-2. The interim report included descriptions of the design, construction, operation, and maintenance of the bridge from its completion in 1928 until its collapse in 1967. Detailed descriptions of the collapse of the bridge were given in the interim report, based upon documentary evidence and witness testimony as presented at the Safety Board's public hearing held in Charleston, West Virginia, May 10 through May 13, inclusive, 1968.

As stated in the interim report, it was determined that the fracture in suspension chain eyebar 330 (north bar, north chain, Ohio side span) was essential to the catastrophic stage of the collapse, but the cause of the fracture had not been determined. Eyebar 330 and its sister eyebar 33 were located in the north suspension chain of the bridge between joints C11 and C13. C13 was the first joint west of the Ohio tower. The north leg of the Ohio tower was joint C15N.

The fracture occurred in the lower half of the head of eyebar 330 in joint C13N. The line of this cleavage fracture was at right angles to the axis of eyebar 330. Then a ductile fracture on the opposite side of the eye from the cleavage fracture resulted in the complete separation of eyebar 330 from joint C13N. It was established that eyebar 33 had slipped from the eyebar pin at joint C13N at some time during the separation of the north eyebar chain at joint C13N. It was not known at the time of issuance of the interim report whether the fractures in eyebar 330 preceded the separation of eyebar 33 from the pin.

When the north eyebar chain was separated at joint C13N, total collapse of the bridge was a certainty due to its design with the towers resting on rocker seats.

Prior to issue of the interim report, the Safety Board's Structural Analysis and Tests Group of the investigative team began supervision of an extensive series of field and laboratory examinations to determine the mechanism of failure and the cause of the fracture at joint C13N. Those examinations were completed in the fall of 1970.

The Safety Board issued a press release on December 31, 1968, describing the discovery during laboratory examinations of evidence of a series of minute cracks penetrating to the interior of the fractured head of eyebar 330. It was stated that stress corrosion was suspected

as the cause of the minute cracks and that such cracks may be entirely undetectable in the present state of the art of bridge inspection without disassembly of members. The press release also noted that the State of West Virginia closed the St. Marys Bridge, a sister structure to the Point Pleasant Bridge, as a safety precautionary measure based upon the information developed during the investigation.

This final report briefly reviews the activities and findings prior to issuance of the interim report, and covers the investigations conducted since that time. The results of the investigations are discussed with relationship to the cause of the collapse, and the consistency of the findings with the observations of survivors and witnesses. This report includes discussion of the status of bridge design technology in the era of 1926 when the Point Pleasant Bridge was designed, the relationship of that philosophy to present-day knowledge of structural behavior, and implications for public safety as regards other existing bridges and those in process of design.

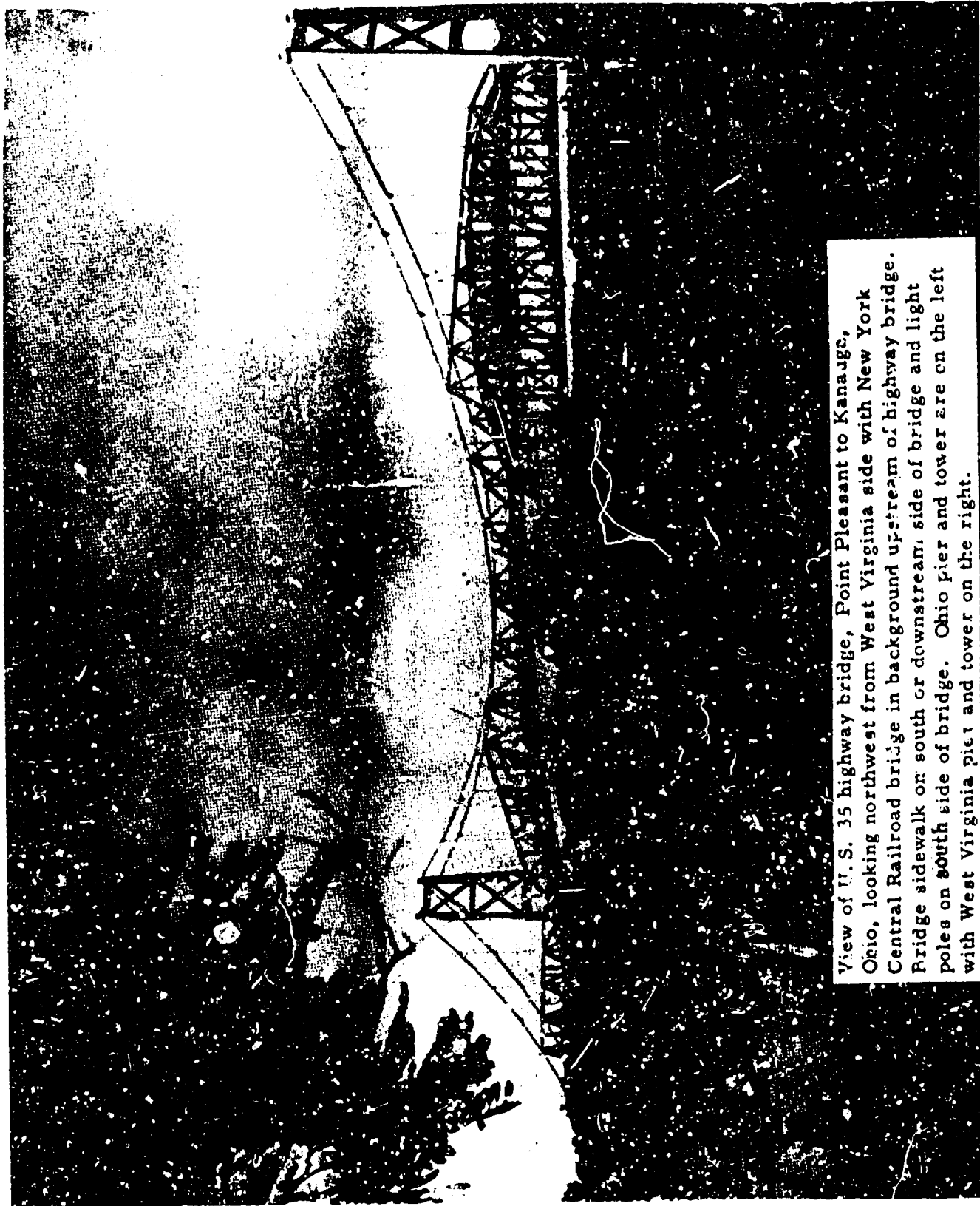
The detailed reports of separate investigations conducted by participating laboratories and consultants are listed as references. Only appropriate key findings and selected results are reported in the text. Certain other documentation not reproduced in formal reports is on file with the National Transportation Safety Board.

The Safety Board gratefully acknowledges the invaluable assistance received during the investigations from the many individuals and organizations that participated. The Corps of Engineers, U. S. Army, completed the massive recovery of the parts of the bridge from the Ohio River and conducted additional searches for missing parts. The Administrator of the Federal Highway Administration gave us continuing support and approval for expenditure of extensive research funds and provided professional assistance to the Safety Board through representatives from the Bureau of Public Roads and the Bureau of Motor Carrier Safety.

The Safety Board also expresses its appreciation to the representatives of the six Parties to the investigation, namely:

1. The States of West Virginia and Ohio
2. The consulting engineering firm of J. E. Greiner Company, Baltimore, Maryland
3. The consulting engineering firm of Modjeski and Masters, Harrisburg, Pennsylvania
4. The consulting engineering firm of Hardesty and Hanover, New York City; and
5. The American Bridge Division of the United States Steel Corporation, Pittsburgh, Pennsylvania

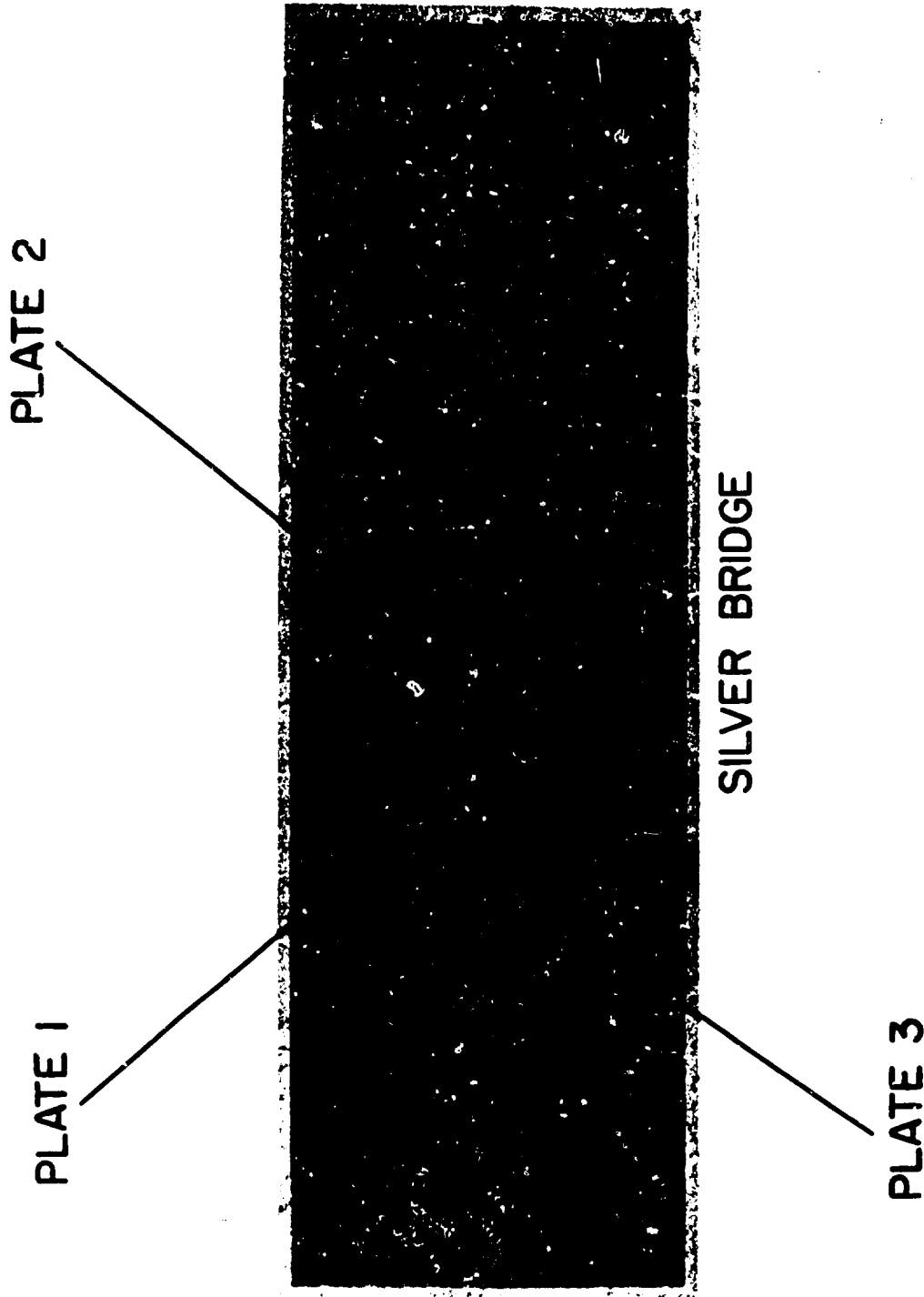
Particular appreciation is extended to Mr. Charles F. Scheffey, Federal Highway Administration, for his untiring efforts and outstanding performance as Chairman of the Structural Analysis and Tests Group of the Safety Board's investigative team.



View of U. S. 35 highway bridge, Point Pleasant to Kanawgo, Ohio, looking northwest from West Virginia side with New York Central Railroad bridge in background upstream of highway bridge. Bridge sidewalk on south or downstream side of bridge and light poles on south side of bridge. Ohio pier and tower are on the left with West Virginia pier and tower on the right.

Figure 1

Figure 2a - View of Bridge from Ohio End, with Locations of Typical Details to be shown in Figures 2b - 2d.



View of U. S. 35 highway bridge, Point Pleasant to Kanauga, Ohio taken from Ohio side looking east toward West Virginia. The three plates which follow numbered 1, 2, and 3 are details of the locations shown on this photograph and marked as plates 1, 2, and 3. On date of collapse, the water level recorder shown in this photograph on the north side of the Ohio pier was on the south side of the Ohio pier.

Detailed diagram of construction of joint U7 of the north truss of the Ohio side span showing the joint pin, the two sets of eyebars, gusset plates attaching members of the north truss to the eyebar joint, retaining plate and the retaining pin which was inserted through a concentric hole in the joint pin and which was installed with two nuts on either end of the retaining pin. The makeup of the retaining pin, retainer plates and the use of double nuts on each end of the retaining pin were common to all eyebar joints except at the tops of the two towers and at the connections of the eyebar chain with the chain bent posts.

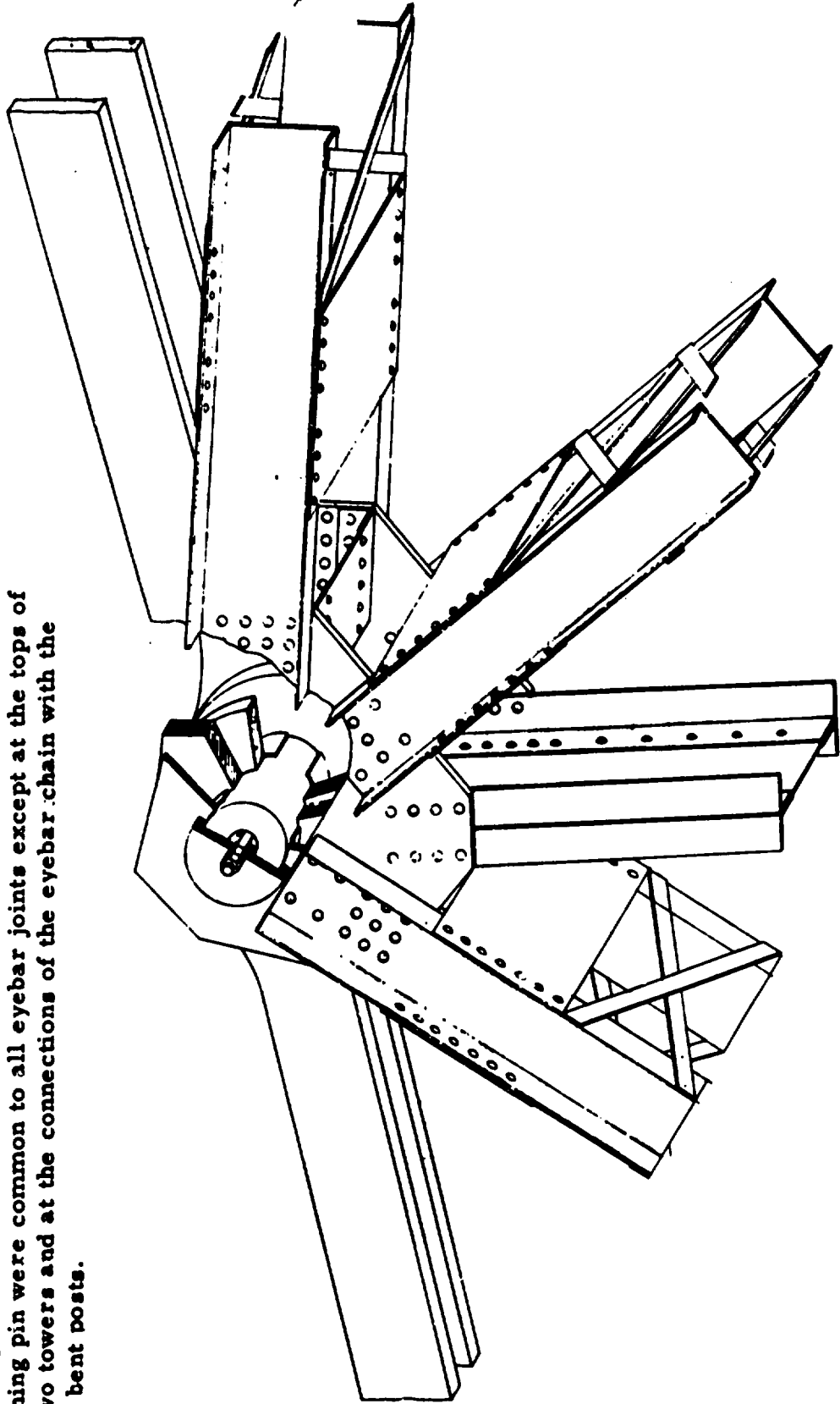


PLATE 1

Figure 2b - Typical Detail of Truss to Chain Connection.

Typical eyebar chain joint for portions of the eyebar chain where the chain was not framed into truss members. Note hanger strap and strap plates in the center of photograph. The strap plate was connected to the top chord of truss members vertically below the eyebar joint. This plate shows makeup of joint C13 north.

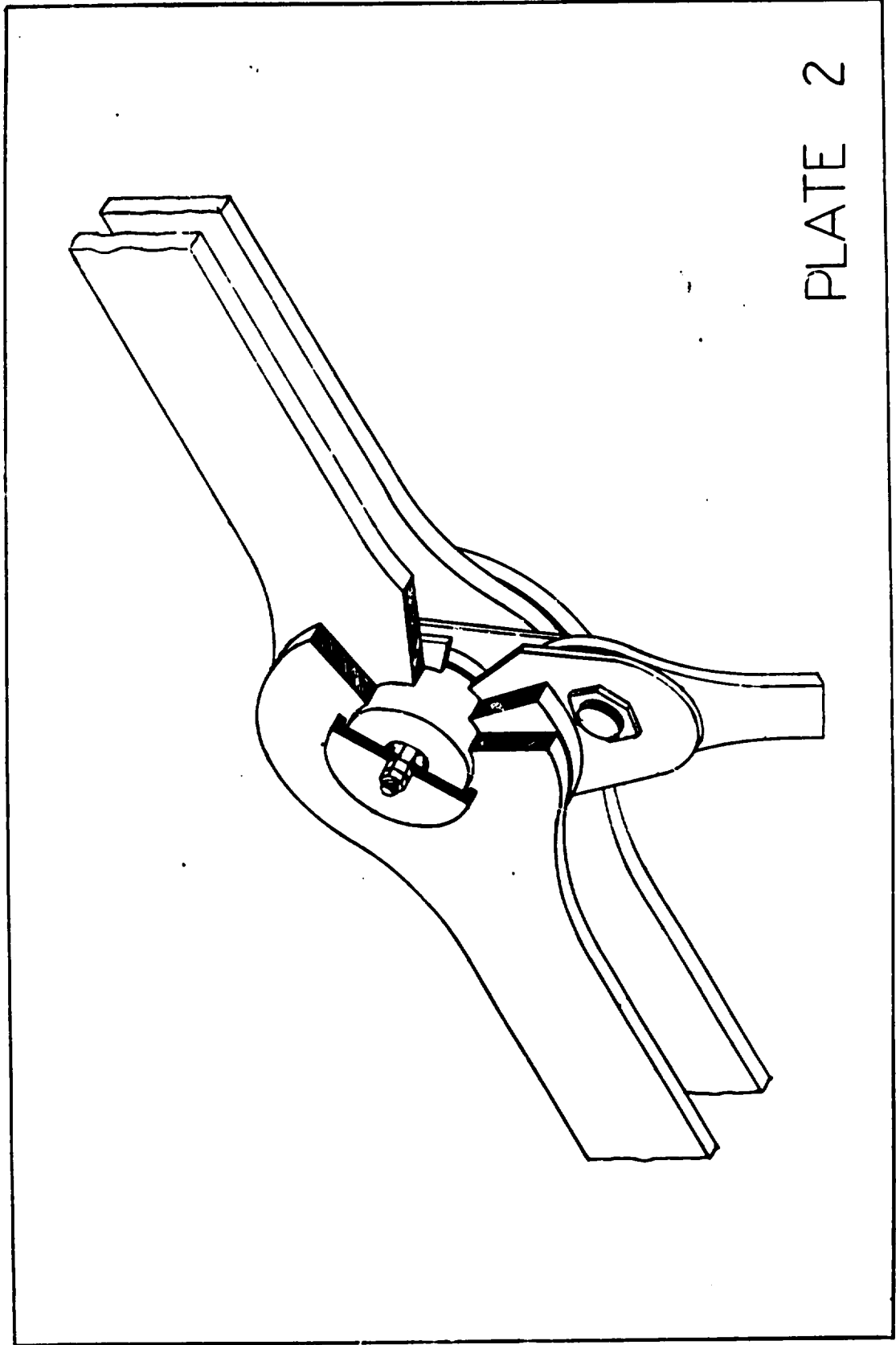
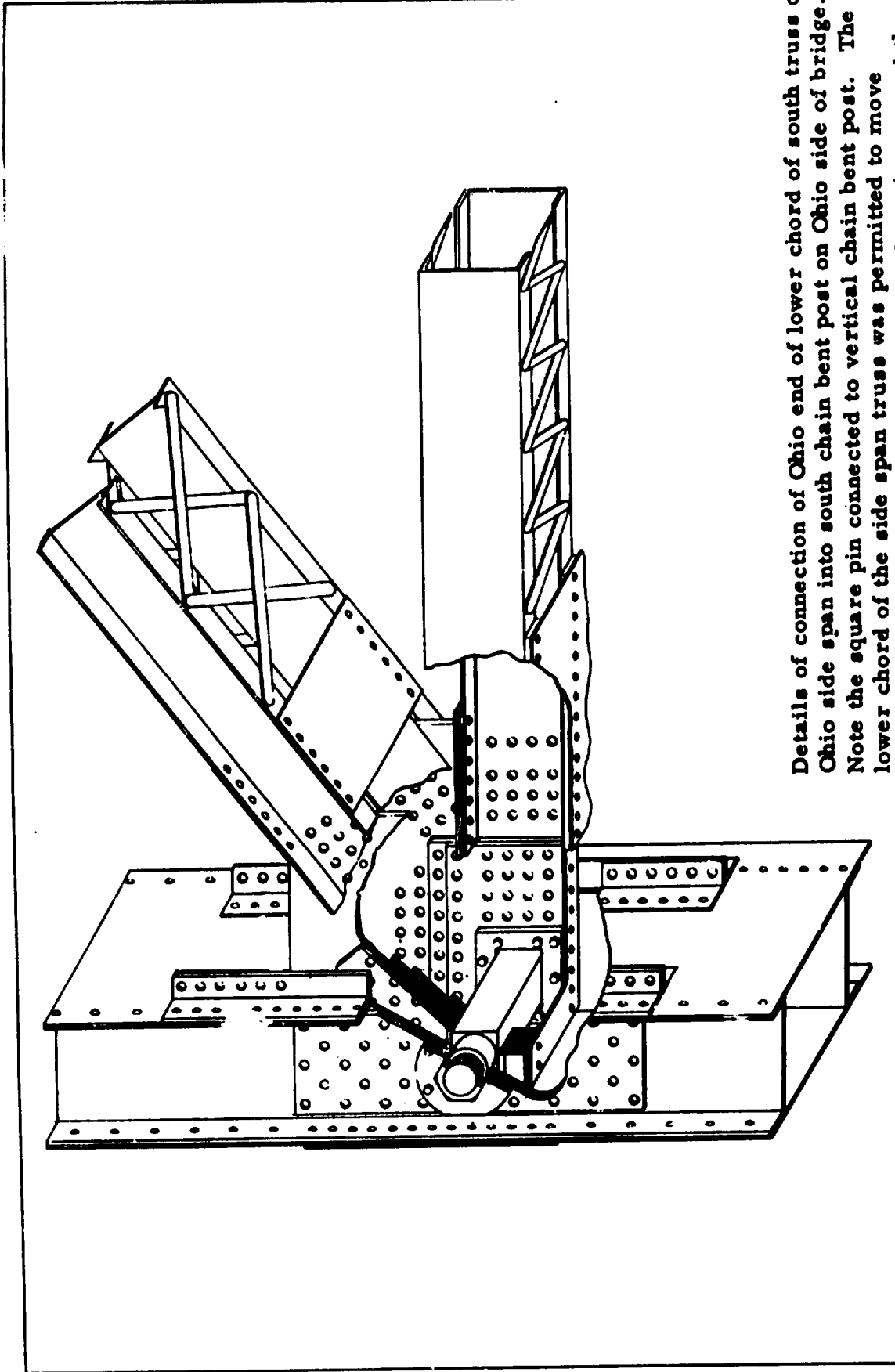


PLATE 2

Figure 2c - Typical Detail of Eyebar Chain and Hanger Connection.

Figure 2d - Detail of Expansion Joint of Connection of Truss to Chain Bent Post.



Details of connection of Ohio end of lower chord of south truss of Ohio side span into south chain bent post on Ohio side of bridge. Note the square pin connected to vertical chain bent post. The lower chord of the side span truss was permitted to move longitudinally through provision of a slotted section around the square pin to equalize expansion and contraction of the bridge due to temperature changes and changes in live load. The detail shown was that used to connect the lower chords of both trusses of the two side spans into the four chain bent posts in the bridge.

II. SYNOPSIS

The U. S. 35 Highway Bridge connecting Point Pleasant, West Virginia, with Kanauga, Ohio, collapsed at approximately 5 p.m. (EST) December 15, 1967. Forty-six persons died in the accident, nine were injured, and 31 of the 37 vehicles on the bridge fell with the bridge. Twenty-four vehicles fell into the Ohio River and seven fell on the Ohio shore. There were no pedestrians on the bridge at the time of collapse.

The initial failure in the bridge structure was a cleavage fracture in the lower limb of the eye of eyebar 330 (north bar, north chair, Ohio side span) at joint C13N, the first eyebar chain joint west of the Ohio tower of the bridge. The cleavage fracture was followed by a ductile fracture in the upper limb of the eye of eyebar 330 at joint C13N, separating eyebar 330 from the chain. Immediately following the separation of eyebar 330 from joint C13N, the sister eyebar 33 slipped from the C13N joint pin, resulting in the separation of the north chain at that location. The collapse of the bridge began in the Ohio side span, moving eastward toward the West Virginia shore, with the result that within a period of about 1 minute, the 700-foot center span, the two 380-foot side spans, and the towers had collapsed.

The Safety Board finds that the cause of the bridge collapse was the cleavage fracture in the lower limb of the eye of eyebar 330 at joint C13N of the north eyebar suspension chain in the Ohio side span. The fracture was caused by the development of a critical size flaw over the 40-year life of the structure as the result of the joint action of stress corrosion and corrosion fatigue.

Contributing causes are:

1. In 1927, when the bridge was designed, the phenomena of stress corrosion and corrosion fatigue were not known to occur in the classes of bridge material used under conditions of exposure normally encountered in rural areas.
2. The location of the flaw was inaccessible to visual inspection.
3. The flaw could not have been detected by any inspection method known in the state of the art today without disassembly of the eyebar joint.

III. FACTS

A. SUMMARY OF WORK PRIOR TO OCTOBER 1968 AND QUESTIONS WHICH REMAINED UNRESOLVED AT THAT TIME

1. Field Operations Completed as of October 1968

As of October 1968, the following major field operations had been completed and are summarized in Report SS-H-2, National Transportation Safety Board, dated October 4, 1968:

a. The wreckage which fell on the Ohio shore had been thoroughly documented by both photography and physical measurements.

b. All visible fractures in the wreckage on the Ohio shore had been carefully examined and extensive notes prepared with respect to evidence found upon the Ohio north chain bent post, gusset plate U7N, markings and deformations associated with the contact of the chain bent frame with the Ohio approach span girders, and the nature of the fractures in floor beam connections (See Figure 1 and Figure 2 for identification of these elements).

c. A precision survey had been completed to determine the positions of the anchorage vaults, piers and pedestals with respect to those indicated on the plans.

d. Approximately 60 percent of the main members in the stiffening trusses and the eyebar chains had been reassembled at the reassembly site.

e. A preliminary investigation of the members of the towers at the reassembly site had been completed, and it indicated that there had been no stability failure in the north leg of the Ohio tower.

f. Detailed measurements were made of eyebar No. 33 (South bar of north chain, link C11-C13), which contained the burr on the bearing edge of the pinhole, and eyebar No. 330 (North bar of north chain, link C11-C13), which contained the brittle fracture in the lower limb of the C13 eye, with a view to explaining the separation of the chain at joint C13N.

g. Parts of the hanger connection system at joint U13N (the joint directly below chain joint C13N) had been located and it was established that this connection had been pulled from the truss, apparently by forces applied through the hanger.

h. Detailed sketches were prepared from the divers' reports indicating the locations in which the principal elements of the wreckage and the vehicles had been found during the salvage operations.

i. Supplemental dredging operations after the completion of the main salvage operations had been successful in locating the outboard piece from the fractured eye of eyebar No. 330, but they had not located the pin from joint C13N in spite of three separate searches.

j. The wreckage on the Ohio shore had been carefully disassembled to obtain additional photographic coverage and to permit examination of freshly exposed pins and pinholes in the eyebar chain. The latter inspections were conducted in part to look for evidence of fretting-fatigue.

k. An experimental program had been conducted on the bridge at St. Marys, West Virginia, which was a near duplicate of the Point Pleasant Bridge, to confirm computed vibrational frequencies and mode shapes, to assess the dynamic effects in eyebars and hangers produced by a single heavy vehicle moving across the structure, and to make strain measurements of certain localized secondary stresses on the chain bent post, gusset plate U7N, and in the eyebar heads.

2. Laboratory Work Reported in Interim Report (Reference 2)

Laboratory work had been initiated at the National Bureau of Standards in order to examine the fracture in eyebar No. 330, the burr and deformation of eyebar No. 33, and the fractures in the chain bent post, gusset plate U7N, and several selected fractures from the lower chord members recovered from the wreckage on the Ohio shore. The Battelle Memorial Institute, Columbus, Ohio, had begun some basic work on the materials used in the eyebars, the hangers and the trusses to determine their susceptibility to brittle fracture due to the presence of small flaws. Studies to determine the fretting fatigue susceptibility of the eyebar material had been initiated at Ohio State University. Additional metallurgical examinations were planned at the National Bureau of Standards and the laboratories of the U. S. Steel Corporation had agreed to perform parallel investigations.

The examination of the brittle fracture in eyebar No. 330 at the National Bureau of Standards had revealed that there was a small radial crack about 1/8-inch deep extending from the eyebar hole surface in the plane of the fracture. The origin of this crack was at a point which was in contact with the pin in the assembled structure. Examination of the hole surface adjacent to the fracture indicated that there were additional smaller cracks of a similar nature generally parallel to the one which had precipitated the fracture. Representatives of the Battelle Memorial Institute were asked to examine a number of eyebar heads at the reassembly site and on the Ohio shore to determine whether or not such cracks were present in other eyebars of this structure.

None of the laboratory work had progressed far enough at the time of the interim report to result in conclusive reports.

3. Observed Facts and Witness Testimony Inadequately Explained at the Time of Interim Report

There was already general agreement among the members of the investigation group that the fracture in eyebar No. 330 was the critical event in the collapse of the structure. It was not clear, however, whether this fracture resulted from the static load which existed at this joint up to the time of the collapse, or resulted from dynamic overload produced by vibration, vehicle effects, or a shock wave produced by a prior fracture somewhere else in the structure. An important part of the subsequent investigations, therefore, consisted of a thorough examination of all fractures in the wreckage in the general vicinity of the Ohio tower, to ascertain if those fractures might have produced such a shock.

There were also questions as to whether the steel in the particular eyebar which fractured was typical of the steel in other eyebars in the structure and whether it met the contract specifications. With respect to the pre-existing* crack, two major questions were unresolved; namely, (1) was this crack sufficiently large to have caused the brittle fracture at the normal stress level expected at this location, and if so, (2) what was the mechanism by which this defect grew to critical size?

Another major unresolved question concerned the order of events in the separation of joint C13N. Was it possible, assuming that the pin retainer cap was missing, that eyebar No. 33 "walked" off the end of the pin prior to the fracture of eyebar No. 330 due to the fluctuating load in the eyebar chain? Such an event would have produced a 100 percent increase of the load on eyebar No. 330. Or did the fracture in eyebar No. 330 come first, with subsequent misalignment causing eyebar No. 33 to slip off the pin? It was in the hope of resolving this question that much effort was expended in attempts to find the missing pin from this joint.

There were a number of questions for which there were no clear answers at the time:

a. If the failure occurred because of weakness or defects in the vicinity of panel point 13, how did the two heavily loaded dump trucks which were in the east bound lane successfully pass this point and reach the center of the main span before collapse occurred?

b. What unusual event accounts for the fact that the saddle casting at the top of the south leg of the Ohio tower appeared to have been pulled vertically upward from its attachments, and how did this leg of the Ohio tower develop two fractures in the length above the portal bracing?

*Pre-existing in the sense that it was present prior to the initiation of collapse, but not necessarily present when the bridge was erected.

c. If the collapse was due to a failure of the upstream chain in the Ohio side span, why did the West Virginia side span rotate in a clockwise direction viewed from the west, with the downstream edge falling first?

d. What explains the presence of the numerous fractures in the entire lower chord system, many of which are distinctly brittle in nature?

e. How did the hanger connection system at U13N get pulled out of the truss if the chain had already failed?

f. In addition, the following observations by one or more eyewitnesses and survivors did not appear to be adequately explained:

(1) The presence of a bolt and/or a retaining caplike object on the deck prior to the collapse.

(2) The rather consistent reports of unusual vibrations just prior to the collapse.

(3) The loud "cracking" and "sonic boom" sounds reported just prior to or during the initial period of the collapse.

(4) The experience on the part of many of the survivors that the bridge dropped a short distance and then there was a momentary hesitation prior to the remainder of the collapse.

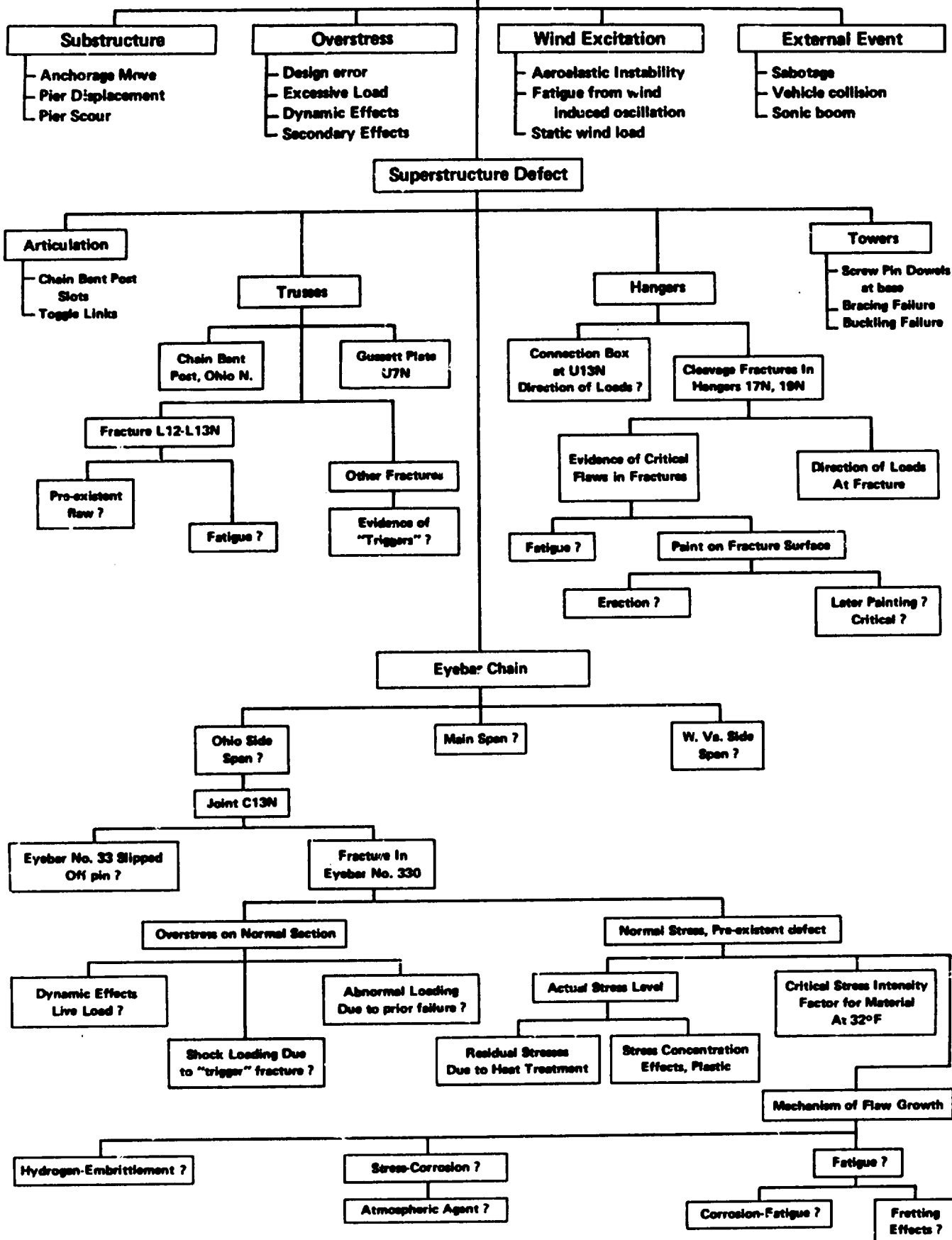
4. Logical Framework for the Conduct of the Investigation

The logical framework on which this investigation has been conducted is shown in Figure 3. The logic "tree" includes the work conducted by the Bridge Design Review and History Group as well as that of the Structural Analysis and Tests Working Group.

The possible causes of failure may be conveniently classified as those due to substructure failure, overload or overstress, superstructure defect, wind excitation, and external events including sabotage, vehicle collisions with the structures, and "sonic booms."

The substructure failures may be further divided into those due to scour around the base of the piers, anchorage movement or pier displacement which may have been caused by foundation failures or by collisions of water craft with the piers. At the time of the interim report it was possible to discard scour as a cause of failure in that the divers had found no abnormal holes or lack of support at the base of the piers during their work on the salvage

POSSIBLE CAUSES OF FAILURE



LOGIC FRAMEWORK FOR CONDUCT OF INVESTIGATION

Figure 3

operation. Cross pier displacement was also eliminated by the fact that the bearing surfaces of the pedestal seats for the tower legs were found to be level and in proper position.

The possibility that small movements of the anchorages or piers could have resulted in misalignment of the towers or sagging of the main chains with consequent overstressing of vital parts was eliminated by the results of the precision survey conducted by Modjeski and Masters (Reference 5, Exhibit Number 4-0). This survey was conducted using a combination of direct chaining over land and direct Geodimeter (an electronic distance measuring device) over water. The latter measurements were checked by a triangulation technique using a Geodimeter measured base line on one shore and precisely measured angles. The results of the survey indicate that all bearings and pedestals were within a few hundredths of a foot of the intended position with one exception. It was found that the distance between the pedestal shoes on the West Virginia tower pier (pier No. 4) and the pier at the east end of the West Virginia side span were approximately 0.25 feet closer than the 370 feet shown on the drawings. It was noted, however, that the distance between the pedestals on the Ohio tower pier and the West Virginia tower pier checked within 0.02 feet of the plan dimension of 700 feet, and that the distance between the pier at the east end of the side span and the next pier eastward also checked very closely with the planned dimension. It was therefore concluded that the erector had chosen to correct a slight error in the original construction by taking advantage of the adjustment provided in the West Virginia side span by the toggle link at the West Virginia tower. With the completion of these surveys and their interpretation, all possibility of substructure failure was precluded.

The computations performed by the Bridge Design Review and History Group (Reference 3 and Reference 5, Exhibit No. 3-E) indicated that the original design had been executed in accordance with normal engineering practice in use at the time of the original design, and that it was without mistakes or significant errors in the original stress computations, although there was a minor error in the computed dead load stress in member L13-L15 of the Ohio side span and corresponding members of the center span and West Virginia side span.* That group also established the fact that the stresses in critical members of the eyebar chain and trusses produced by the loading on the structure at the time of collapse were well below the specified maximum stresses provided for in the original design. Computations were carried out by the American Bridge Division of U. S. Steel using a digital computer, and were independently checked by the firm of Modjeski and Masters.

Both the original design computations and the check computations were computed on the following basis:

a. The structure was assumed to be linear in its behavior. The full implications of this statement will be discussed in the analysis section of this report.

*Such minor error, however, was of no significance as regards the collapse.

b. Only primary stresses in the members of the eyebar chain and the stiffening stresses were considered. Secondary effects because rigidity of the joints in the truss induced bending in the members as the structure changed shape due to various patterns of traffic loading were not taken into account. Other secondary effects due to transverse bending of the floor beams, distortion of the chain bent post frame, and possible effects in the eyebar heads if they did not rotate freely on the pins were also ignored.

c. The dynamic stresses introduced in the floor system by moving traffic were estimated by simple percentage increases in live load stress, which was the common practice at the time of the design of the structure. No allowance for dynamic effects was included in the analysis of eyebar chain, towers or stiffening truss.

There were therefore questions with respect to the actual levels of dynamic stress which were appropriate for this structure and the possible significance of uncomputed secondary stresses. These questions were studied during the experimental work conducted on the St. Marys Bridge during the Spring of 1968 and the subsequent interpretation of the data obtained from these experiments.

The questions associated with the superstructure defect branch of the logic tree had been only partially resolved at the time of the interim report (refer to Figure 3). Fortunately, positive evidence from the salvage operation showed that both towers fell toward the West Virginia shore. This permitted elimination of the possibility of a failure in the eyebar chains in either the central span or the West Virginia side span. It was clear that if a chain failure were responsible, it would have to be in the Ohio side span, since a break in the central span would have caused each tower to fall toward its respective end of the structure. Correspondingly, a break in the West Virginia side span would have caused both towers to fall toward Ohio.

The only failure in the eyebar chain within the Ohio side span was the separation of the joint at C13N. As noted above, the mechanism of this joint separation had not been adequately explored. The possibility that there had been initial failures elsewhere in the truss or in the hanger system was responsible for much of the effort since the issue of the interim report.

The possibility of failure in the towers was quickly eliminated by the fact that the north leg of the Ohio tower was in a single piece and was free from major distortions or plate buckling failures. The inspection of the pins in the pedestal shoes showed clearly that no tower leg had slipped off its pedestal at its base. The general nature of the failures in the tower bracing connections gave no indication that any of these failures had occurred prior to the general collapse.

There existed the possibility that wind excitation of the structure might have produced a failure of the Point Pleasant Bridge of the same type as that which occurred in the Tacoma Narrows Bridge in 1940. At the time of collapse of the Point Pleasant Bridge, however, the wind was blowing in a direction parallel to the axis of the bridge and at a velocity of about six mph. Mr. George Vincent, a well recognized authority on the aeroelastic oscillation of suspension bridges as a result of his participation in the investigation of the Tacoma Narrows Bridge failure and his many years of subsequent research on this class of problem, testified at the public hearing in May 1968 that these circumstances made it highly improbable that aerodynamic excitation was the direct cause of the catastrophe on December 15, 1967.

Nevertheless, it was conceivable that at certain periods during the lifetime of the structure there may have been wind at right angles to the axis of the structure sufficiently strong to induce aeroelastic vibrations and that these vibrations, if of sufficient magnitude, could have contributed to reducing the life of the structure by fatigue crack growth. The further investigations conducted to examine this possibility are discussed within this report.

Among the causes related to external events, the possibility of sabotage had been checked during the initial phases of the investigation. The results of inspections of all of the salvaged vehicles by a team of experts from the U. S. Army Ordinance Group showed no evidence of explosions in any of the vehicles. Subsequent inspections of the structural members at the reassembly site have not produced any indication of explosions in critical members, and no other evidence of deliberate sabotage by cutting or burning has been found.

The design of the structure was such that it would be virtually impossible for a vehicle to collide with the tower structure. Examination of the tower legs at the reassembly site showed no evidence of such vehicle collisions. A collision on some part of the stiffening truss was possible. This might have produced large distortions and local deck failures but would not constitute a failure in the critical load supporting structures in the towers and chains. However, the shocks involved in such a collision and the subsequent loads on the eyebar chain could have produced critical failures. The positions of the vehicles known to be on the bridge at the time of collapse makes this possibility remote, in that the deck adjacent to the north truss was occupied by standing traffic from the Ohio shore to the middle of the main span. Had a collision occurred, it is unlikely that it would have escaped the notice of all of the witnesses who survived the collapse of the structure. The eastbound traffic consisted of the two heavily loaded dump trucks and five passenger vehicles moving as a group across the structure. Since eyewitness testimony indicates that this group of vehicles moved continuously from the Ohio shore

to the center of the main span, the only possibility of a collision with a part of the structure which could have precipitated the collapse would have been in this area. Had a collision occurred due to a vehicle in the eastbound lane the damage would have been to the south stiffening truss. This would have most likely produced a failure in the south eyebar chain if any point in the main suspension system were vulnerable to shocks. As discussed above, it is known on the basis of physical evidence that the initial break occurred somewhere within the Ohio side span and it has been confirmed that the eyebar chain associated with the south stiffening truss was intact from the Ohio anchorage to the top of the Ohio tower. Further search for evidence due to this cause was therefore abandoned.

There were rumors in the Point Pleasant area that a sonic boom had occurred just prior to the collapse of the structure. A check with nearby military installations indicated that no aircraft likely to produce such effects were operating in the vicinity of the Point Pleasant Bridge at that time, and there were no other complaints of even minor damage in this area. Those witnesses that were either on the structure or nearby at the time of collapse testified that they heard a loud noise, or a series of loud noises, just prior to the collapse which some described "like a sonic boom." The chains of this bridge were designed to carry a live load of 1400 pounds/foot applied at the deck level, which is approximately 50 pounds/square foot on the deck. This is a heavier unit loading than that for which most roof structures are designed and it seems improbable that such an overpressure could have been exerted on the deck of the structure without having caused extensive damage to houses and other buildings in the Point Pleasant area. Further pursuit of this possible cause for the collapse was, therefore, abandoned.

B. FIELD INVESTIGATIONS SINCE SEPTEMBER 1968

1. Further Examinations at Reassembly Site

Adequate answers to the question of whether there had been fractures in the stiffening truss or the hanger system which could have preceded the brittle fracture in eyebar No. 330 required the completion and detailed inspection of the two-dimensional reconstruction of the bridge at the reassembly site. This work was carried on by the West Virginia State Road Commission until October of 1968, resulting in the identification and placement of approximately 90 percent of the eyebar chains and 70 percent of the stiffening trusses, plus the principal elements of the Ohio and West Virginia towers.

In September of 1968 a special team of the staff of the Office of Research of the Federal Highway Administration and representatives of Robert A. Hechtman and Associates, consultants to the Federal Highway Administration, took over operations at the reassembly site in order to complete as much additional identification and placement work as possible and to document all significant fractures for the record. This work was completed in October 1969 with approximately 90 percent of all available wreckage identified and placed. The detailed inspection of fractures resulted in the correction of a number of previous identifications. When layout was completed, a special series of low altitude vertical photographs were taken of the entire reassembly from a boom supported platform. These photographs were taken from positions about 30 feet above the ground and at a spacing such that an overlap of adjacent photographs of approximately 40 percent was obtained. In addition, all the fractures in the main chord members of the trusses were photographed at close range from two or more directions to document their features for the record. Each fracture was inspected to determine whether it was predominantly a cleavage fracture or a shear fracture, and where cleavage fractures were found, a careful inspection was made to determine whether there was any indication of a pre-existent defect. At the time of these inspections, a considerable accumulation of rust had formed on the fracture surfaces so that it was not possible to make positive judgments on the existence of such prior defects by field examination.

In view of this condition, a program of additional laboratory samples was established, in which the ends of members containing fractures of special interest or those in which it was deemed there was a possibility of a pre-existent defect were burned off and shipped to the National Bureau of Standards for cleaning and metallurgical examination.

The documentation work done at the reassembly site during this period is contained in Reference 7, excerpts of which are presented in Appendix A. The principal exhibit of this appendix consists of a

diagram which shows the status of the reassembly at the completion of this work, classifies all fractures in principal members of the stiffening trusses and eyebar chains, and shows the locations where laboratory specimens were removed. Further documentation of this work is covered in References 11 through 14, consisting of reports of examinations of fractures in the stiffening trusses, hangers, and towers. A few of the significant observations made in these reports as a result of this activity are as follows:

a. All but one of the fragments of the various parts of the hanger connection at joint U13N were identified and examined. It was established that the failure of this connection initiated in the rivets which fastened the west diaphragm channel to the inboard gusset. On a basis of the field examination of the fragments, it appeared that the failure had occurred in two stages, the first being initiated while the hanger was in a nearly vertical position with respect to an east-west plane, but inclined with respect to the north-south plane. Final separation appeared to have occurred when the hanger was inclined at a considerable angle with respect to the joint in the east-west plane. This material was shipped to the laboratory for further examination.

b. Cleavage fractures were found in the hangers in panel points 17 and 19 of the north truss, which are the two hangers just east of the Ohio tower in the upstream eyebar chain and truss system. Portions of both of these fractures were removed and shipped to the National Bureau of Standards for further examination. Similar fractures also were found in the hangers of the south truss of these same panel points, and in the hangers of both trusses just east of the West Virginia tower at panel points 45 and 47.

c. Two cleavage fractures were found in the lower chord of the north stiffening truss between panel points 12 and 13. The extraction of samples from these fractures was not completed until January of 1970, when they were removed, and taken to NBS for examination.

d. A detailed examination of deep scars and bruises on parts of the Ohio tower provided a highly consistent explanation of the sequence of events in the collapse of this tower and a possible explanation of why the saddle casting at the top of the south leg appeared to have been pulled away from the top of the tower leg along an axis parallel to the leg itself. Details of this sequence of events are covered in Reference 14, but may be summarized as follows:

- (1) Initially the top of the north leg of the tower moved eastward as a result of the separation of joint C13N in the Ohio side span.

(2) The bracing connecting the two tower legs pulled the top of the south leg in a northeasterly direction to conform to the movement of the north leg. After perhaps two feet of eastward motion of the top of the north leg, the eccentricity of the vertical load imposed on the south leg by the still intact south eyebar chain produced severe bending stresses in the south leg as indicated by the fact that there is a permanent bend in this leg above Strut PS1 (See Figure 35). Further bending resulted in failures in the tower bracing system and a fracture through the south leg about 69 feet below the top of the tower. This portion of the tower leg continued to tilt northward falling with considerable velocity because it was still carrying the south eyebar chain. This tilt dragged all portions of the south stiffening truss attached to the eyebar chain toward the north.

(3) This northward leaning of the upper 69 feet of the south leg continued until it made contact with the west side of the north leg of the tower which was falling to the east. At about this time fractures apparently occurred in the south eyebar chain in the main span.

(4) The next contact of the upper portion of the south leg occurred when a point about 26 feet below the saddle casting struck the southwest corner of the north leg about six feet above the top of the girder G1 (See Figure 35). As is evidenced by heavy gashes in the north leg at this location and corresponding marks on the south leg, this violent collision resulted in a complete cleavage fracture in the south leg about 26 feet below the saddle casting. The partially inverted position of the portion of the south leg to which the saddle casting was attached and the violence of the collision were apparently responsible for the manner in which the saddle separated from the top connection angles of the south leg.

e. The presence of numerous cleavage fractures in the lower chord of both stiffening trusses in the center of the main span was noted, indicating that some specific cause existed for these fractures.

2. Detailed Survey of the Extent of Corrosion on Eyebar Chains and Stiffening Trusses

A detailed examination of all recovered portions of the stiffening trusses and eyebar chains was conducted by the firm of Modjeski and Masters to determine what influence surface corrosion may have had upon the load carrying capacity of the eyebar chain, stiffening trusses, towers, and chain bent posts. Reference 15, "Corrosion Survey of the Silver Bridge (No. 1663)," is a complete documentation of this work. The diagrams indicating the locations at which detailed examinations were made are keyed to both the conventional panel point designations and the piece identification numbers painted on the member fragments by the Federal Highway Administration team which conducted the work at the reassembly site. Thickness measurements were made with calipers to determine the extent of corrosion at selected locations in the top chord members and on all bottom chord pieces where there was measurable corrosion. Similar measurements were made on approximately 13 percent of the diagonal and vertical members of the stiffening trusses selected on the random basis. Similar measurements were made on a large number of eyebars. The summary of this report reads as follows:

"The degree and location of corrosion observed on the primary truss members of the Silver Bridge did not significantly alter the ability of the individual members to carry the amount and type of stress to which they were subjected. Measurable corrosion was found on parts of many primary members below the roadway level. This metal loss appears to be the result of corrosive attack by roadway drainage. The corrosion was sufficiently advanced to indicate a need for replacement of some lower chord secondary material, principally lacing bars and stay plates.

"Pitting corrosion was observed on eyebar heads and pin hole surfaces. The maximum metal losses caused by corrosion amounted to less than three percent of the eyebar head, by conservative estimate. The pitting on pin hole surfaces removed substantially less than one percent of the critical cross-section through the pin hole.

"The corroded portions of the eyebar heads and pin holes were not accessible for maintenance of any type while the structure was standing. The eyebar heads between the abutments and chain bent posts were below the roadway level, and therefore, subject to corrosive attack by roadway drainage. The vast majority of the eyebar heads were located between Panel Points 0 and 58, above the roadway. Corrosion pitting of these eyebars is related to atmospheric conditions, but could not be related to roadway drainage."

3. Experimental Measurements on the St. Marys Bridge

The field work to make experimental measurements of the vibration characteristics and check certain secondary effects was completed in May of 1968 by the Structures and Applied Mechanics Division of the Office of Research, Federal Highway Administration. Reference 16 titled "The Dynamic Response of the Eyebar Chain Suspension Bridge Over the Ohio River at St. Marys, West Virginia," documents this activity. There are five results of particular interest in the discussions and conclusions of this report:

a. The dynamic behavior of the structure with respect to natural frequencies and mode shapes is in good agreement with the computations performed by Mr. George Vincent, strengthening the conclusion that the aeroelastic excitation of this structure by wind to significant amplitudes was improbable. The pin connections at numerous points in this structure provided a high level of energy absorption, producing a logarithmic decrement of 0.10 for damping in the fundamental vertical mode.

b. The response of the structure to a moving, heavy vehicle showed that there was lateral as well as vertical oscillations generated in the deck structure and that relative lateral motions of the deck system with respect to the eyebar chain were produced. These motions induced bending stresses in the hangers which were superimposed on the tension stresses which these members were designed to carry. The range of frequencies of motion induced by the moving vehicle was from approximately three to seven cycles per second, which is within the range of from 2 to 15 cycles per second to which a seated human is most sensitive. Dynamic increase of strain produced by these oscillations as compared to the static strain produced at crawl speed varied from as low as 20 percent of the static strain in the chain bent post to as much as 250 percent of the static strain in the hangers. It is important to note, however, that even the dynamic strains involved were very small. These live loading effects due to a single vehicle constitute only a small fraction of the total live load stress possible from traffic loading over the full length of the structure, and live load stress in the members is but a small portion of the total stress in the member. For example, the end span hanger at panel point 11 showed a static unit strain of 12 microinches/inch with the load in the middle of the center span, six microinches/inch when the load was in the middle of the side span (both of these strains being the average of the two faces of the hanger), and a dynamic unit strain of 16 microinches/inch with the load passing through the side span. This dynamic increment represents only about 480 psi. of bending stress.

c. Secondary effects in the northwest chain bent post produced live load tension on one corner of this post under certain positions of load, whereas certain other positions of the load produced compression at the same point. The gage at the southwest corner of the chain bent

post showed maximum unit strains of 42 microinches/inch in tension and 23 microinches/inch in compression. These correspond to stresses of approximately 1300 lbs. per square inch tension and 670 lbs. per square inch compression. These alternating stresses occurred in a member designed to carry a primary compression load at an allowable design stress of 20,000 lbs. per square inch. A fatigue failure is therefore improbable. Secondary stress effects were also measured in gusset plate U7N and in an eyebar head at joint C11S.

d. A supplemental study to determine whether the eyebars did in fact rotate on the pins produced indications that such rotation does occur when large live load tensions are produced in the chain by loadings in the main span, but not when the loadings are within the side span.

e. An additional secondary effect was observed with the live load in one lane only. Such loading produced distortion of the floor beam-truss-vertical rigid frame, inducing lateral motion of the deck with respect to the eyebar chain. This distortion therefore produces not only bending stresses in the hangers but also bending moments at the connections of the floor beams to the trusses.

C. LABORATORY INVESTIGATIONS SINCE SEPTEMBER 1968

This section is a summary of each of the laboratory investigations which have been conducted since September 1968 or which were not completed to the point of reduction of data and presentation of a report at that time. Investigations are reported and summarized on a basis of the laboratory conducting the work. Complete details are available in the formal reports by the individual laboratories listed in the references. The discussion of the significance of the results of each of these investigations will be deferred to the next section of this report.

A guide to the location and identification of the various laboratory specimens removed from the wreckage of the Point Pleasant Bridge is given in Figure 4 and Figure 5. Figure 4 indicates the locations in the structure from which the major specimens were removed and the laboratory to which they were shipped initially. Figures 5a through 5f indicate subsequent subdivision of these major specimens and the individual laboratory designations assigned to these subdivisions for various portions of the work. Specimen material being held for possible supplemental tests is indicated by the designation "reserve specimen."

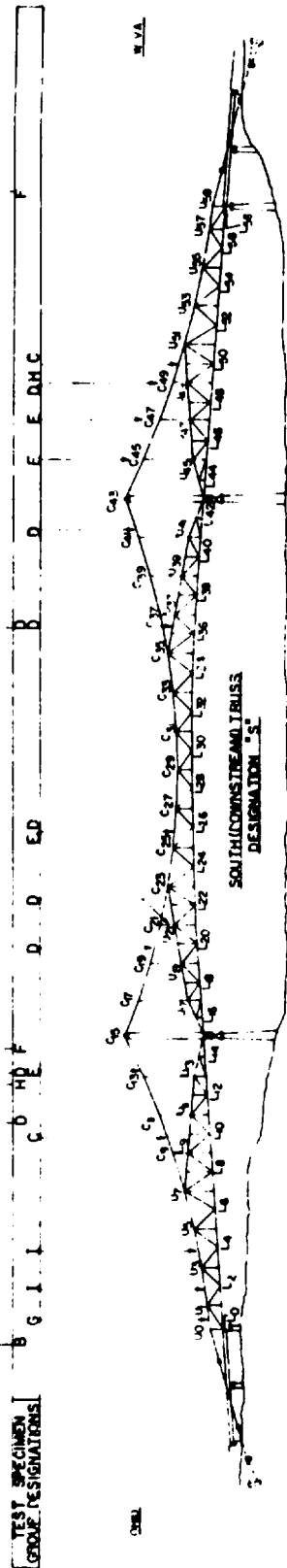
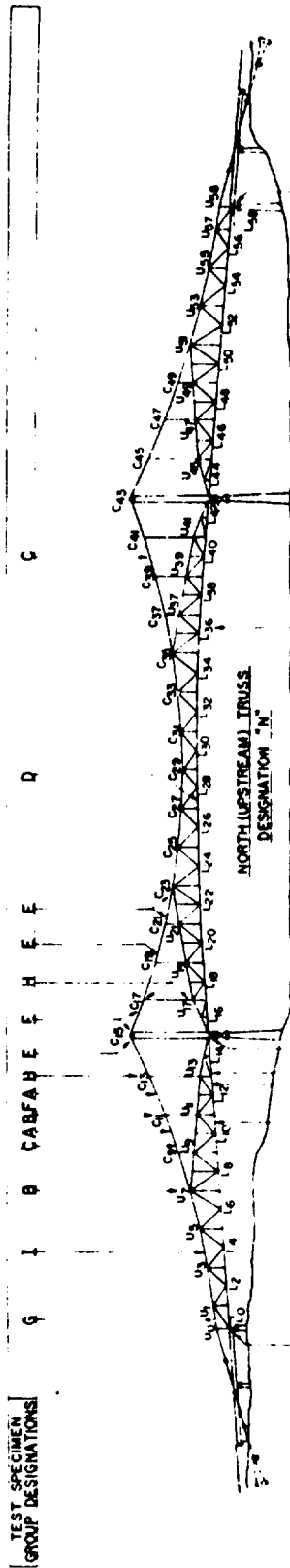
1. Laboratory Investigations at the National Bureau of Standards

The results of the investigations conducted at the National Bureau of Standards are documented in a series of seven reports from that laboratory (References 17 through 23).

a. The first report describes the initial examinations made of the material in eyebar No. 330 (the north bar of the north chain, connecting points C11 and C13), to determine chemical composition, metallurgical and mechanical properties, and the results of the initial fractographic examination of the brittle fracture in the lower limb of the C13N head of this eyebar. Results of this investigation are summarized as follows:

(1) The chemical composition of the steel was in general conformance with the specifications for 1060 carbon steel (detailed results are given in Appendix B).

(2) The heat treatment which consisted of quenching in water from the austenitizing temperature (approximately 1600°F.) and tempering from between 1150 and 1200°F. produced a non-homogeneous micro-structure. It may therefore be characterized as a "slack-quenched" steel in which martensite was formed in a layer 1/4" to 3/8" thick adjacent to the surfaces and a ferrite-pearlite structure was formed in the interior. The outer 1/16 to 1/3-inch of the martensite layer was heavily decarburized. These facts were confirmed by hardness profiles taken through the thickness of the bar, with results as indicated in Figure 6.

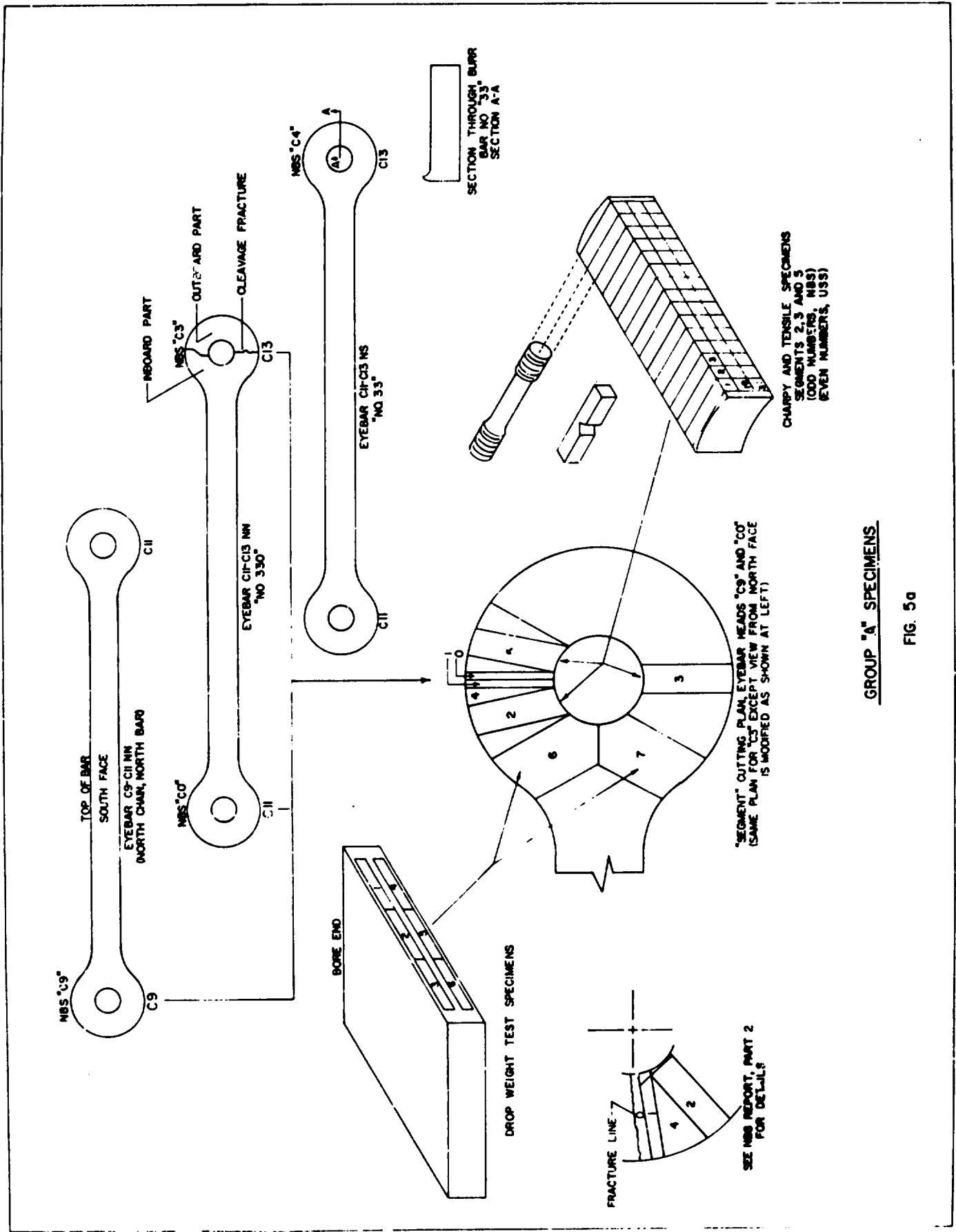


GROUP A	GROUP B	GROUP C	GROUP D	GROUP E	GROUP F	GROUP G	GROUP H	GROUP I
<p>GROUP A</p> <p>1 EYEBARS NO 330 AND 33 PORTION OF CHAIN BENT SHIPPED TO SPR FOR SHIPPED TO BATTLE SHIP ED TO U.S. STEEL SHIPPED TO LDHGH LMV SHIPPED TO NBS FOR SHIPPED TO NBS AND HELD FOR FUTURE PULL</p> <p>2 POST, QUARTZ U7N, FATIGUE TESTS AND EYEBAR HEADS FOR NOT LABORATORY BY MAZESKI AND WAS INSPECTION EXAMINATIONS SCALE TESTS (PULL</p> <p>3 SEE FIGURE 5a AND HEADS OF EYEBARS OTHER SPECIAL INVESTIGATION CHECK AND OTHER BAR TESTS (PULL EYEBARS)</p> <p>4 CB-CB TO NBS SEE FIGURE 5b</p>	<p>GROUP B</p> <p>1 SHIPPED TO SPR FOR SHIPPED TO BATTLE SHIP ED TO U.S. STEEL SHIPPED TO LDHGH LMV SHIPPED TO NBS FOR SHIPPED TO NBS AND HELD FOR FUTURE PULL</p> <p>2 FATIGUE TESTS AND EYEBAR HEADS FOR NOT LABORATORY BY MAZESKI AND WAS INSPECTION EXAMINATIONS SCALE TESTS (PULL EYEBARS)</p> <p>3 SEE FIGURE 5a AND HEADS OF EYEBARS OTHER SPECIAL INVESTIGATION CHECK AND OTHER BAR TESTS (PULL EYEBARS)</p> <p>4 CB-CB TO NBS SEE FIGURE 5b</p>	<p>GROUP C</p> <p>1 SHIPPED TO SPR FOR SHIPPED TO BATTLE SHIP ED TO U.S. STEEL SHIPPED TO LDHGH LMV SHIPPED TO NBS FOR SHIPPED TO NBS AND HELD FOR FUTURE PULL</p> <p>2 FATIGUE TESTS AND EYEBAR HEADS FOR NOT LABORATORY BY MAZESKI AND WAS INSPECTION EXAMINATIONS SCALE TESTS (PULL EYEBARS)</p> <p>3 SEE FIGURE 5a AND HEADS OF EYEBARS OTHER SPECIAL INVESTIGATION CHECK AND OTHER BAR TESTS (PULL EYEBARS)</p> <p>4 CB-CB TO NBS SEE FIGURE 5b</p>	<p>GROUP D</p> <p>1 SHIPPED TO SPR FOR SHIPPED TO BATTLE SHIP ED TO U.S. STEEL SHIPPED TO LDHGH LMV SHIPPED TO NBS FOR SHIPPED TO NBS AND HELD FOR FUTURE PULL</p> <p>2 FATIGUE TESTS AND EYEBAR HEADS FOR NOT LABORATORY BY MAZESKI AND WAS INSPECTION EXAMINATIONS SCALE TESTS (PULL EYEBARS)</p> <p>3 SEE FIGURE 5a AND HEADS OF EYEBARS OTHER SPECIAL INVESTIGATION CHECK AND OTHER BAR TESTS (PULL EYEBARS)</p> <p>4 CB-CB TO NBS SEE FIGURE 5b</p>	<p>GROUP E</p> <p>1 SHIPPED TO SPR FOR SHIPPED TO BATTLE SHIP ED TO U.S. STEEL SHIPPED TO LDHGH LMV SHIPPED TO NBS FOR SHIPPED TO NBS AND HELD FOR FUTURE PULL</p> <p>2 FATIGUE TESTS AND EYEBAR HEADS FOR NOT LABORATORY BY MAZESKI AND WAS INSPECTION EXAMINATIONS SCALE TESTS (PULL EYEBARS)</p> <p>3 SEE FIGURE 5a AND HEADS OF EYEBARS OTHER SPECIAL INVESTIGATION CHECK AND OTHER BAR TESTS (PULL EYEBARS)</p> <p>4 CB-CB TO NBS SEE FIGURE 5b</p>	<p>GROUP F</p> <p>1 SHIPPED TO SPR FOR SHIPPED TO BATTLE SHIP ED TO U.S. STEEL SHIPPED TO LDHGH LMV SHIPPED TO NBS FOR SHIPPED TO NBS AND HELD FOR FUTURE PULL</p> <p>2 FATIGUE TESTS AND EYEBAR HEADS FOR NOT LABORATORY BY MAZESKI AND WAS INSPECTION EXAMINATIONS SCALE TESTS (PULL EYEBARS)</p> <p>3 SEE FIGURE 5a AND HEADS OF EYEBARS OTHER SPECIAL INVESTIGATION CHECK AND OTHER BAR TESTS (PULL EYEBARS)</p> <p>4 CB-CB TO NBS SEE FIGURE 5b</p>	<p>GROUP G</p> <p>1 SHIPPED TO SPR FOR SHIPPED TO BATTLE SHIP ED TO U.S. STEEL SHIPPED TO LDHGH LMV SHIPPED TO NBS FOR SHIPPED TO NBS AND HELD FOR FUTURE PULL</p> <p>2 FATIGUE TESTS AND EYEBAR HEADS FOR NOT LABORATORY BY MAZESKI AND WAS INSPECTION EXAMINATIONS SCALE TESTS (PULL EYEBARS)</p> <p>3 SEE FIGURE 5a AND HEADS OF EYEBARS OTHER SPECIAL INVESTIGATION CHECK AND OTHER BAR TESTS (PULL EYEBARS)</p> <p>4 CB-CB TO NBS SEE FIGURE 5b</p>	<p>GROUP H</p> <p>1 SHIPPED TO SPR FOR SHIPPED TO BATTLE SHIP ED TO U.S. STEEL SHIPPED TO LDHGH LMV SHIPPED TO NBS FOR SHIPPED TO NBS AND HELD FOR FUTURE PULL</p> <p>2 FATIGUE TESTS AND EYEBAR HEADS FOR NOT LABORATORY BY MAZESKI AND WAS INSPECTION EXAMINATIONS SCALE TESTS (PULL EYEBARS)</p> <p>3 SEE FIGURE 5a AND HEADS OF EYEBARS OTHER SPECIAL INVESTIGATION CHECK AND OTHER BAR TESTS (PULL EYEBARS)</p> <p>4 CB-CB TO NBS SEE FIGURE 5b</p>	<p>GROUP I</p> <p>1 SHIPPED TO SPR FOR SHIPPED TO BATTLE SHIP ED TO U.S. STEEL SHIPPED TO LDHGH LMV SHIPPED TO NBS FOR SHIPPED TO NBS AND HELD FOR FUTURE PULL</p> <p>2 FATIGUE TESTS AND EYEBAR HEADS FOR NOT LABORATORY BY MAZESKI AND WAS INSPECTION EXAMINATIONS SCALE TESTS (PULL EYEBARS)</p> <p>3 SEE FIGURE 5a AND HEADS OF EYEBARS OTHER SPECIAL INVESTIGATION CHECK AND OTHER BAR TESTS (PULL EYEBARS)</p> <p>4 CB-CB TO NBS SEE FIGURE 5b</p>

NOTES: 1 FOR DETAILS OF SPECIMEN POSITION AND DIMENSIONS, SEE APPENDIX A
2 FOR SPECIMEN SUBDIVISION AND SUBSEQUENT SHIPMENT, SEE FIGURES 9a-9c

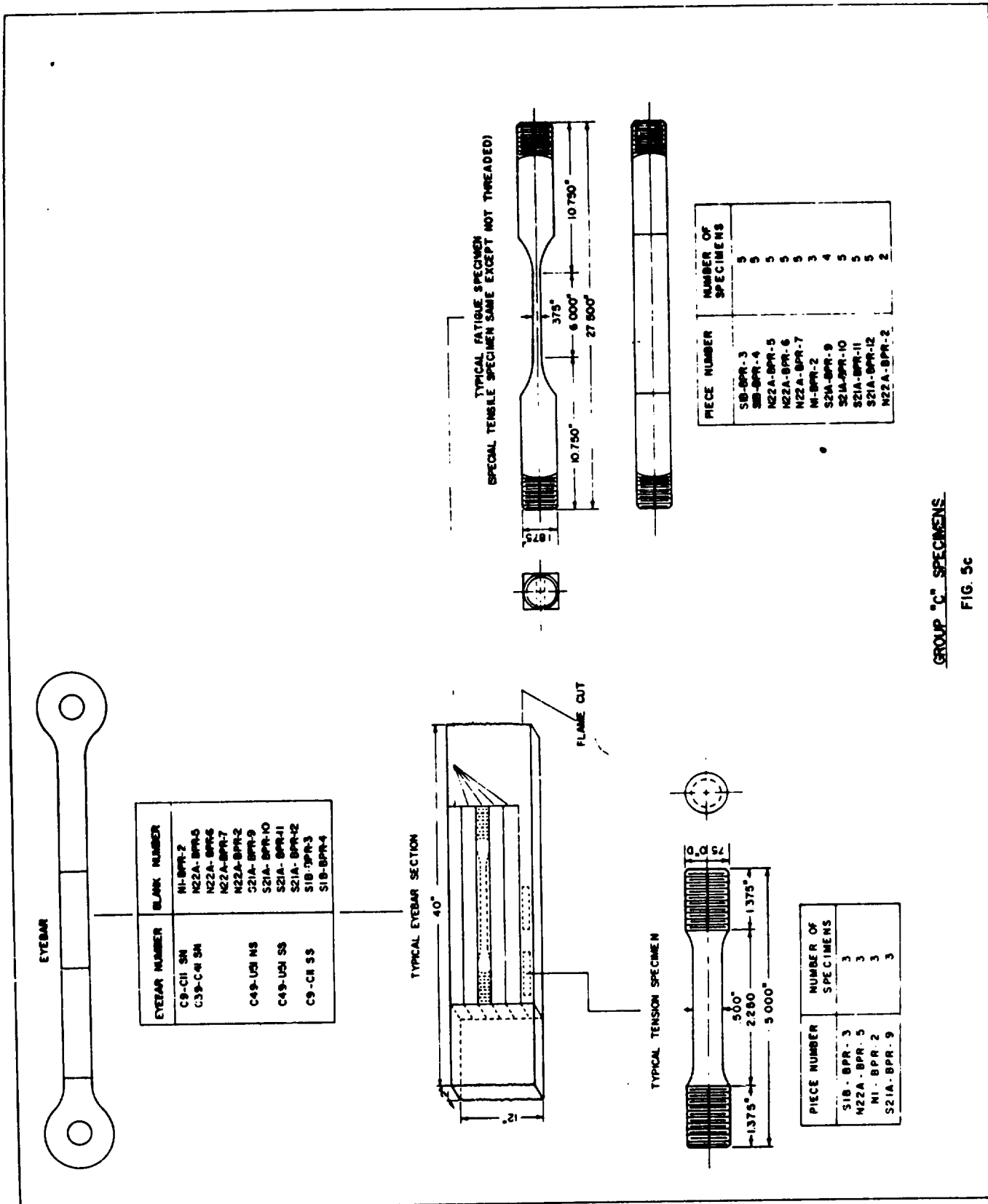
MASTER CHART FOR LOCATION OF LABORATORY SPECIMENS

FIG 4



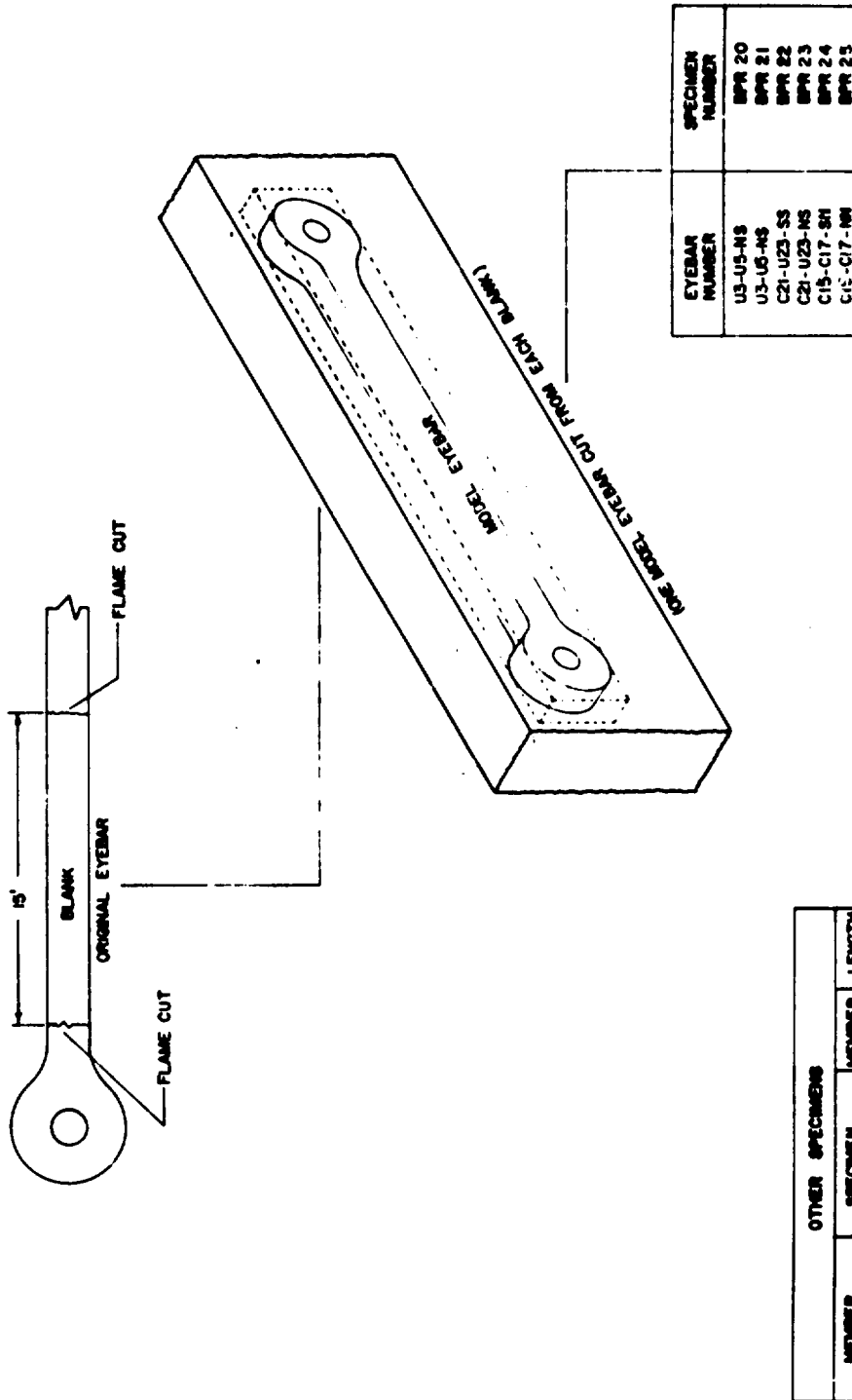
GROUP "A" SPECIMENS

FIG. 5a



GROUP "C" SPECIMENS

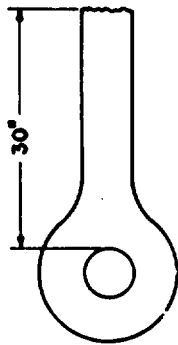
FIG. 5c



OTHER SPECIMENS			
MEMBER NUMBER	SPECIMEN NUMBER	MEMBER TYPE	LENGTH
L0-L1-SH	BPR-H17	CHANNEL	5'
L27-L30-MM	BPR-H19	CHANNEL	3'
C19-C21-NS	BPR-HH15	EYEBAR	3'
C21-U21-S	BPR-HH14	EYEBAR	3'
C28-C27-SS	BPR-S9B	EYEBAR	66"
L36-L37-SH	BPR-HH5	CHANNEL	4'
U26-U37-NS	BPR-HH10	CHANNEL	3'

GROUP 'D' SPECIMENS

FIG. 5d



TYPICAL EYEBAR HEAD

BATTLE AND BUREAU OF PUBLIC ROADS IDENTIFICATION OF EYEBARS INSPECTED AT BATTLE		BPR	
BTL IDENTIFICATION	IDENTIFICATION	FROM WRECKAGE ON OHIO SIDE	EYEBAR LOCATION
BTL-1	OS-41	•	U25-U27-N8
BTL-2	MM7	•	U25-U27-S8
BTL-3	OS-MM14	•	C13-C15-S8
BTL-4	OS-7	•	C13-C15-N8
BTL-5	OS-7	•	C15-C17-SN
BTL-6	OS-5	•	C15-C17-NN
BTL-7	OS-5	•	C15-C17-SN
BTL-8	OS-3	•	C13-C15-NN
BTL-9	OS-3	•	C13-C15-SN
BTL-10	OS-MM11	•	C19-C21-SN
BTL-11	S8AW	•	C19-C21-NN
BTL-12	S8BW	•	C21-U23-NN
BTL-13	S3B	•	C21-U23-SN
BTL-14	S3A	•	C21-U23-SN
BTL-15	N4A	•	U23
BTL-16	N4B	•	C46-C47-N8
BTL-17	N5A	•	C46-C47-N8
BTL-18	N5B	•	C46-C47-S8
BTL-19	N3A	•	C46-C47-S8
BTL-20	N3B	•	C46-C47-S8
BTL-21	N8BW	•	C46-C47-S8
BTL-22	N8AW	•	C46-C47-S8
BTL-23	N9BW	•	C46-C47-S8
BTL-24	N9AW	•	C46-C47-S8
BTL-25	N9AE	•	C46-C47-S8
BTL-26	N9BE	•	C46-C47-S8
BTL-27	S19AW	•	C46-C47-S8
BTL-28	S19BW	•	C46-C47-S8
BTL-29	S19AE	•	C46-C47-S8
BTL-30	S19BE	•	C46-C47-S8

NOTE: OS-OHIO SIDE

GROUP "E" SPECIMENS
FIG. 5e

(3) The fracture of the lower limb of the C13 head of this eyebar was precipitated by the existence of a small semi-circular crack about 1/8-inch in radius and an auxiliary crack about 1/16-inch in radius (See Figure 7). Both of these small cracks originated on the inside surface of the pinhole near the south face of the bar and on a plane roughly through the center of the pin at right angles to the longitudinal axis of the eyebar. The remainder of this fracture showed two zones of fracture propagation, the first of which extended from the crack roots to about 0.6 inch from the pinhole surface. The fracture in this zone is cleavage without any evidence of branching or secondary cracking. Such secondary cracking becomes apparent in the second zone, which extends through the remainder of the fracture.

(4) Cracks similar to that associated with the fracture were found on the inside surface of the pinhole approximately 1/16 inch from the plane of fracture and near the same face of the eyebar as those associated with the fracture. Further examination disclosed that there were additional cracks at distances up to about 1/2 inch from the fracture on the inboard piece of the eyebar (that which was still attached to the shank) and at about 0.1 inch from the fracture in the outboard piece which separated. Sectioning and examination of these cracks under high magnification indicate that they originated from small corrosion pits on the pinhole surface and penetrated radially into the eyebar material, approximately at right angles to the lines of principal stress.

(5) The faces of both the pre-existent crack associated with the main fracture and the similar cracks in adjacent areas were covered with dark oxides of a distinctly different color and texture than the surface rusting which developed on the remainder of the fracture surface.

b. Part 2 of the National Bureau of Standards report (Reference No. 18, "Metallurgical Examination and Mechanical Tests of Materials from the Pt. Pleasant, West Virginia Bridge,") describes further metallurgical work on eyebar No. 330 and on eyebar No. 33, which was the south bar of the pair in the north chain, panel point C11-C13, and which contained the burr on the north edge of the pinhole surface of the C13 head of this bar. The important conclusions of this report are as follows:

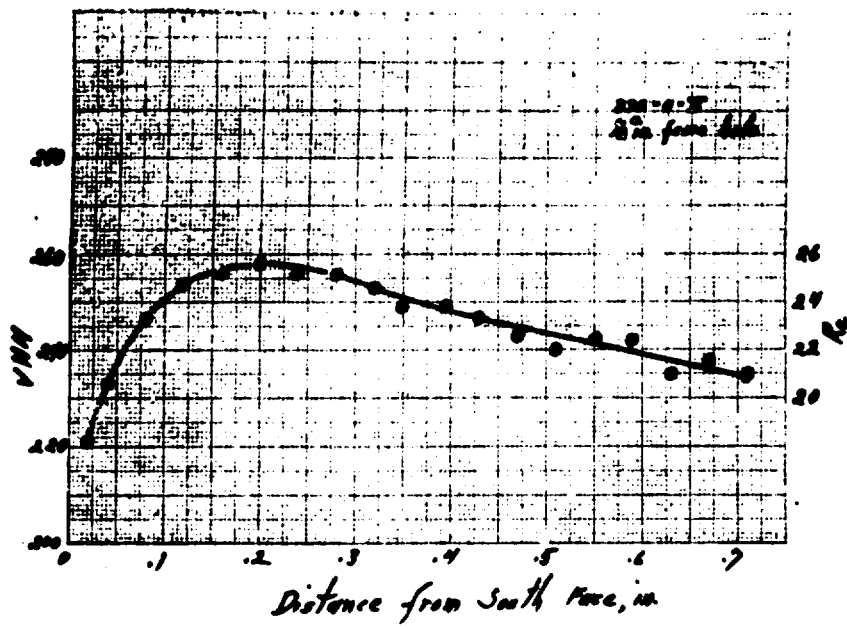


Figure 6 - Variation of Hardness through Thickness of Eyebar Materials.
(NBS Photo)



Figure 7 - Small Semi-circular Crack (upper left of photo) which existed prior to Fracture in Eyebar No. 330. (NBS Photo)

(1) The microstructure and hardness of the steel varied markedly with distance from the faces of the bar, as would be expected for material of this composition, size and heat treatment.

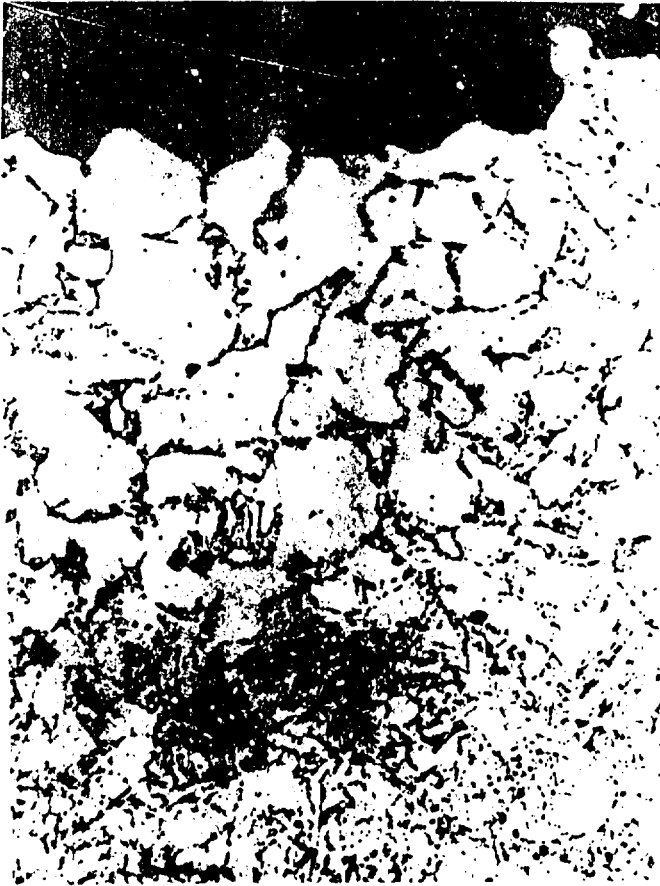
(2) The material in eyebar No. 330 did not appear to differ in any important respect from other eyebar material removed from the structure.

(3) The tests of mechanical properties and chemical composition showed that the materials in eyebar No. 330 and in the eyebar from panel C9-C11, north chain, north bar, were similar in composition and strength to the sample bars that were tested by the American Bridge Company at the time of manufacture (See Appendix B). The mechanical properties fall within a range that satisfies the requirements stipulated in the material specification for the structure.

(4) Results of Charpy V-notch and drop weight tests indicate that this material had limited fracture toughness (2 to 4 foot pounds in the Charpy tests) at 32°F., the approximate temperature at the time of the bridge collapse (See Appendix B). The 15 ft. lb. transition temperature measured in the Charpy tests was about 220 degrees Fahrenheit, and the NDT (Nil-Ductility Temperature) measured by crack-starter drop weight tests was between 130°F. and 170°F. Figures 8a, 8b, and 8c, illustrate the typical microstructure found in the decarburized area near the surface of a bar, the martensite structure at slightly greater depth, and the somewhat softer material found in the interior of the bar.

(5) The burr on the north face of the bearing section of the eyebar hole in the C13 end of eyebar No. 33 was sectioned through the thickness of the bar and along a plane in the longitudinal axis. Figure 9 shows the general geometry of this section and Figure 10 shows a detail of a magnification of the burr itself after polishing and etching. This detail indicates that this burr was formed in a single step as the bar slid off the end of the pin, with no indication that a series of terraces was formed during progressive movements of the bar relative to the pin.

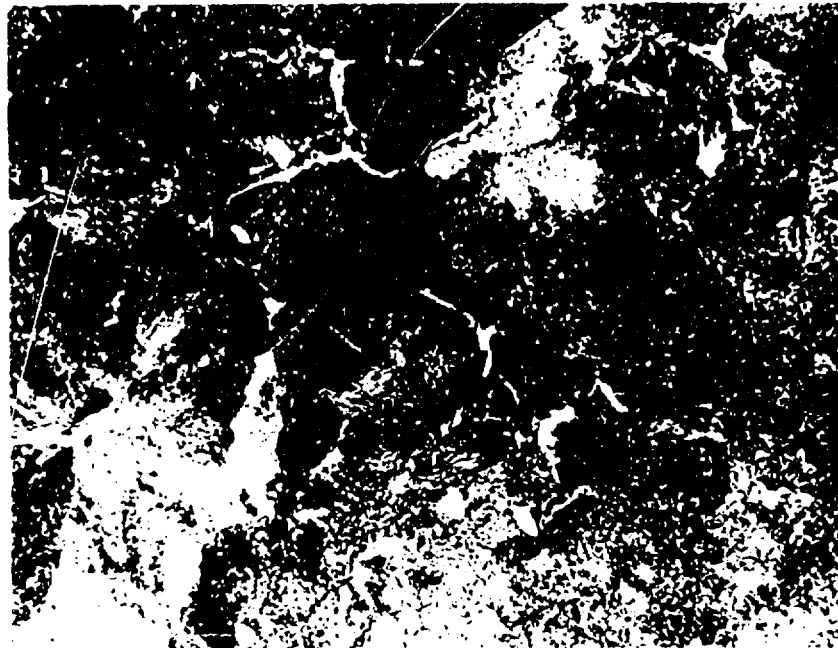
c. Part 3 of the National Bureau of Standards report (Reference 19) discusses the results of fractographic analyses of the fracture in eyebar No. 330 performed with the scanning electron microscope and



(a) Outer Surface



(b) Martensite at 0.2" depth



(c) Interior

Figure 8 - Micro Structure of Eyebar Material (NBS Photos)

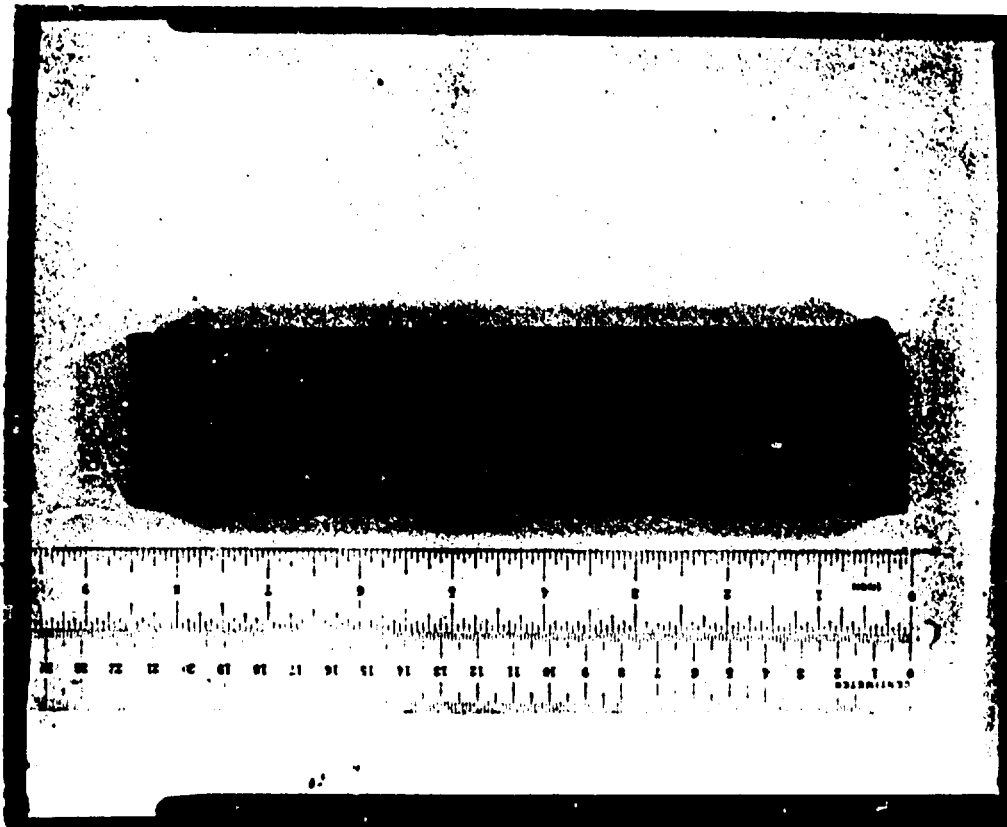


Figure 9 - Location of Burr on Eyebar No. 33 (NBS Photo)

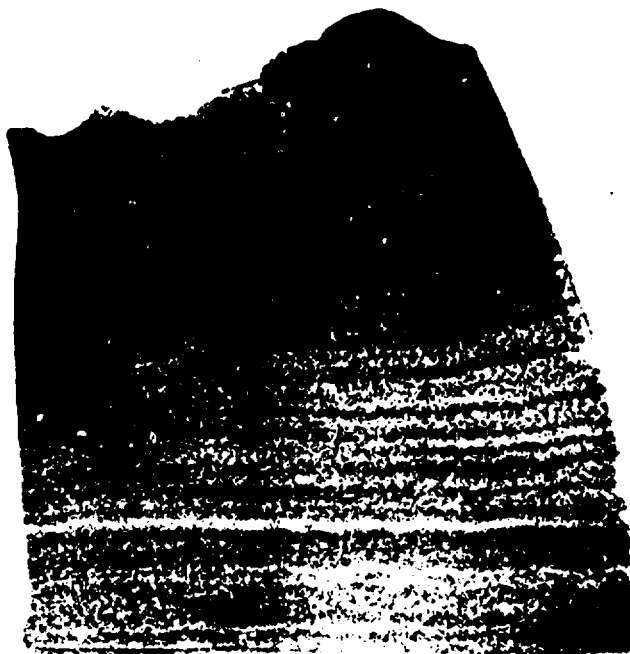


Figure 10 - Detail of Burr on Eyebar No. 33 after Polishing and Etching (NBS Photo)

the use of microprobe and x-ray diffraction techniques to identify the nature of the deposits on the crack surfaces. The principal conclusions of this work were as follows:

(1) Cracks appeared to have initiated in the rather hard material on the surface of the pinhole.

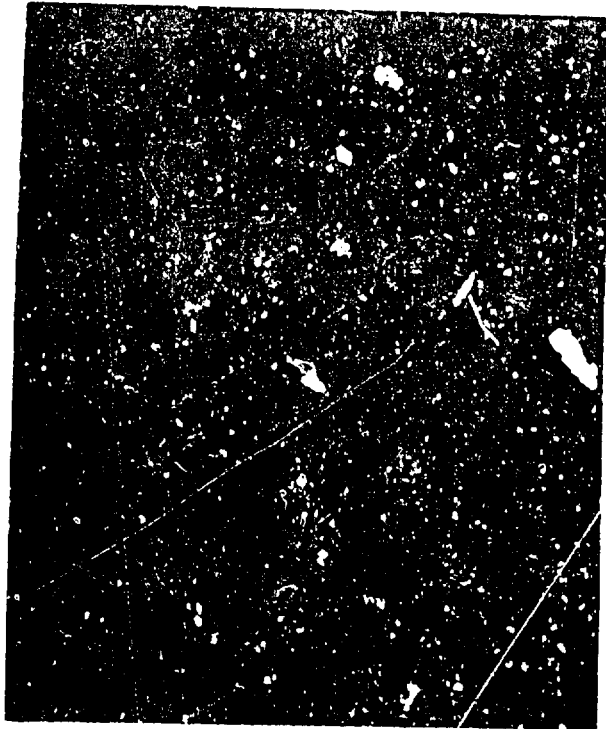
(2) Microprobe analyses indicated the presence of more than normal amounts of sulfur compounds in the crack surface. This indicates that sulfur bearing gases such as sulfur dioxide or hydrogen-sulfide in the atmosphere may have penetrated into the cracks and caused them to grow by the stress-corrosion cracking process.

(3) The cracks propagated along the carbide structures within the material, probably by a combination of stress-corrosion and mechanical loading effects. Figures 11a and 11b indicate the marked difference in sulfur levels on the surface of the pre-existent crack and on the surface of steel in the interior which was freshly exposed.

(4) During the conduct of the studies of the mechanism of crack propagation, the Bureau of Standards also made some limited tests to examine the stress-corrosion cracking susceptibility of the eyebar steel. A portion from eyebar No. 330 was used for this test.

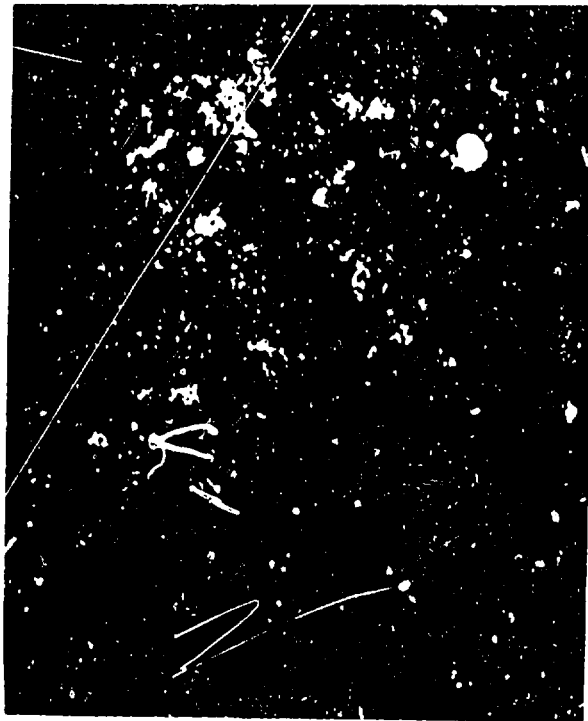
This specimen was approximately 2" x 2-3/4" x 3/16" and had one concave face, since it came from the end of the specimen block next to the pinhole. This specimen was subjected to a static bending moment by a three point loading fixture so as to produce a maximum tensile stress of 113,000 psi on the outer fiber. After 60 hours of exposure to a solution in which H₂S gas was dissolved, a black corrosion product (presumably iron-sulfide) formed, most intense at the area of highest stress. The specimen was returned to the corrosion cell for an additional 49 days and, after this exposure, exhibited extensive cracking. These cracks were most numerous in the area of highest stress and were found to extend to a depth of at least 0.033 inches below the surface.

d. The investigations of the chemical composition and mechanical properties of the A7-24 steel of the trusses, hangers, and chain bent posts are covered in Part 4 (Reference 20). Specimens were cut from the 13/16-inch thick gusset plate at joint U7N and from the 5/8-inch thick web of the channel from the north Ohio chain bent post. The



(a) Freshly exposed steel surface

NOT REPRODUCIBLE



(b) Near lip of pre-existent crack

Figure 11 - Micro-Probe Evidence of Sulfur (NBS Photos)

test program consisted of chemical analyses; metallurgical examinations; tension tests for yield, tensile strength, and ductility; and Charpy impact tests to assess notch-toughness. The general results of these investigations are given in Appendix B. In general, the material met the specifications for A7-24 steel, the detailed requirements of which are also indicated in Appendix B. The "15 foot pound transition temperature" for pieces from the various elements and with indicated orientation with respect to rolling were as follows:

U7N gusset plate (longitudinal specimen).....80°F
U7N gusset plate (transverse specimen).....92°F
North chain bent post (longitudinal specimen)...74°F

The major conclusions of this work are as follows:

(1) This material meets the requirements for A7-24 steel called for in the specifications for the Point Pleasant Bridge.

(2) Variations of properties are noted for material taken from different thickness members, but these were all within the specification range.

(3) This material was operating well below its "15 foot pound transition temperature" at the time of collapse of the structure (at 30°F.) such that fractures could be propagated at low energy levels compared to those required for propagation in the ductile range. The 15 foot pound transition temperatures for material of different thicknesses were all in the upper end of the range of service temperatures at which the structure was required to perform, although the transition temperature for the chain bent post material was lower than that of the thicker gusset plate material. This was attributed to the finer grain size associated with the thinner material and higher manganese content of the post material in comparison to the gusset plate material.

e. Part 5 of the National Bureau of Standards report series (Reference 21) discusses the examination of a sample of hanger material designated as 12C, which was obtained from the upper end of the hanger at panel point 17 in the north truss and which had a cleavage fracture surface on its upper end. The cleavage fracture extended across the 1-1/4 inch x 6 inch hanger bar at an angle of about 75 degrees to the longitudinal axis of the hanger. Chemical and mechanical tests on

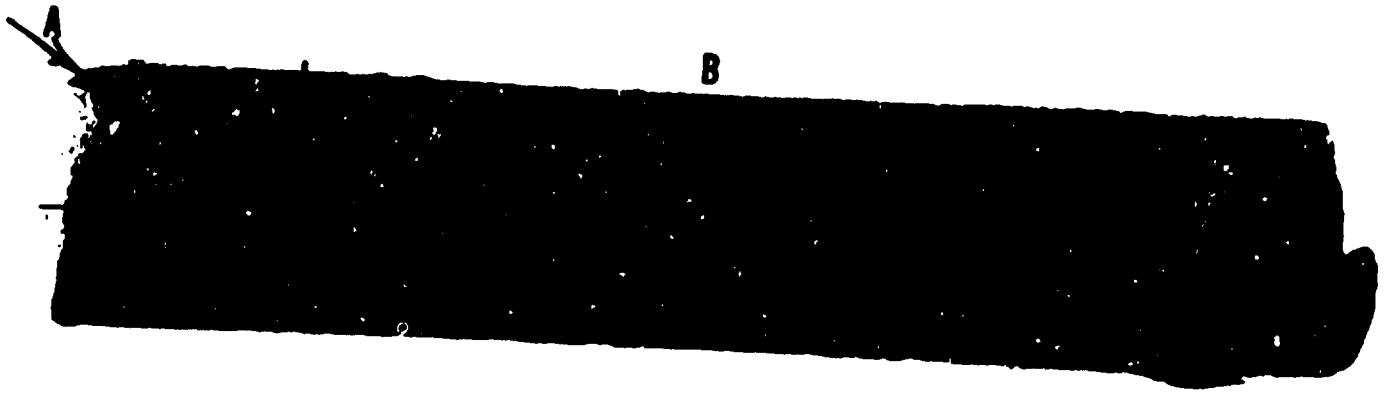
samples removed from the lower end of this specimen indicated that its composition and properties were typical of the other A7-24 material in the structure (See Appendix B). The examination of the cleavage fracture surface showed that it had propagated from a pre-existent crack in the southwest corner of the cross section, that the propagation of the crack had occurred at high velocity and apparently under the influence of a high loading rate. Two photographs of the fracture surface are given in Figures 12a and 12b. The pre-existent crack surface was metallurgically examined and found to be decarburized and to be characterized by rather large grain size.

This crack area also showed evidence of tightly adhered particles of both aluminum and orange colored lead paint. An analysis of these paint particles was conducted by the FBI laboratory. The report of the laboratory is included as an appendix to Reference 21 and indicates that:

- (1) The fracture surface in this area includes small areas of both aluminum and orange colored lead paint which the evidence indicates to have been deposited when wet.
- (2) The composition of aluminum paint on the fracture surface corresponds to those on the outer layers of a total of three layers found on the area of the non-fractured outer surface of the specimen. The orange paint in the fracture surface corresponds with the lowest of five layers on another portion of the outer non-fractured face. These findings were the subject of lengthy discussions within the working group, since the presence of paint in this region of the fracture surface would appear to indicate that the pre-existing defect extended to the outer surface and might have been a crack large enough to be observed during inspection or painting operations.

The possibility that this fracture acted as a "trigger" producing shocks on the eyebar chain was considered. The distortion of the cross section of the specimen, however, indicates that the fracture occurred at a time when there was considerable torsion as well as tension on the member. The narrow faces of the bar are distorted at an angle of about 3-1/2 degrees with respect to the normal to the wide faces.

At the time of preparation of this report, communications from the National Bureau of Standards indicated that the cleavage fracture



(a) Normal view showing paint in upper left and longitudinal crack in center



(b) Oblique view showing evidence of torsion

Figure 12 - Cleavage Fracture in Hanger U17 - C17 N
(NBS Photos)

in hanger C19-U19 north contained no pre-existent crack and showed evidence of both bending and high strain rate.

f. In the further pursuit of fractures in the structure which might have occurred prior to the fracture in eyebar No. 330, a careful examination was made of the cleavage fracture in lower chord member L12-L13 of the north truss (Reference 22). This was one of two such cleavage fractures within this panel length of the lower chord and occurred some six feet from the connection at panel point L12N. The fractures in the two channels composing the lower chord at this point both originated at rivet holes where lacing was attached to the member and were therefore staggered by approximately 8 inches. Metallurgical examinations showed that these fractures had originated in small pre-existent cracks at the edges of the rivet holes (See Figure 13a). The fracture surface showed clear evidence of a high rate of loading and of crack propagation, with branching or secondary cracks extending into the material below the plane of the fracture.

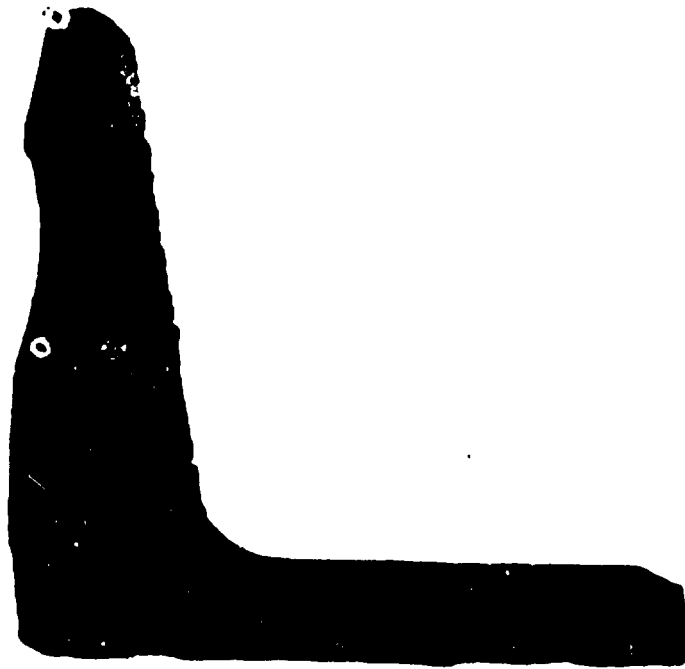
Some unusual small reflective specks (See Figure 13b) were noted within the fracture surface of the south channel of the pair. Microprobe analyses indicated that these reflective specks contained both lead and calcium. Although there was speculation that a tightly closed crack may have existed in this area for some time prior to the collapse and that lead may have migrated there from lead oxides in the paint by virtue of the establishment of an electrolytic "cell," the metallurgical and fractographic examinations contradicted and disproved this speculation. They indicate that the entire fracture surface with the exception of a small area near the origin was formed during the application of a single load at a high loading rate.

g. A further report discusses the investigations of the rivet failure in joint U13N (Reference 23). As mentioned above in the discussion of the field investigations, the hanger connection at this joint was pulled from the truss. This hanger connection is made up of a pair of channels with reinforcing plates attached, through which the pin at the lower end of the hanger passes, connected in turn to two other channels known as diaphragm channels which were riveted to the inboard and outboard gusset plates. Several of the rivets showed unusual fracture surfaces and were, therefore, examined metallurgically to determine the nature of these fractures.

Figure 14 shows the fractures in the group of rivets which fastened this channel to the outboard or north gusset plate. The failure plane was at the interface between the channel flange and the gusset plate. Rivets A and B, which were the two lowest rivets in the joint show rather unusual fractures. The metallurgical examination indicates that the fractures originated in small discontinuities at the outside surface of the rivets in areas that exhibited significant decarburization. Fracture was by cleavage in these initial zones, but by mixture



(a) Crack origin at rivet hole



(b) Reflective specks in south channel

Figure 13 - Cleavage Fracture in Chord L12 - L13 N (NBS Photos)



Figure 14 - Rivet Fractures in Hanger Connection at U13 N (NBS Photo)

NOT REPRODUCIBLE

of cleavage and shear as the fracture progressed through the cross section of the rivet. No evidence of pre-existing cracks or flaws in the rivets was found. The conclusion of this report states in part

"Strain-hardening of the rivets occurred as stress was applied. In the process of fracturing, the energy absorbed was evidently high and the fracture stress was higher than the ultimate* strength of the material. Accordingly, the fracture behavior could be characterized as being ductile. It appears that fracture of the rivets resulted from overloading of the steel in the plastic range. The appearance of the fracture profiles indicates a relatively high strain rate."

h. A number of other minor examinations have been conducted by the National Bureau of Standards laboratories. Significant data resulting from these investigations are contained in the official records of the investigation, as follows:

- (1) Measurements of the deformations in the C13 heads of eyebars No. 33 and No. 330.
- (2) Miscellaneous metallurgical data on eyebar steel and A-7 steel examined.
- (3) Results of an attempt to identify pin C13N by "ballistic matching" of markings in eyebars and in pins available.

2. Studies at the Battelle Memorial Institute (Columbus, Ohio)

The Battelle Memorial Institute was requested to conduct extensive studies to supplement those conducted at the National Bureau of Standards for the following purposes:

- (1) To determine whether small cracks on the inside surfaces of the eyebar pinholes existed in other eyebars in the Point Pleasant Bridge wreckage.
- (2) To assess the fracture toughness characteristics of the two steels used in the structure in order to determine whether pre-existent cracks found in various members by the National Bureau of Standards were of the critical size necessary to induce brittle fracture at stresses computed to have existed in the structure at the time of collapse.

*The author of the report apparently intended this to mean the static tensile strength of the material.

(3) To investigate the mechanisms by which small initial cracks or defects could have grown to critical size.

(4) To investigate the residual stress patterns which were present in the eyebar heads due to the combination of fabricating and heat treatment processes and subsequent loading history.

The results of these investigations are presented in Reference No. 24, "Inspection and Evaluation of Two Steels from the Silver Bridge."

a. Section 1 of the Battelle report describes nondestructive test techniques applied to five eyebar heads then stored at the National Bureau of Standards and to heads of twenty eyebars from the wreckage of the Point Pleasant Bridge which were still at the reassembly site or on the Ohio shore where they fell. Dye penetrant techniques and magnetic particle techniques were used in the field investigations, with inconclusive results. Thirty eyebar heads were therefore burned off and taken to the Battelle laboratories at Columbus for examination under more favorable conditions. After cleaning and visual inspection, Zyglo dye penetrant techniques and wet magnetic particle techniques were applied. The net result of this program was that positive indications of cracks on the pinhole surface were found in five of the eyebar heads.

b. Section 2 of the Battelle report describes the experimental techniques employed to determine the residual stress that existed in typical eyebar heads of the Point Pleasant Bridge wreckage. These residual stresses arise from the differential cooling which occurs during the heat treatment process and also from the fact that some of the material around the pinhole is subjected to strains above the yield point strain when maximum dead load and live load effects occur in the structure. The residual stresses of the first kind vary sharply with the distance from the outside surfaces of the bar where cooling was most rapid. The stresses of the second kind occur with more or less uniform levels through the thickness of the bar, but vary in magnitude from the pinhole surface to the outer circumference of the eyebar head.

The laboratory used two techniques to assess the magnitude of these residual stresses. Surface residual stresses were measured by the application of strain gages to the surface and noting the changes in strain produced by removal of small amounts of material directly below the strain gage by careful work with a dental drill. The second method was also destructive in nature and involved the removal of a 2-inch wide slice of material by two parallel cuts across one limb of the eyebar head, followed by successive removal of layers of

material through the thickness of this slice (See Figure 15). In general the results after the initial cuts (See Figure 16) show that residual stresses existed at the edge of the pinhole which were as high as 27,325 lbs. per square inch, with marked differences between the residual stresses at the two faces of the bar. The patterns of residual stress through the thickness were quite complex (See Figure 17) and in general the magnitudes were highest in the sections closest to the pinhole, indicating that stresses in excess of the yield strength of the material had existed at this point at some time during the life of the structure.

c. The next section discusses the investigation of the fracture toughness properties from the point of view of the modern discipline of fracture mechanics. The basic problem is to determine the parameter K_{Ic} , the "critical stress intensity factor" for the material, from which the stress level at which a given flaw size can produce a brittle fracture may be computed. Two types of specimens were employed. The first type, a notch bend specimen two inches thick, eight inches deep and thirty-six inches long, was tested as a beam at a temperature of 0°F. and at room temperature (about 70°F.). The test arrangement for the 0°F. tests is shown in Figure 18. The specimen was wrapped with foil over layers of steel wool, through which liquid nitrogen was circulated to establish the proper test temperature. Three specimens were tested at 0°F. and two at room temperature, all of which were cut from the shank of eyebar No. 330. All specimens contained chevron notches sharpened by fatigue cracking to about half the depth of the specimen.

The surface-flawed specimens were made from 1" x 2" x 24" blanks cut from eyebar No. 330, with the 2" side parallel to the thickness dimension of the bar. Tab extensions were welded to the ends for engagement of the loading grips. Each specimen was given a deliberate flaw by means of electronic discharge machining at mid length and across the center of the two-inch face. The flaw was then sharpened to a fatigue crack by fatigue loading prior to the static tension test in which fracture toughness data was obtained.

The results of these tests are summarized in Table 1. Complete data are presented in Appendix B. There is good agreement between the values of the K_{Ic} parameter obtained with the two types of specimen. All fractures were 100 percent "flat" cleavage.

A computation of stress level to produce a brittle fracture with a flaw the size of the primary pre-existent crack in eyebar No. 330 (0.12" x 0.28"), using the minimum value of stress intensity factor of 43.2 ksi $\sqrt{\text{in.}}$ found for specimens at 32°Fahrenheit, indicates that a unit stress of 88,000 psi is required. This is about 10 percent above the yield strength of the material, but since no consideration was given to the presence of the smaller secondary crack, it

II-7

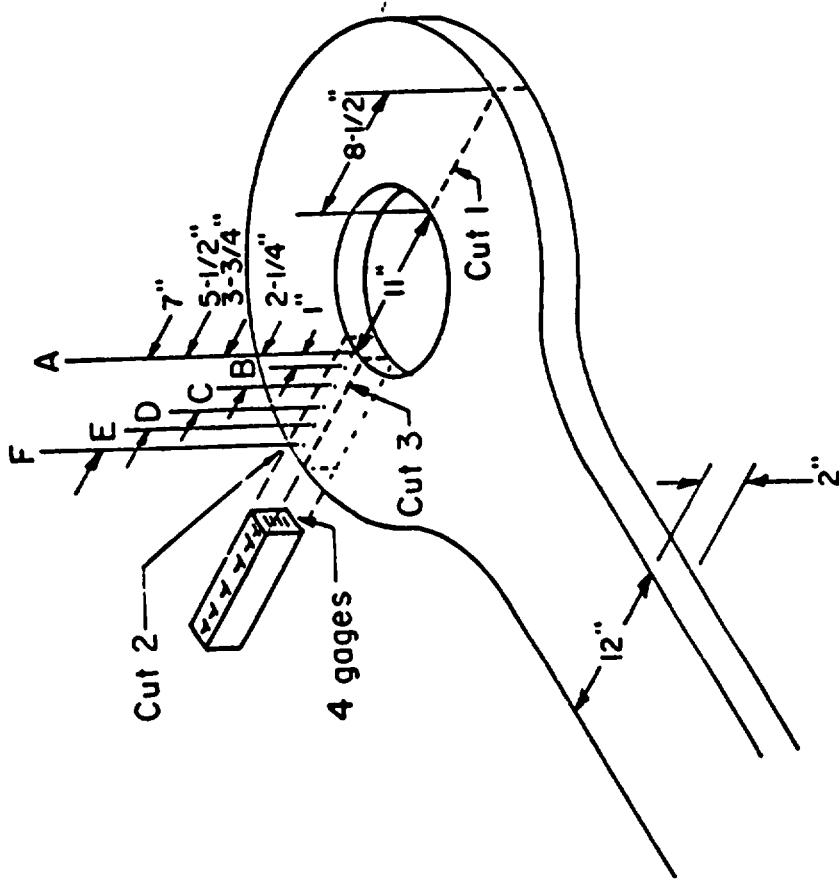


Figure 15 - EYEBAR WITH GAGE LOCATIONS AND INITIAL CUT LINES

(Battelle Memorial Report)

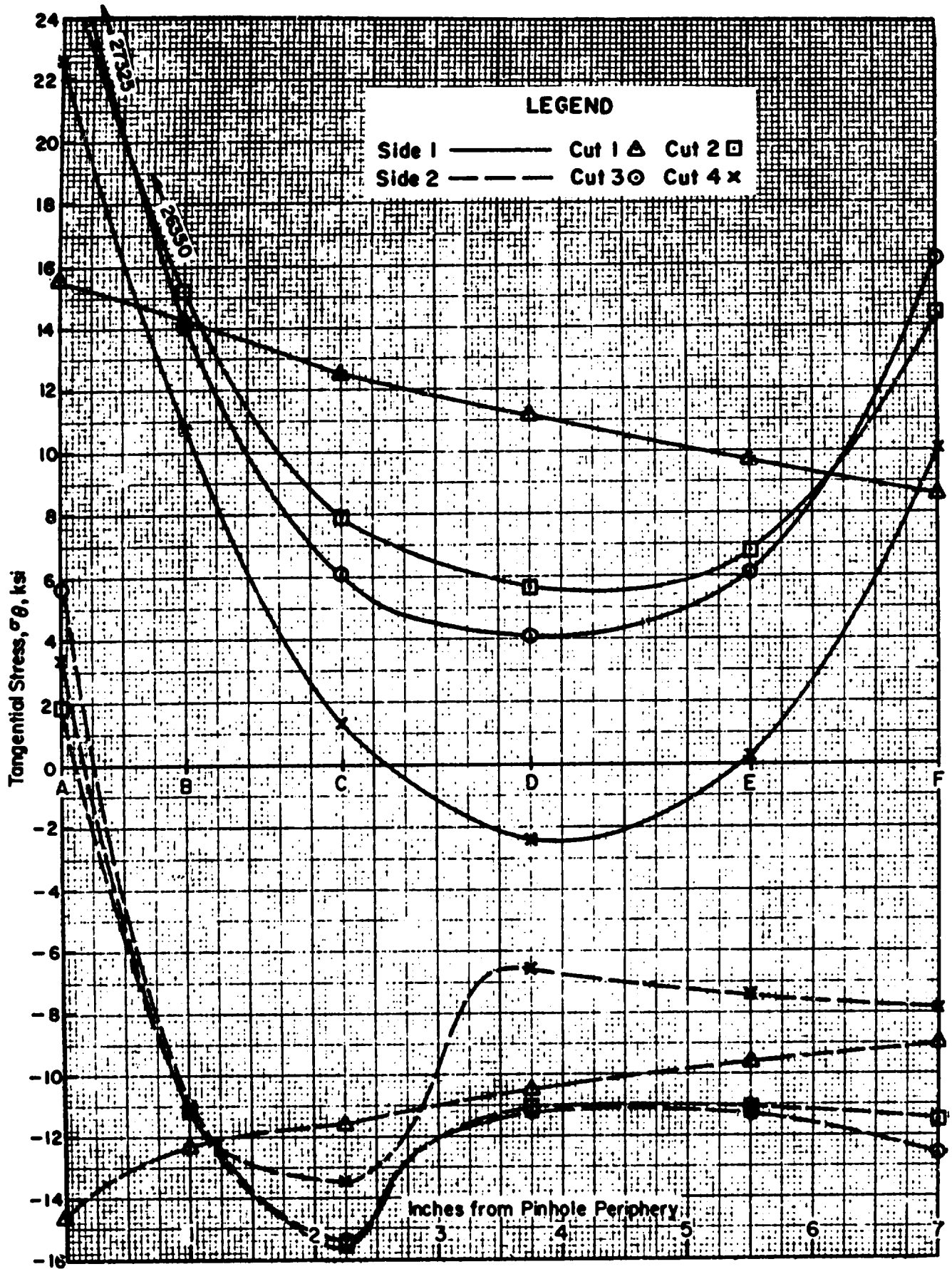


Figure 16 - CIRCUMFERENTIAL STRESS CONTOURS FOR INITIAL CUTS, SPECIMEN B-17

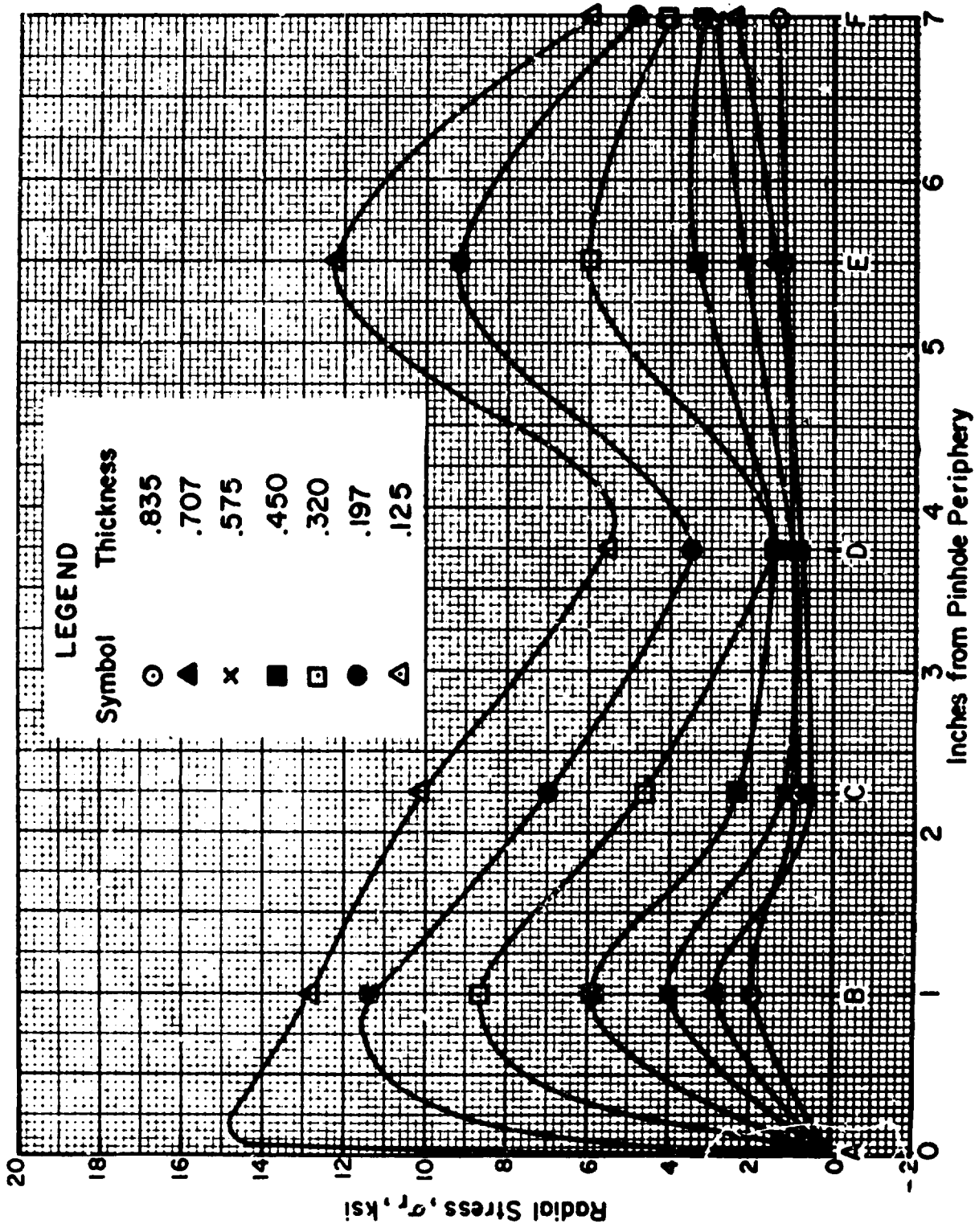


Figure 17 - RADIAL STRESS PRODUCED BY LAYER REMOVAL, SPECIMEN B-17, SIDE 2

(Battelle Memorial Institute)

NOT REPRODUCIBLE

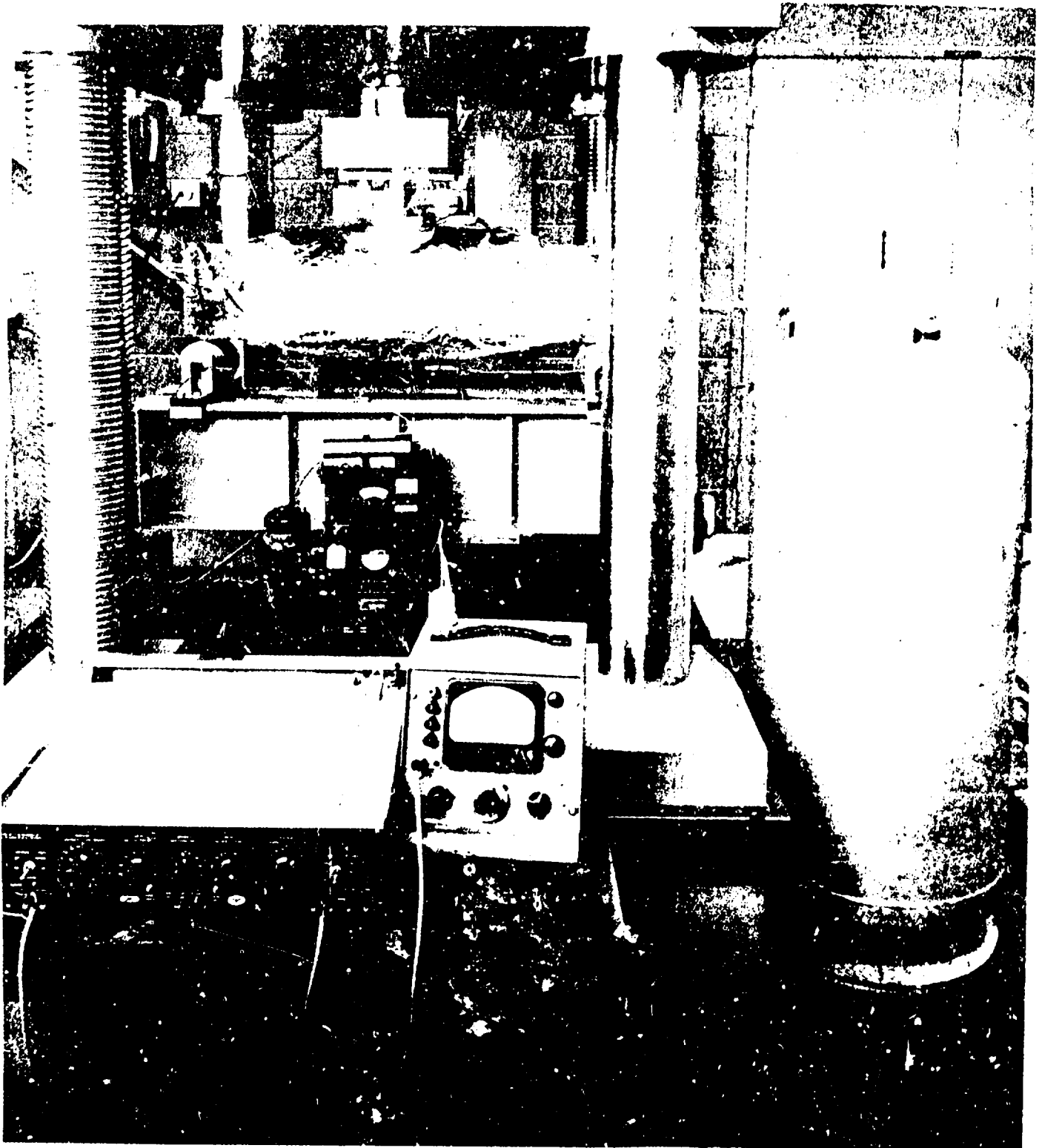


Figure 18 - Fracture Toughness Test Arrangement for 0° F. Temperature
(Battelle Memorial Institute)

must be concluded that brittle fracture was possible at a stress about equal to the yield strength of the steel.

The validity of these data was confirmed later by a test of a full scale eyebar head under loading conditions which produced a strain distribution across one limb of the eye similar to that existing in the prototype structure under load. The purpose of this latter test was to determine whether the type of fracture found in the lower limb of the C13 eye of eyebar No. 330 could have been produced by static load alone. A static load test at room temperature of a piece of the south eyebar from C9-C11 of the north chain, which contained a crack similar to those found in eyebar No. 330, had been conducted at the U. S. Steel laboratories. The fracture had shown an intermediate zone of ductile fracture between the pre-existent crack and the zone of brittle fracture. The Battelle laboratories were, therefore, asked to break a full scale eye at a temperature of about 32° Fahrenheit.

The specimen for this test was prepared from one of the eyebar heads in which the non-destructive test work had indicated the existence of a pre-existent crack on the pinhole surface in approximately the same location as that which produced the fracture of eyebar No. 330. The general arrangement is shown in Figure 19. The left side of the eye was severed by a saw cut. Two 2.74" diameter holes were drilled on a line parallel to the longitudinal axis of the eyebar at a location such that a tensile load applied through pins at these holes generated a stress gradient across the right limb of the eye similar to that existing in the case of normal loading of the eye in the chain. Strains along the expected line of fracture were monitored by bonded electrical strain gages.

On the first attempt at loading, in which a stress of 90,000 psi was produced near the crack, no failure occurred. The specimen was partially unloaded and again checked by dye penetrant. It was found that the "crack" was actually a shallow surface defect. An artificial defect was therefore introduced by means of a hardened steel wedge and then enlarged and sharpened by fatigue loading. At the second attempt at loading to failure, fracture took place during a partial loading imposed to check instrumentation. The stress in the vicinity of the crack was about 57,000 psi. Fortunately, all instrumentation worked properly, so it was possible to measure the flaw size (0.345" x 0.780") and to compute the effective critical stress intensity factor, K_{Ic} . A value of $46.2 \text{ ksi}\sqrt{\text{in.}}$ was obtained, which compares closely with the average value of $46.4 \text{ ksi}\sqrt{\text{in.}}$ at 32° Fahrenheit measured on the surface flaw specimens. No intermediate ductile zone was present in the fracture.

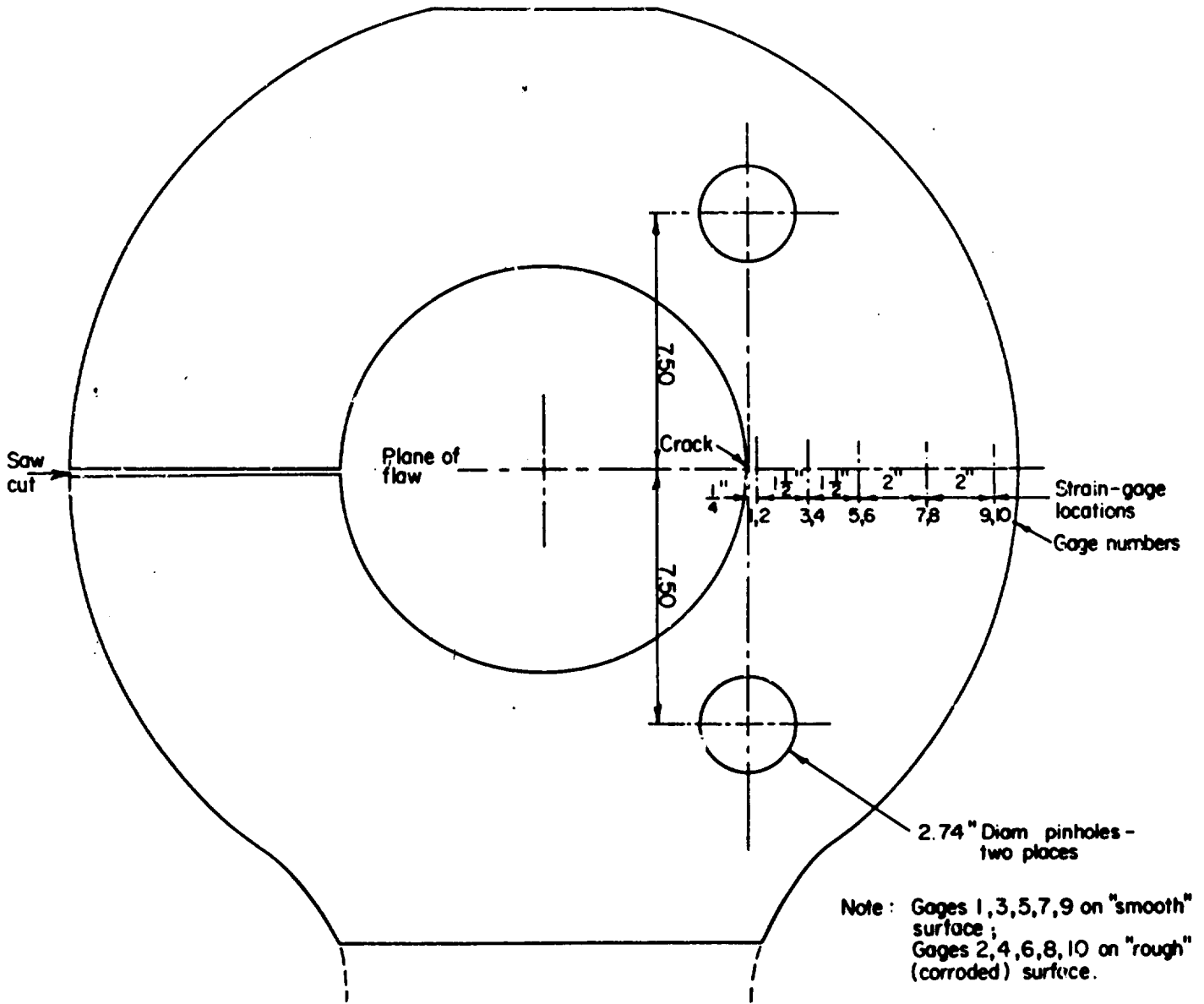


Figure 19 - Specimen Configuration with Strain-Gage Locations for Full-Scale Fracture Test

(Battelle Memorial Institute Report)

d. Three different possible mechanisms by which the critical flaw in eyebar No. 330 might have grown to critical size were explored; namely, fatigue cracking, hydrogen-stress-cracking, and stress-corrosion.

The fatigue crack propagation rates were measured in dry laboratory air, at room temperature, in dry air at 32 degrees Fahrenheit, and in air moistened by a water spray. Results are presented in Figures 20a, and 20b, which show the rate of change of crack depth per cycle versus the stress intensity factor range for the imposed nominal stress range. It can be seen that this measure of crack propagation was virtually independent of the temperature and environmental factors tested.

The nominal live load stress range in eyebar No. 330 was 12,500 psi from dead load to full live load. However, the maximum live load stress could be produced only by loading both lanes of the bridge from end to end with the full design loading, a situation of rare occurrence. A more typical maximum stress would probably be that associated with the loading at the time of collapse, which produced a live load unit stress in the shank of the eyebar of 4900 psi. The range of stress at the edge of the hole in the eyebar would be approximately three times as much, or 15,000 psi. Computations based on the fatigue crack propagation data indicates that to grow a defect from a small pit assumed approximately 0.020 inches deep to a crack 0.100 inches deep corresponding to the critical crack in eyebar No. 330 would require about 541,000 cycles of such loading. This is equivalent to 37 cycles of such loading per day for the forty years of life of the structure. The Battelle report concludes that while fatigue might have been a significant contributing factor, it was probably not in itself the primary method of crack propagation.

Experiments were conducted to determine the hydrogen-stress-cracking susceptibility of the eyebar material. This mechanism of crack growth may exist in steels processed to a tensile strength level of the order of 110,000 psi which are subjected to continuous loading above some minimum level, and which are subjected to an environment which contains hydrogen which is free to diffuse through the lattice structure of the steel. It was therefore necessary to determine whether the steel could absorb enough hydrogen from the service environment and whether or not the stress level was above the critical level. Surface flawed specimens made of the material from the outer layers of eyebar No. 330, which because of its hardness would be most susceptible to such cracking, were exposed to four different environments:

Condition A: 4% by weight of sulfuric acid in distilled water, plus a poison (phosphorus dissolved in carbon disulfide).

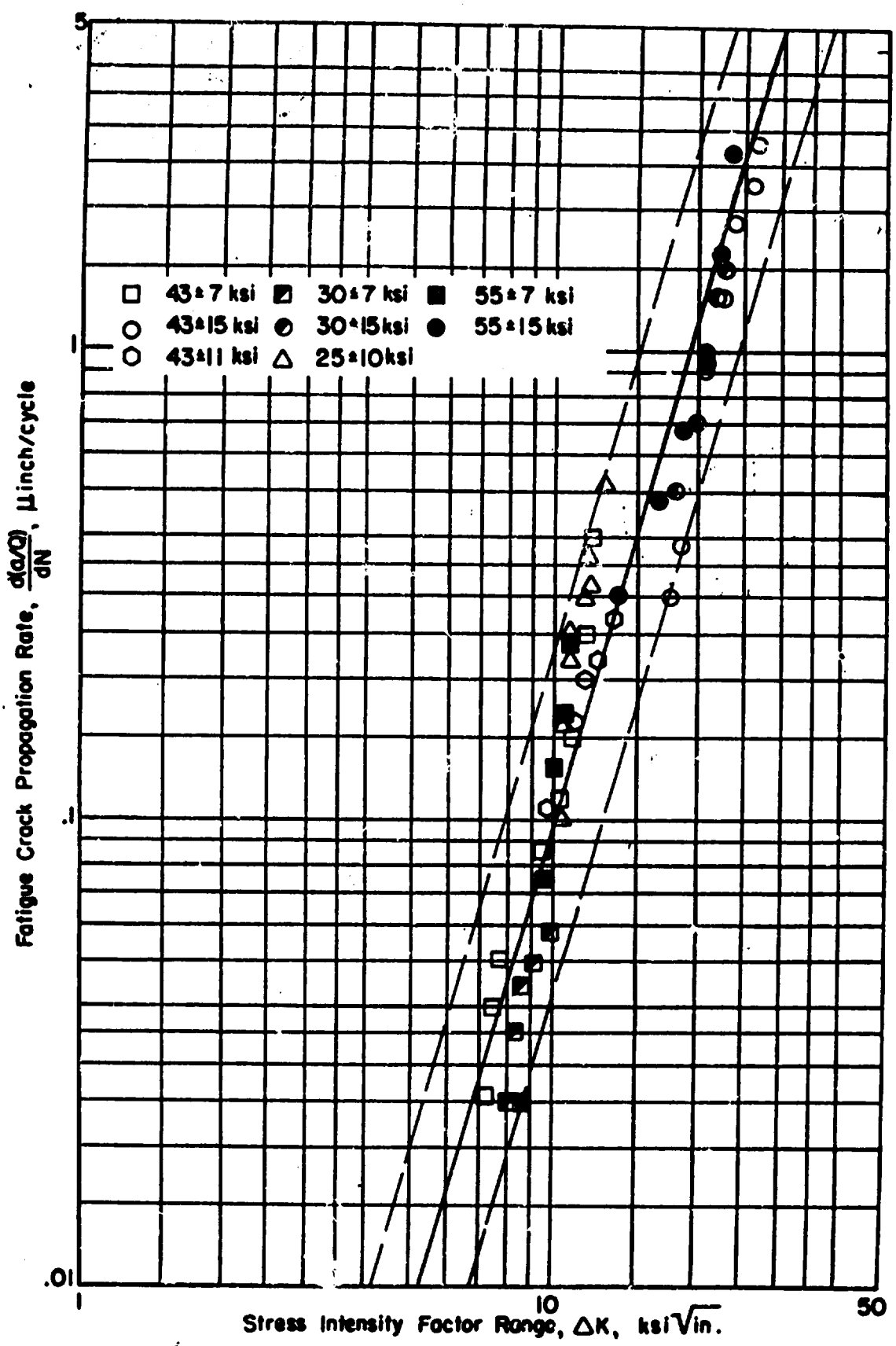


Figure 20a - Room-Temperature Fatigue-Crack-Propagation Rates for Eyebars Material

(Battelle Memorial Institute Report)

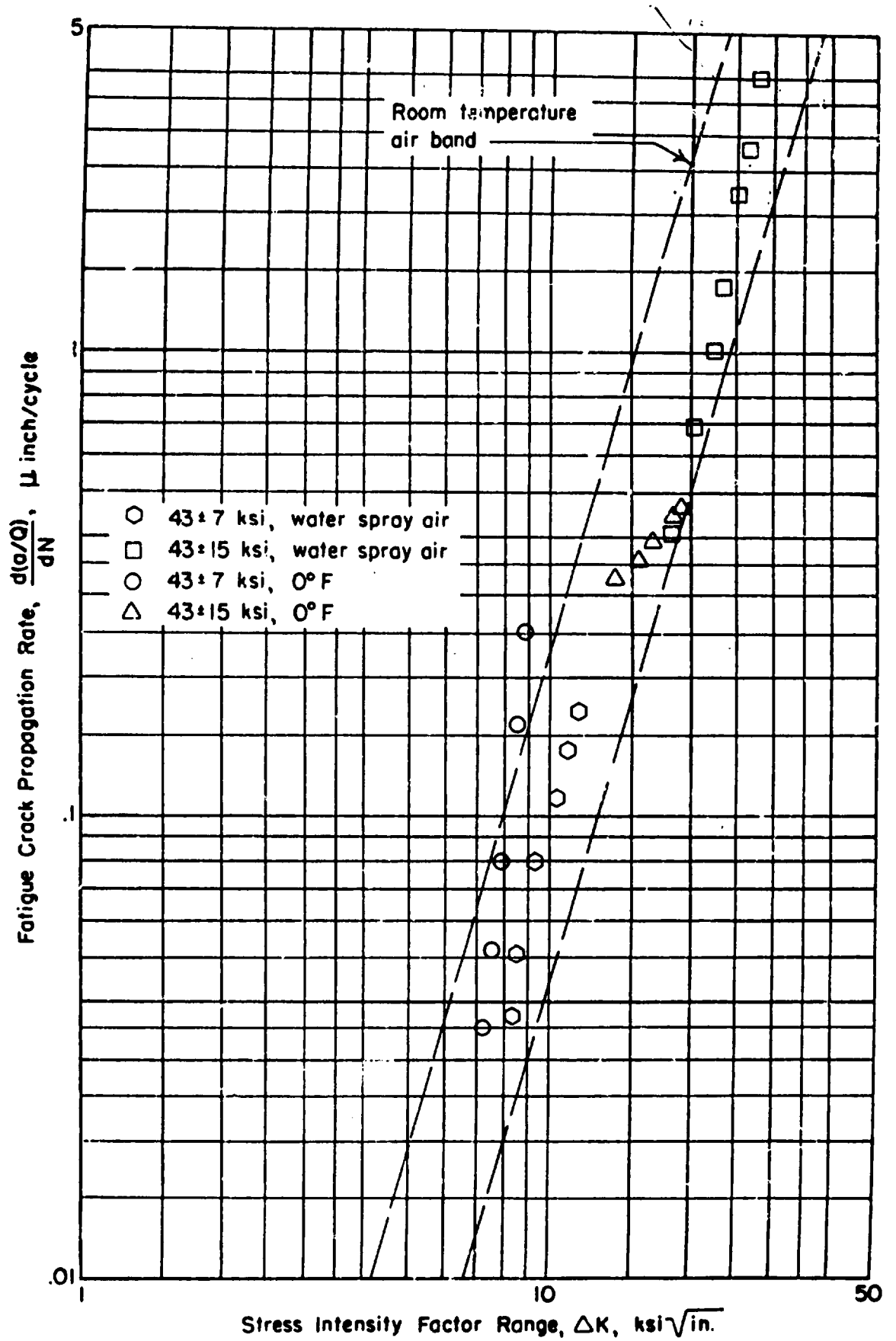


Figure 20b - Effect of Temperature and Environment on the Fatigue-Crack-Propagation Rates for Eyebars Material

(Battelle Memorial Institute Report)

Condition B: 0.004% by weight of sulfuric acid in distilled water, plus a poison.

Condition E-1: Hydrogen sulfide gas dissolved in water by continuous bubbling.

Condition E-2: Same as E-1, except that the specimen was coupled with a commercially pure aluminum anode.

The charging currents established by these exposures were measured. Sustained loads applied to the specimens produced stress intensity factors between 26.4 and 45.0 ksi. $\sqrt{\text{in.}}$ Hydrogen entry rates under the same set of environments were independently measured by samples exposed in a vacuum-permeation cell. The study showed that the steel without pre-existing defects was susceptible to hydrogen-stress-cracking only under severe cathodic charging conditions and high stress levels.

The investigators also made the following observations:

(1) The steel from the inside surface of the pinhole was more susceptible than that from the outer surface of the eyebar because of the removal of the decarburized layer in the machining of the hole, exposing the harder material. Some of this material was extremely hard (51 Rockwell C by conversion), due apparently to localized cold working.

(2) There was considerable metallurgical variation between specimens, which may account for some of the apparent inconsistency of results.

(3) There was an indication that the hardest layers of steel were susceptible to stress-corrosion cracking (not requiring the presence of atomic hydrogen) in a hydrogen sulfide environment.

Further investigations of the stress-corrosion cracking susceptibility are reported in Section VI of the Battelle report. In these investigations, the emphasis was on the determination of the threshold value of the stress intensity factor below which no stress-corrosion crack propagation could occur in each of two environments; namely, 100 percent relative humidity air, and a solution of 0.5 percent hydrogen sulfide and 5 percent salt in distilled water. Two types of specimens were used. Six ordinary surface flawed specimens were exposed to each environment at various static stress levels to obtain values for plotting curves from which the threshold value could be determined. "Wedge loaded" specimens were also tested in each environment. This form of specimen has the advantage that, as cracking proceeds, the

stress intensity factor decreases. Thus, a point is reached where the crack stops growing because the stress intensity factor falls below the threshold value. The experimental set-up for these tests is shown in Figure 21. The specimen itself is not visible in the photograph since it is inside the plastic environmental enclosure, but the pins in the loading device which apply the loads to the ends of a machined slot in the specimen can be seen. This slot was about one quarter of an inch wide and parallel to the direction of loading. Stress raisers were initiated in the sides of the slot by a saw cut and were sharpened to cracks by fatigue loading prior to the sustained static load test.

In this experiment, it was found that the material was not susceptible to crack growth in 100 percent humidity air, but that it was quite susceptible to crack growth in the hydrogen sulfide and salt solution, based on data from the surface-flawed specimens. The indicated threshold value of the stress-intensity factor was $15 \text{ ksi} \cdot \sqrt{\text{in}}$. The wedge loaded specimens failed to show any flaw growth at the stress intensities used, even in the severe environment. This was attributed to the difference in microstructure in the material in the interior of the specimen in which the "through the thickness" cracks were located.

Crack growth rates were also measured on the surface flawed specimens and were found to be an exponential function of the stress intensity factor. This implies that, for very long service lifetime, even very small cracks would result in sustained load crack growth in this hydrogen sulfide and salt solution environment.

e. In Section V of the Battelle report, the results of fractographic examination and microprobe analysis of one of the pre-existent cracks on the pinhole surface of the C11 head of eyebar C9-C11, north chain, south bar, are discussed. The portion of eyebar head C11 containing the cracks was cut from the eyebar at the National Bureau of Standards and shipped to the U. S. Steel laboratory. It was broken open in the presence of representatives of U. S. Steel and Battelle Memorial Institute, who were part of a special test group appointed on May 23, 1969, to attempt to resolve the question of what mechanism of crack growth was responsible for extending such cracks. After breaking open, one side of the fracture was retained by U. S. Steel and the other taken to Battelle for independent evaluation. The results of the investigation of the fracture surface by the U. S. Steel laboratory are discussed in the next subsection of this report, and the report of the chairman of the task group, is discussed in Section IV.

The examination of this fracture at Battelle disclosed the following:

- (1) The origin of the pre-existent crack was a small corrosion pit about 0.01 inch in diameter.

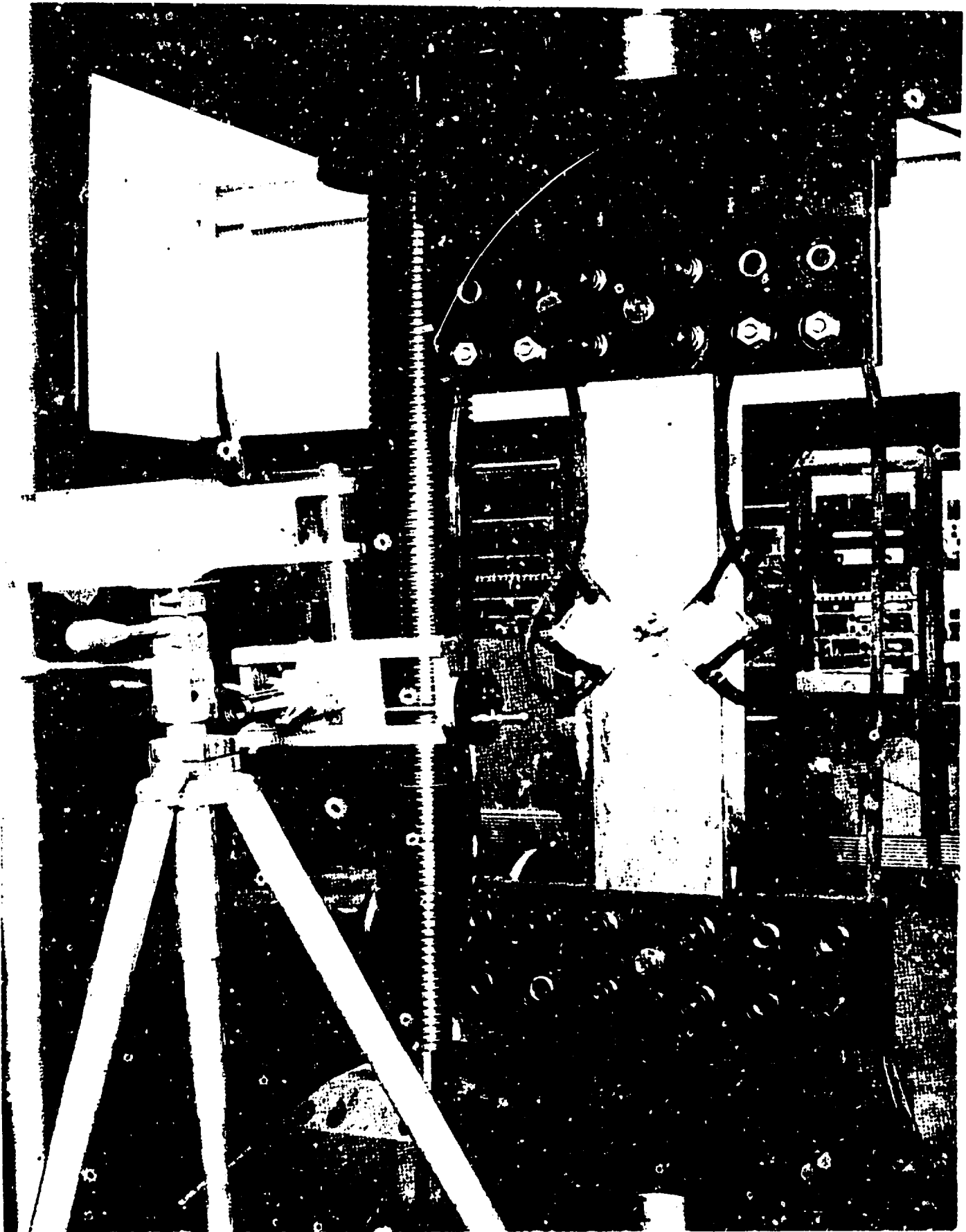


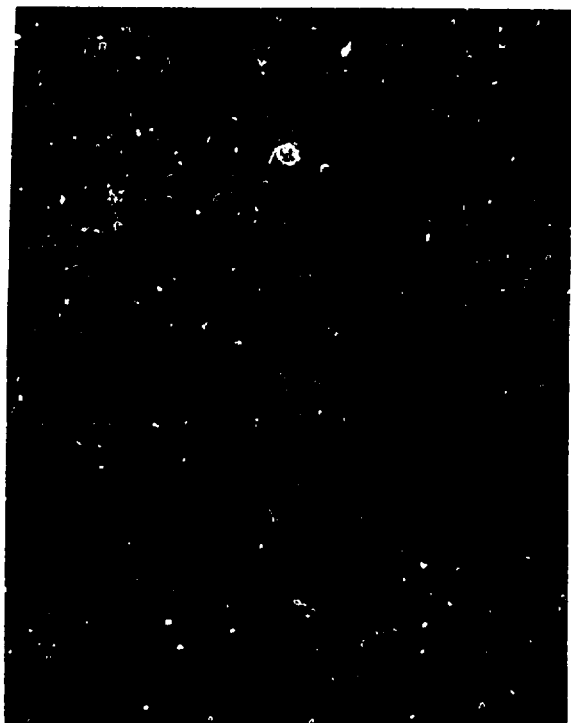
Figure 21 - Test Setup for Wedge-Force Loaded Specimens under Environmental Conditions

(Battelle Memorial Institute Report)

- (2) A black acicular oxide covered much of the pre-existent crack surface.
- (3) No distinct fractographic features such as fatigue striations were found after the oxide was removed.
- (4) Near the tip of the pre-existent crack, there were many small branching cracks, suggesting that the crack growth was by stress-corrosion cracking.

Area scans and line scans were made with the electron microprobe. In the area scan work, the resulting x-rays emitted by elements on the surface were displayed and photographed on a cathode ray tube. By selective control of the x-ray detection, those due to separate elements could be identified. This permitted the general distribution of the elements in the crack fracture surface to be determined. It was found that aluminum, chlorine, potassium, and sulfur were prominent at the outer lip of the crack (the original pinhole surface), and except for the aluminum and potassium, generally decreased in concentration as one proceeded along the crack surface. Figure 22 shows the pattern of concentration for sulfur. An examination of the area near the crack tip showed higher concentrations of sulfur and chlorine on the pre-existent crack surface than on the freshly cracked ductile fracture. Sulfur in the freshly cracked area was found to be identified with sulfide inclusions in the metal. Line scans across the entire crack and into the freshly opened surface confirmed this result. A test to distinguish sulfide from sulfate ions showed that both were present on the pre-existent crack surface. A chemical test using sodium azide gave only a very weak indication of sulfide in the crack surface, and no detectable indication in the freshly opened crack. The conclusion of this study reads in part as follows:

"The crack morphology is quite typical of that normally associated with stress-corrosion cracks. No evidence was found to suggest that the crack may have been associated with corrosion fatigue. A pit near the mouth of the crack was identified as the possible origin of the crack... Also, the highest chlorine concentrations were found at both the mouth and tip of the crack, whereas sulfur was greatest just at the mouth of the crack... Examination of the secondary crack in the eyebar corroborated the work done by Lane et. al. on eyebar No. 330. The failure mechanism was probably sulfide-stress corrosion. Hydrogen sulfide in the atmosphere from industrial or exhaust gases could have dissolved in moisture condensed on the bridge. H₂S could then react with the steels and form iron sulfide in the oxide scale. Restricted areas where moisture would remain for long periods would become sulfide



500X

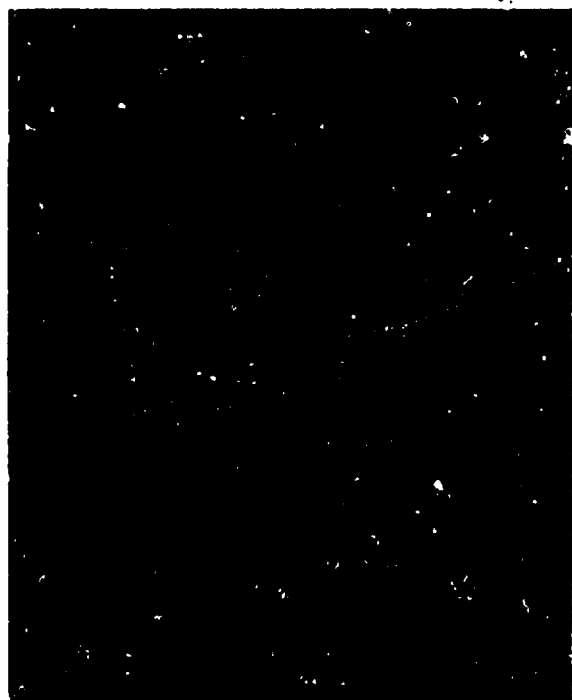
a. Aluminum



500X

b. Chlorine

NOT REPRODUCIBLE



500X

c. Potassium



500X

d. Sulfur

Figure 22 - Microprobe Area Scans at Site A

(Battelle Memorial Institute Report)

concentration points. The presence of sulfides, by their restriction of the H_2 recombination reactions, would inhibit the escape of hydrogen produced during corrosion from the steel surface. Atomic hydrogen would diffuse to stressed areas in the steel and cause embrittlement and eventual failure. The role of the chloride ion probably was not to initiate a crack by itself but to reinforce the corrosion reaction thereby facilitating cracking in the presence of H_2S ."

f. The final section of the Battelle report covers investigations of the fracture toughness properties of the A7 steel, based on samples extracted from the chain bent post at panel point zero, north truss, Ohio shore, which was believed to be typical of the steel used in the stiffening trusses.

It was doubted from the outset that linear fracture mechanics techniques would be appropriate for use with this steel because of its ductility at normal temperatures and static loadings. The first attempt to determine the critical stress intensity parameter by use of a surface flaw specimen confirmed these doubts. The fractures were accompanied by much ductile deformation, and the nominal stress level at fracture was 55,000 psi., well above the yield point for this material. A second test at 0°F. gave similar results.

Since it was evident that brittle fractures could be produced only at high strain rates or at low temperatures, the program was modified to make use of the Charpy impact test to obtain the required data. Although a conventional Charpy specimen and apparatus were used, the tests were supplemented with special instrumentation which permitted the measurement of the instantaneous loading imposed on the specimens throughout the period of loading and rupture. This technique permitted the detection of any plateau in the load-deformation curve associated with ductile yielding prior to fracture. The results of these experiments, together with the results of slow bend tests on Charpy type specimens are displayed in Figure 23. The instrumented Charpy tests were conducted at a temperature range from -120 degrees Fahrenheit to +220 degrees Fahrenheit. The test points are those associated with the solid lines on the figure. General yielding prior to fracture was detected only for tests above zero degrees Fahrenheit and are associated with the straight line in the diagram. It will be noted that the loading at which general yield occurred, decreased from about 2900 lbs. at zero degrees Fahrenheit to approximately 2300 lbs. at 220 degrees Fahrenheit. The fracture of these specimens occurred at higher loadings for the region above zero degrees Fahrenheit as indicated by the upper solid line. Loadings were in general in excess of 3000 lbs. at fracture. Below zero degrees Fahrenheit, fracture occurred prior to any ductile yielding and at decreasing loads with further reduction in temperature. The data indicate a transition

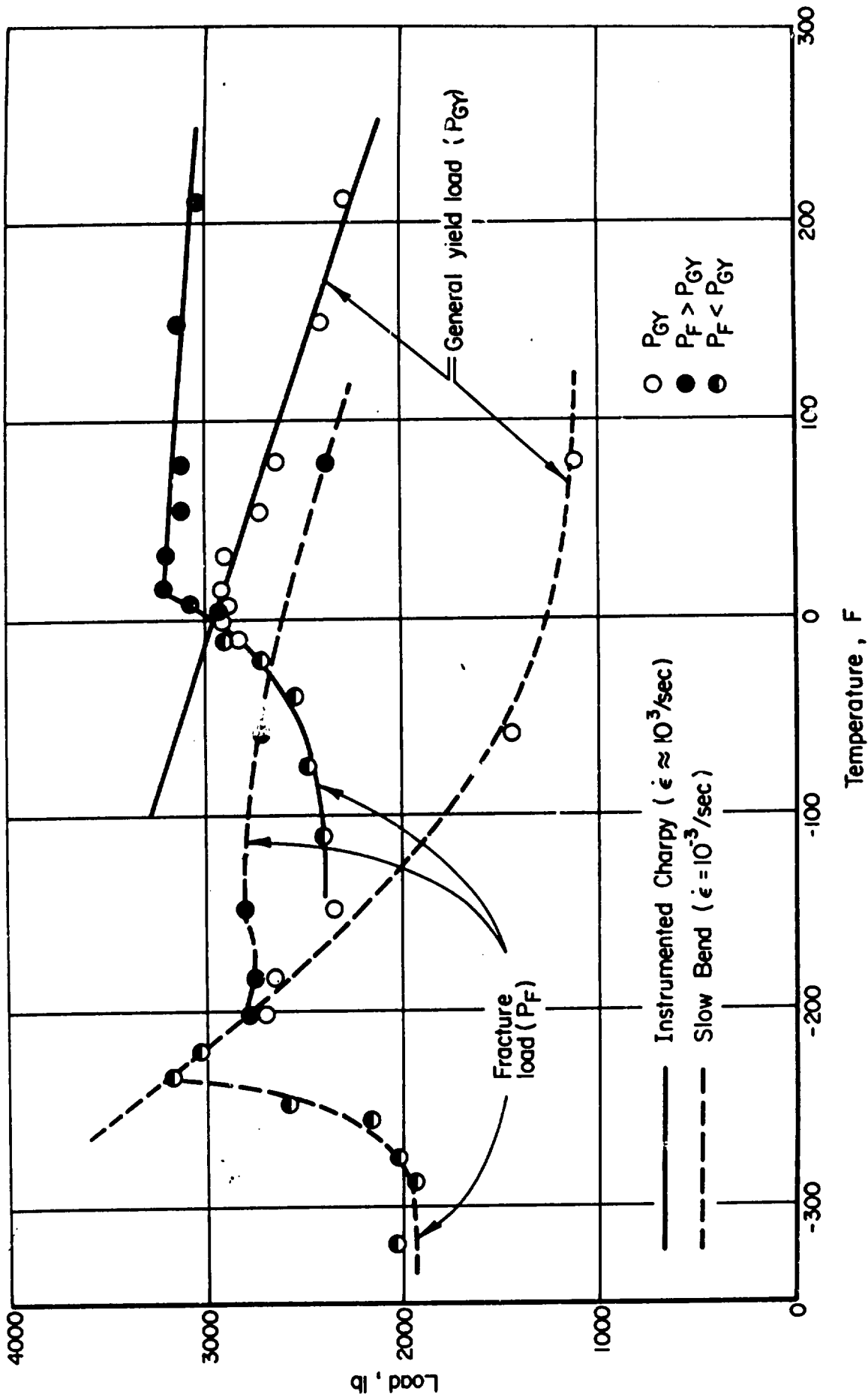


Figure 23 - The Effect of Strain Rate on the Three-Point Bend Properties of A-7 Steel Charpy V-Notch Specimens (Battelle Memorial Institute Report)

from ductile to brittle fracture behavior at about 0°F. for the high strain rates associated with the Charpy test, which are on the order of 10^3 microinches/inch per second.

The dramatic change in the fracture behavior at essentially static load rates in the slow bend tests are indicated by the dotted curve in the diagram. For these strain rates, which are estimated at approximately 10^{-3} microinches/inch per second, the transition from ductile to brittle behavior occurs at much lower temperatures than those in the dynamic Charpy test.

The Charpy impact data were also used to construct the conventional transition temperature curve by plotting energy at fracture against temperature. This technique of data interpretation resulted in an estimate of 36°F. for the "15 Ft. Lb. transition temperature." Further discussion of these results is deferred until they are compared with the results from other laboratories in the analysis section of this report.

3. Investigations at U. S. Steel Applied Research Laboratory

Tests and investigations at the United States Steel Corporation's Applied Research Laboratory at Monroeville, Pennsylvania, were conducted partly to obtain independent checks on materials properties, metallurgical and fractographic results, and also to study certain special problems. This work was conducted without charge to the Government by U. S. Steel, functioning as a Party in Interest in the investigation.

a. The early test results of this laboratory on the properties of the eyebar and truss steel, as submitted to the working group on February 14, 1969, and supplemented on March 3, 1969, are included in Appendix B. These include tests to determine chemical composition, tensile properties, hardness variations through the thickness, and Charpy impact test properties for the eyebar steel; and chemical composition, tensile and Charpy impact properties of a sample of the A7-24 steel. The samples of eyebar steel were taken from the C9 head of eyebar C9-C11 north chain, north bar (designated C9) and the C11 head of eyebar C11-C13 north chain, north bar, (designated sample C0), which was also known as eyebar No. 330. Supplemental results of tests on another sample removed from the C13 head of eyebar No. 330, submitted in May 1969, are also included in Appendix B.

These results, in general, corroborate those obtained by the NBS laboratory. Minor differences are discussed in the analysis section of this report. They established that there were no significant differences in chemical composition or mechanical properties between eyebar No. 330 and other eyebars in the structure. The C13 head of eyebar No. 330 showed slightly lower carbon, manganese and sulfur contents, but insignificant differences in resulting mechanical properties. Hardness profiles across the thickness and from pinhole surface to interior of the

eyebar also showed results similar to those obtained by NBS. There was a layer approximately 0.10 inches thick on each face in which the Rockwell C hardness (obtained by conversion from Vickers diamond point hardness, DPH) averaged about 24, then a layer extending to a depth of about 0.40 inches in which the hardness was between 25 and 30, and followed by a gradual decrease of hardness toward the core material at the center of the thickness, where the hardness averaged about 21. This is a result of the slack quench obtained in the heat treatment and the decarburization of the outer surface. The profiles beginning at the pinhole surface show similar effects, but the layer of apparently decarburized steel was either thin or absent.

The results on the A7-24 steel also corroborated the work at other laboratories, indicating that its chemical composition and mechanical properties were within the limits of the specifications for the material. The 15 ft. lb. transition temperature, based on results of Charpy impact tests, was between 50 and 70 degrees Fahrenheit.

b. A single slow bend test of a notch beam specimen was performed at 32°F. to check the fracture mechanics parameters developed at Battelle. The specimen of eyebar material used was somewhat smaller than those tested at Battelle, being 1.82 inches thick, 5.80 inches deep and about 28 inches long. It was tested in three point loading on a span of 24 inches and fractured at a load of 21,100 pounds. The depth of the notch and fatigue crack totaled 2.29 inches. The value of the critical stress intensity factor computed from these results is $39.3 \text{ ksi}\sqrt{\text{in.}}$, about nine percent below the minimum obtained by Battelle, which was $43.2 \text{ ksi}\sqrt{\text{in.}}$ The indicated failure stress for the critical flaw in eyebar No. 330 based on this lower value of the critical stress intensity factor is 75,000 psi.

c. A careful examination of the depth of pitting on various surfaces of the C13 head of eyebar No. 33 was conducted, in which the pit depths were measured by noting the change of focusing adjustment necessary for the microscope between the surface near the pit and the bottom of the pit. The results of this examination are summarized as follows:

<u>Surface</u>	<u>Number of Pits</u>	<u>Average Pit Depth, in.</u>	<u>Maximum Pit Depth, in.</u>
Two inch wide strip, pinhole to outside edge, south face			
Half inch nearest hole	31	0.014	0.038
Remainder of surfaces	7	0.008	0.013
Two inch wide strip, pinhole to outside edge, north face			
Five inches nearest hole	60	0.027	0.053
Outer four inches	42	0.049	0.105
Pinhole surface (normally in contact with the pin)			
First 6/16" from north face	4	0.0045	0.006
Next 9/16" from north face	27	0.005	0.007
Next 10/16" from north face	51	0.006	0.008
Remaining 6/16" to south face	23	0.0075	0.012

d. Reference 25, "Examination of Point Pleasant Bridge Eyebars," dated May 18, 1970, reports the studies conducted by U. S. Steel as a part of the work of the special task group appointed to investigate the mechanism by which the crack in eyebar No. 330 grew to critical size. The specimen was taken from eyebar C9-C11 north chain, south bar, which contained a tight crack similar to the pre-existent crack in eyebar No. 330. As noted in the discussion of the work by the Battelle group, this specimen was broken open by a static load to extend the crack at the USS laboratory. The general appearance of the piece retained by USS for examination is shown in Figure 24a. Four distinct regions were noted in the fracture surface, designated A, B, C, and D in Figure 24b. When first examined, the black oxides in region A were noted to be wet with water. An attempt was made to measure the pH, but there was not sufficient water for a valid reading. Within five minutes, the surface was dry. This region marks the limits of the crack originally in the piece.

Zones B, C, and D were formed when the specimen was loaded to failure. Zones B and C were both gray in color, but zone D was light in color, and a zone of definite fast fracture.

In addition to examination of all regions by fractography using the scanning electron microscope, the material present in zone A was checked for the presence of certain elements with the x-ray spectroscopy attachment, by electron probe analysis, and by x-ray diffraction techniques. The black oxides were identified as iron oxides (Fe₃O₄ and possibly Fe₂O₃), and other particles in this region contained calcium, silicon, chlorine, aluminum, and sulfur. The calcium and silicon were frequently associated, and most sulfur indications were associated with manganese, indicating that these particles may have been manganese sulfide from the underlying steel. An azide test for detection of sulfide was conducted on zones A and D. Both zone A and zone D gave moderate indications, with that in zone A being somewhat



Figure 24a - Appearance of Freshly Opened Crack in Eyebar Steel
(U. S. Steel Photo)

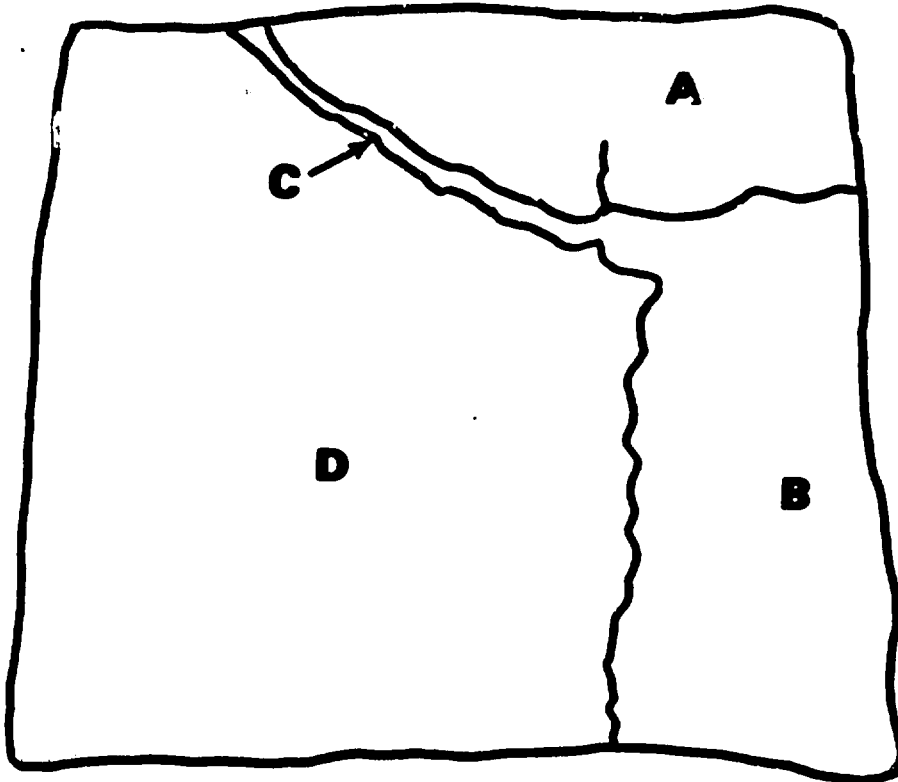


Figure 24b - Fracture Regions in Freshly Opened Crack in Eyebar Steel
(U. S. Steel Photo)

more pronounced. The degree of reaction, however, was no greater than that found on other corrosion products found on steel exposed in rural atmospheres where hydrogen sulfide is not believed to have been present, indicating that the positive reaction noted may have been the result of manganese sulfide originally in the steel.

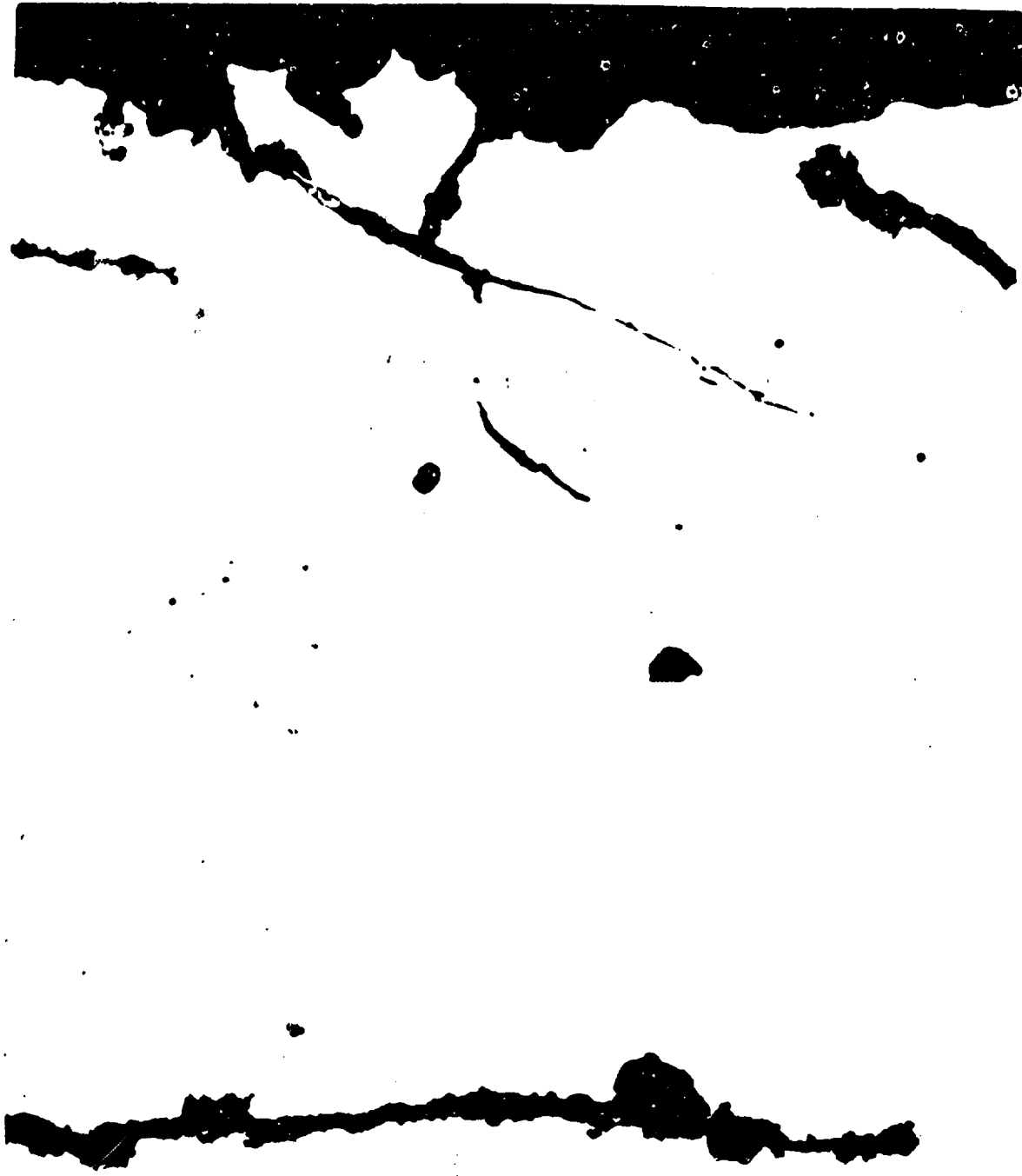
The scanning electron examination of the fracture surfaces of zones B and C showed that these were fractures of ductile-dimple type, whereas zone D was flat cleavage. Apparently the original crack (zone A) was extended through the transition zone (zone C) as a ductile fracture during the slow bending load until it reached critical size, resulting in the fast cleavage fracture of the remainder, except for zone B. This zone had a more favorable microstructure. The existence of the ductile zone C raised questions as to whether the lack of such a zone in the critical fracture in eyebar No. 330 indicated that this fracture might have been caused by forces other than a static load alone. This led to a decision to attempt to fracture a full scale eye containing a crack at 32°F. at Battelle, as described above.

Further examinations of typical cracks were made. An attempt to examine one in Battelle specimens BTL-15, where work at that laboratory had indicated a crack existed, failed because no crack could be found. A mounted sample from the NBS laboratory which had been cut from eyebar No. 330 along a plane perpendicular to the fracture was carefully examined to check the nature of the propagation of secondary cracks roughly parallel to the primary crack of the fracture itself. These cracks were found to be relatively straight and unbranched, transgranular, relatively blunt at the tip, and filled with corrosion product. All of them started at pits on the original pinhole surface. A photomicrograph of the tip of one of these cracks which was about 0.01" from the fracture and which penetrated about 0.03" is given in Figure 25a. The different appearance of the branch cracks emanating from the primary fracture is shown in Figure 25b. Even those cracks showed some corrosion, most likely due to environmental exposure after collapse of the structure.

The author of the report expressed the opinion that the cracks starting at the pinhole surface showed evidence more characteristic of corrosion-fatigue than of stress-corrosion, due to the fact that they conform to the behavior typical of the former type of propagation; namely, initiation of the cracks at pits or trenches in the surface, transgranular propagation, and relative absence of branching. This observation was at variance with the opinions expressed by both the NBS and Battelle laboratories, and resulted in a meeting of the special task group which is discussed in Analysis.

4. Laboratory Tests at Structures Laboratory, Fairbank Highway Research Station, Federal Highway Administration

Two types of laboratory studies were conducted by the Structures and Applied Mechanics Division, Office of Research, Federal Highway



(a) Secondary Crack Tip

(b) Branch Crack along Main Fracture

Figure 25 - Appearance of Branch and Secondary Cracks Associated with Fracture in Eyebar No. 330

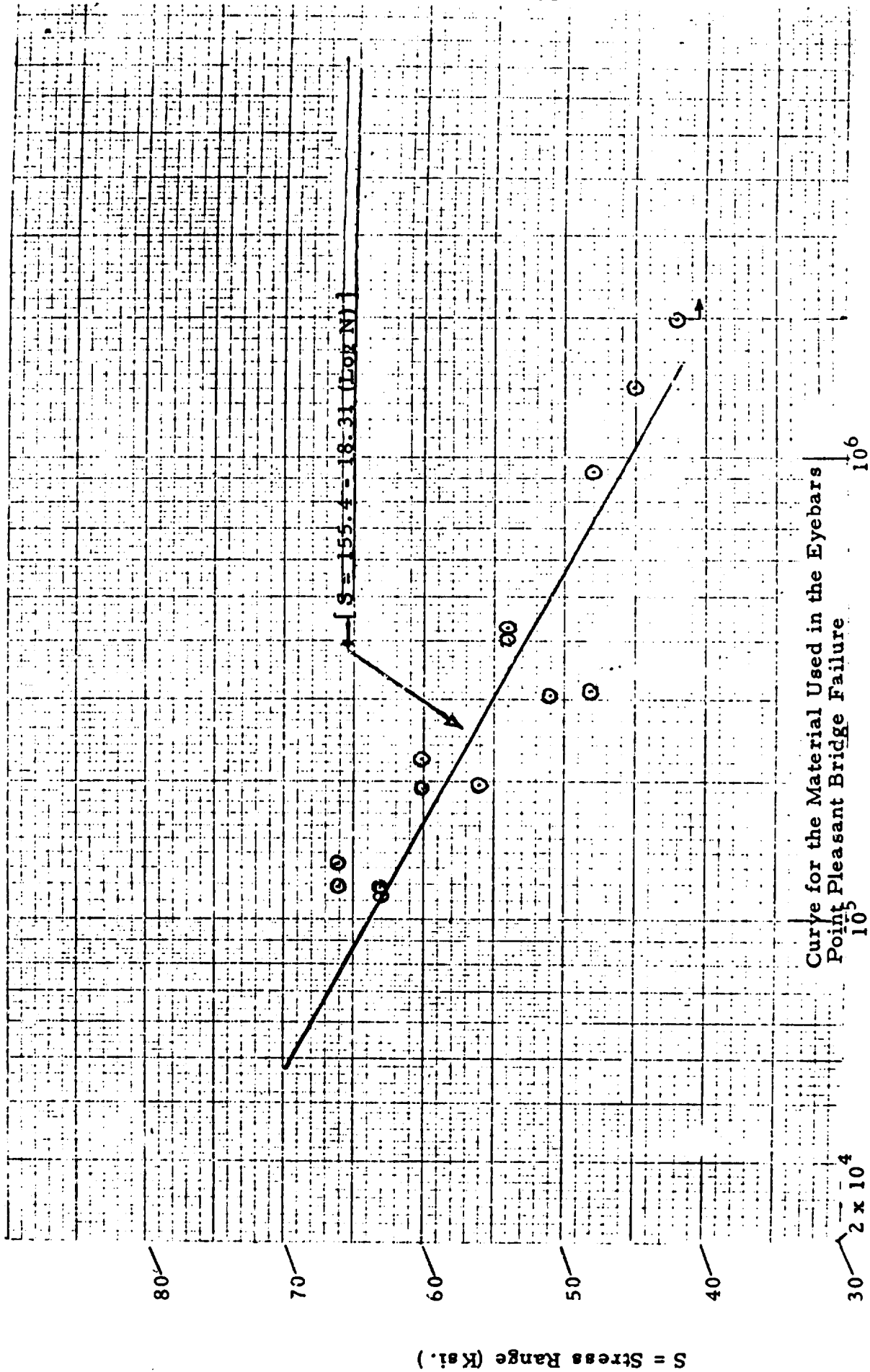
(U. S. Steel Photos)

Administration. The first of these developed basic data on the fatigue properties of the eyebar steel (Reference 26) and the second consisted of scale model tests of a portion of the eyebar chain in which the possible modes of separation of joint C13N were investigated (Reference 27).

a. The results of the fatigue tests are summarized by the data presented in Figure 26. This figure shows the relation between the stress range (the change of stress between minimum and maximum loads) and the number of cycles to produce a fatigue fracture. As is customary in such data interpretation, the number of cycles to failure is presented on a logarithmic scale. It is significant to note three specific points on the line of best fit to these data. Namely, (1) the indicated numbers of cycles to failure if the stress range were equal to the full 50,000 lbs./sq. in. allowable stress is 230,000 cycles; (2) a stress range of approximately 45,000 lbs./sq. in. would carry about a million cycles prior to failure; and (3) a stress range of 15,000 lbs./sq. in., which is probably typical of that which occurred near the edge of the eyebar hole indicates a life in excess of one billion cycles.

The specimens for these fatigue experiments were prepared from eyebars salvaged from the wreckage of the Point Pleasant Bridge which appeared to have suffered least damage from the collapse and subsequent salvage operations. The form of the specimen used is shown in Figure 27. It will be noted that the original surfaces of the eyebar form the narrow edges of the specimen, and that these edges were left in their natural state. Inspection of a number of the fatigue fractures obtained in the experiment showed that these fractures invariably originated on this original bar face, and usually at the location of a small corrosion pit. Where large corrosion pits were responsible for the fracture, the number of cycles to failure was typically lower than the curve of best fit for all data. Control tests on tensile specimens cut from material from the same eyebars showed an average of 79,000 lbs./sq. in. yield strength and 116,000 lbs./sq. in. tensile strength, indicating that the material used in the fatigue experiments was typical of material examined by other laboratories and of eyebars Nos. 33 and 330.

b. The scale model tests were performed to resolve the question of the sequence of events in the separation of joint C13N. In test A, a brittle fracture was induced in the eyebar corresponding to prototype eyebar No. 330, the north bar connecting C11N and C13N. In test B, an attempt was made to cause the eyebar corresponding to prototype bar No. 33 to "walk off" the pin by canting the pin at an angle of approximately 0.5 degrees and imposing a loading regime patterned after the prototype deadload and liveload variations. Complete details on the two tests are covered in Reference 27. A general view of the test



N = Cycles to Failure

Figure 26 - Fatigue Properties of Eyebars 5 Steel (Based on Federal Highway Administration Tests)

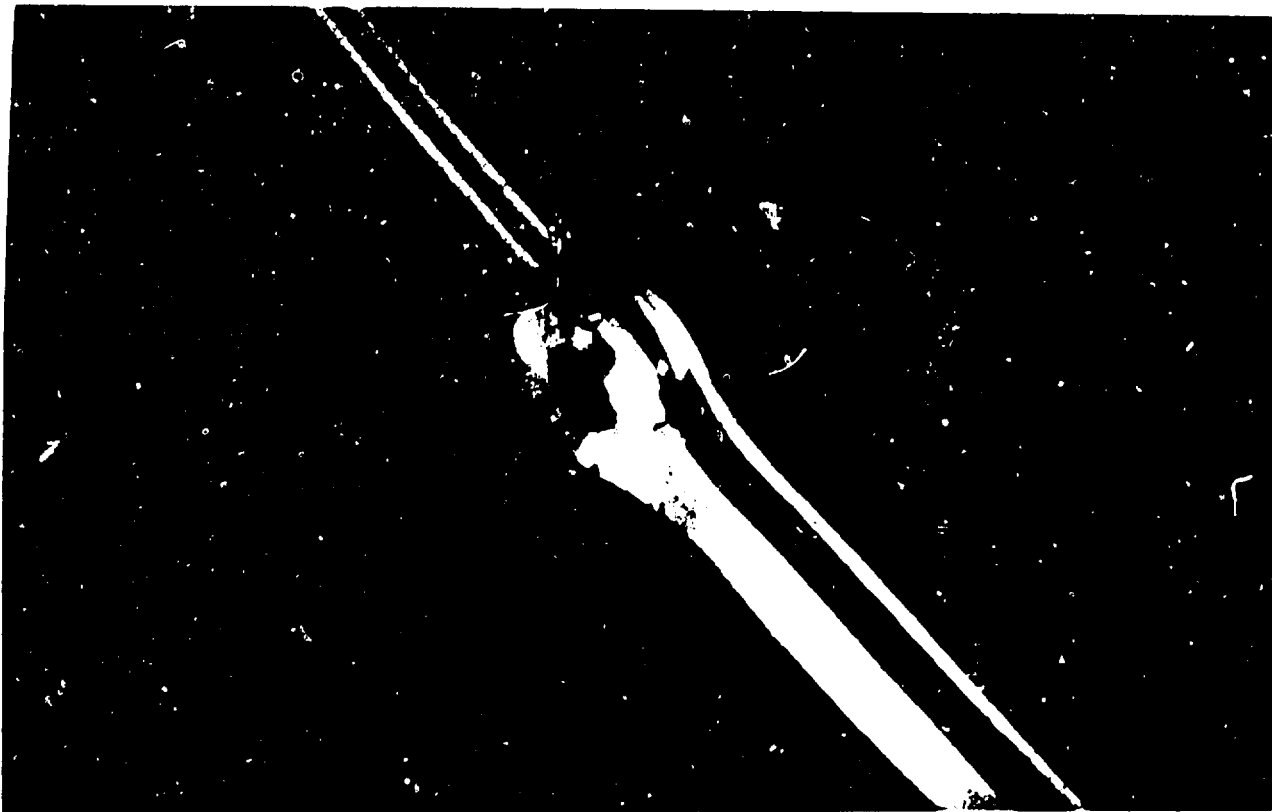
arrangement is given in Figure 28. The model consists of joints C15, C13, and C11 of the eyebar chain at 1/5 scale. Eyebars connecting joints C11 and C13 were machined from the midthickness and midwidth of eyebars salvaged from the wreckage. The other eyebars and fixtures in the model were machined from a modern high strength steel of similar strength properties. Careful attention was given to scaling the tolerances in the fabrication of the pinholes and pins to insure similarity of fit. Loading was applied by means of servo-hydraulic actuators. Strains were measured at selected locations around the pinhole in the eyebar corresponding to prototype No. 330 and on both faces of all eyebars in the model at midwidth and midlength.

In test A, a small deliberate defect was introduced at the edge of the pinhole in model eyebar No. 330 in the location at which the pre-existent crack was found in the prototype eyebar. This deliberate defect was produced by a sawcut through the thickness of the bar at this point 1/32 of an inch deep, with a kerf width of 0.007 inches. It was subsequently sharpened to a fine crack by loading with a fluctuating load of 20,000 lbs., and was grown to a length of 0.020 inches prior to loading to failure. The failure load was provided by automatic control systems which increased the load linearly from a base loading of approximately 1/3 of the expected failure load to the capacity of the system or a specified maximum in about three seconds. The actual failure load for the model was 104,290 lbs., corresponding to a nominal unit stress in the shank of the eyebars of 55,400 lbs./sq. in. Stresses at the root of the fatigue crack were above the yield strength of the material. Events during the failure were photographed with a motion picture camera operating at 1,000 frames/second. Figures 29a and 29b show two of the critical stages of the joint separation. In Figure 29a the brittle fracture in the lower limb of the C13 head of model eyebar No. 330 has just occurred. In Figure 29b, which is 1021 frames later, the ductile fracture in the upper limb of this eyebar has been completed and eyebar No. 33 has just slipped off the opposite end of the pin.

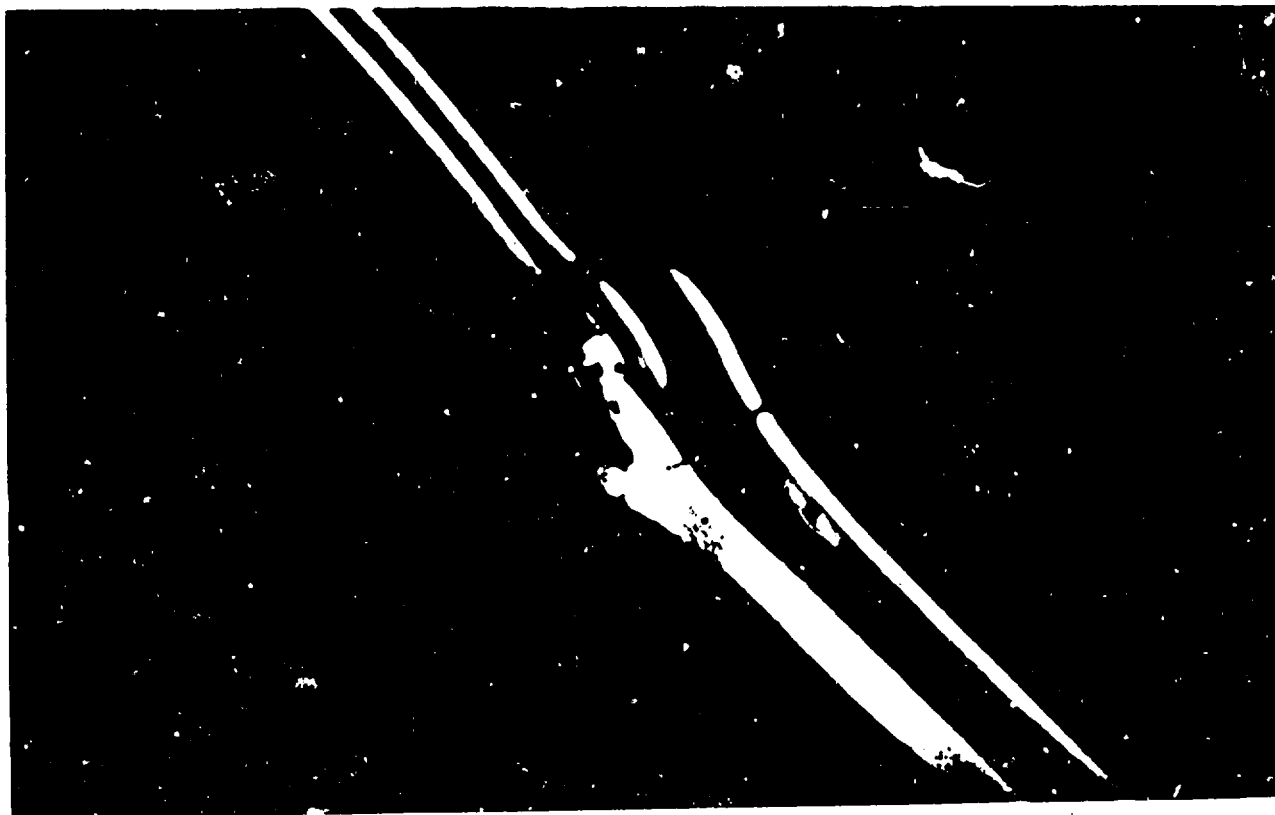
The deformation and the appearance of the fractures in the model parts bear a remarkable resemblance to those of the prototype parts salvaged from the wreckage. Figures 30a and 30b show the comparison between the model and prototype pieces which fractured from eyebar No. 330. The only distinguishable difference between these pieces is the direction which the fracture in the ductile side of the failure traveled after reaching approximately the midwidth of the section. It will be noted, however, that there is a crack in the prototype part which corresponds to the direction which the fracture followed in the model after reaching this point. Subsequent investigations of the mating piece of the model eyebar showed a similar crack extending in the initial direction of the prototype fracture. Model eyebar No. 33 also displayed a similar burr very much like that observed on prototype eyebar No. 33, although it was somewhat larger in relation to the thickness of the bar. Scratches on pinhole surfaces also resemble those of the prototype elements.



Figure 28
General View of Model Test
of Eyebar Chain Joint
(Federal Highway Admin. Photo)



**Figure 29a - Model Eyebar Test A at Instant of Brittle Fracture
in Lower Limb, Model Eyebar 330.**



**Figure 29b - Model Eyebar Test A at Instant of Final Separation
of Model Eyebar 330. (This photo is 1,021 frames
later than Figure 29a; approximately 1.021 seconds later.)
(Federal Highway Administration Photos)**



Figure 30a - Outboard Fragment of Eyebar 330, Test A Model
(Federal Highway Administration Photo)

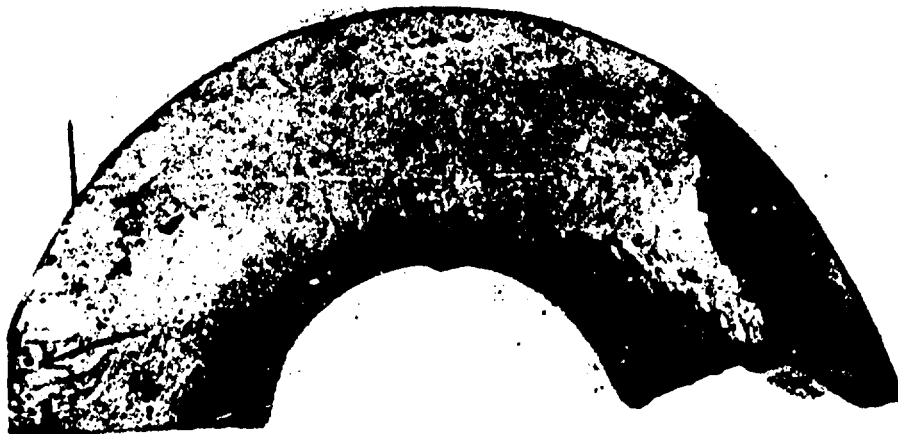


Figure 30b - Outboard Fragment of Eyebar 330, Prototype
(NBS Photo)

When an attempt was made to simulate the second type of joint separation it was found that eyebar No. 33 could not be forced to "walk" along the pin with the loading regime corresponding to that in the prototype. This was in spite of the 0.5 degree pin cant which had been introduced. The dead load was reduced to one-half its proper value, but the eyebar still did not walk. Only when the dead load was reduced to a very small value was any walking of eyebar No. 33 along the pin produced, and even then it was arrested before any portion of the eyebar hole extended out beyond the end of the pin. Further attempts to simulate the type B failure were, therefore, abandoned.

Some supplemental tests were conducted with a spare set of eyebars to measure stress concentration effects and residual stresses produced by application and release of loads. Strain gages were applied to the outside face of the bar representing eyebar No. 330 along a line through the center of the pinhole at right angles to the longitudinal axis of the bar. These gages were 0.08", 0.23", 0.38", 0.54", 0.88", and 1.56" from the edge of the hole on the lower limb, and 0.08", 0.81" and 1.55" from the edge of the hole on the upper limb, the last gage in each set being near the outer edge. The measured strains for a load which placed a nominal stress of 16,000 psi on the shank of the bar indicate (by extrapolation) a strain at the edge of the hole of 1600 microinches/inch for the upper limb and 1100 microinches/inch for the lower limb. These strains correspond to stresses of 46,500 psi and 31,900 psi, respectively, assuming a modulus of elasticity of 29×10^6 psi. The stress concentration factors are 2.90 and 2.00, with an average of 2.45. The difference between these factors in the upper and lower limb is believed to be due to a difference in the transverse bending effects, but this could not be confirmed because there were no strain gages on the inside face of the bar.

A loading producing a unit stress of 36,600 psi in the shank of the bar, corresponding to the dead load stress in eyebar No. 330, produced strains of 4000 microinches/inch and 2600 microinches/inch at the edge of the hole in the upper and lower limbs respectively. Both these strains are above the strains of 2410 microinches/inch at the yield strength of 70,000 psi appropriate to the material from which the model eyebar was made, since this was cut from the core or inner layers of a prototype eyebar. The initiation of plastic strain was also indicated by the change in the strain concentration factors, which became 3.17 and 2.06 for the upper and lower limb respectively. A further increase in load to that which produced a unit stress of 46,200 psi in the shank of the bar raised the unit strains at the edge of the hole to 6200 microinches/inch and 4300 microinches/inch for the upper and lower limbs respectively. After release of this load, the strain gage 0.08" from the edge of the hole in the lower limb indicated a residual compression of 22,000 psi. Values at the edge of the hole, estimated by extrapolation, were 37,000 psi for the lower limb and 59,000 psi for the upper limb.

5. Investigations of the Possibility of Fretting-Fatigue by Professor W. L. Starkey of Ohio State University

When the wreckage which fell upon the Ohio shore was disassembled, Professor W. L. Starkey, under contract with the Federal Highway Administration, was invited to examine freshly opened pin connections in the eyebar chain to look for possible signs of fretting-fatigue. Such a mechanism takes place when metal parts in contact under high loads undergo very small relative movements which tend to break the microscopic asperities of the metal surfaces. These broken pieces undergo corrosion, producing iron oxide, usually Fe_2O_3 , which is very hard and which occupies more space than the steel particle from which it came. The presence of these hard particles, under great pressure because of their own expansion and some small relative motion, produces a grinding action between the two steel surfaces. If the movements are large, the particles escape; but if small, they are trapped and result in the development of pits and then cracks perpendicular to the mating surfaces. Professor Starkey's inspection of the freshly opened joints, in his opinion, showed some evidence of such fretting action near the "90 degree" positions of the hole, where a plane perpendicular to the longitudinal axis of the bar through the center of the hole intersects the hole surface. Pin surfaces were scored and there was a reddish-brown oxide present (Reference 28). Professor Starkey also believed there was evidence of fretting on the fragment of eyebar No. 330 and on one of the pins.

In order to assess the possible importance of this observation, simulated fretting-fatigue studies were conducted on material taken from the C11 head of eyebar No. 330 and the shank just adjacent to this head. The specimens were prepared in the shops of the FHWA laboratories from blanks cut from the eyebar at the NBS laboratory. Before machining, the ends of the blanks were checked for hardness by the NBS laboratory. The material was found to be typical of other material in eyebar No. 330 in this respect, with hardness between Rockwell C 20 and 25. The 19 specimens themselves were tapered pins 4-1/4 inches long, 0.144 to 0.146 inches in diameter at the small end, 0.322 to 0.324 inches in diameter at the large end, with a Brown and Sharpe taper of 0.502 inches per foot. Collars of the same material were also prepared and each test was conducted on a combination pin-collar set. A contact pressure of 5000 psi was obtained by forcing the pin into the collar until a brittle lacquer on the outside surface showed initial cracking, then forcing the pin an additional fixed distance. The reliability of this technique was checked by dummy specimens in which the collars were strain gaged to measure hoop stress. The specimen combination was placed in a specially constructed rotating beam fatigue testing machine which held the collar so as to support the tapered pin as a loaded cantilever beam, thus causing minute longitudinal relative motions between the pin and collar as the whole assembly rotated. An additional 19 standard rotating beam fatigue specimens were also prepared and tested to get basic fatigue data.

The results of these investigations, reported in February 1969 (Reference 29), show that the material of the eyebars was susceptible to fretting-fatigue, and that such action could reduce the fatigue life at a given stress range, as compared to rotating beam specimens of equal initial surface finish, by about 17 percent, as indicated by the S-N curves of Figures 31a and 31b. On a basis of these data, Professor Starkey estimated that the material in the critical location at the edge of the pinhole would have a life expectancy of about 200,000 cycles, assuming nominal stresses in the shank of the eyebar to vary from 40,000 psi. to 50,000 psi. and considering the effects of stress concentration and fretting. However, he also pointed out that the presence of water in the joint would contribute further to the acceleration of fatigue damage by the mechanism of corrosion-fatigue, possibly reducing the life by as much as 50 percent, thus approaching the 73,000 cycles would correspond to five cycles per day for 40 years. Professor Starkey concluded his report with the observation that the static proof tests of the eyebars did not relate in any way to the ability of the bar to sustain the high local stresses in the head over a long period of time and under variations of load.

6. Static Tests of a Full-Scale Eyebar at Lehigh University

A tension test of a full scale eyebar removed from the wreckage on the Ohio shore was performed at Lehigh University in April of 1969 at the direction of the firm of Modjeski and Masters, consultants to the West Virginia Department of Highways. The eyebar used had a nominal length of 25 feet, 4 inches between pin hole centers, and was one of the elements in the north chain between panel points 0 and 1. The bar was loaded in the large universal testing machine by means of clevis connections. The pins were 10 inches in diameter but were fitted with sleeves made from one of the 11-1/2 inch diameter pins removed from the Point Pleasant Bridge wreckage. The length of the pin between the inside faces of the clevis yoke was 10-1/2 inches.

The eyebar was loaded in increments of 50,000 lbs. up to a load of 400,000 lbs., then by increments averaging about 100,000 lbs. until some definite yielding was observed at 1,775,000 lbs. At this time, load was reduced, then the extensometer was removed. Loading was then applied and raised until a fracture was produced in the shank of the bar near its midlength at a load of 2,450,000 lbs. This corresponds to a unit stress of 112,000 psi. in the shank of the bar. Analysis of the data from the test indicated that the actual yield load was 1,650,000 lbs., corresponding to a unit stress of 76,040 psi. in the shank. The percent of elongation measured over an 18 foot gage length was 8.54 percent. The reduction of area at the fracture was 30.55 percent.

Both faces of one head of this eyebar were extensively strain gaged to assess stress concentration factors under load. The stress concentration factors averaged 2.64 on the left side of the hole and

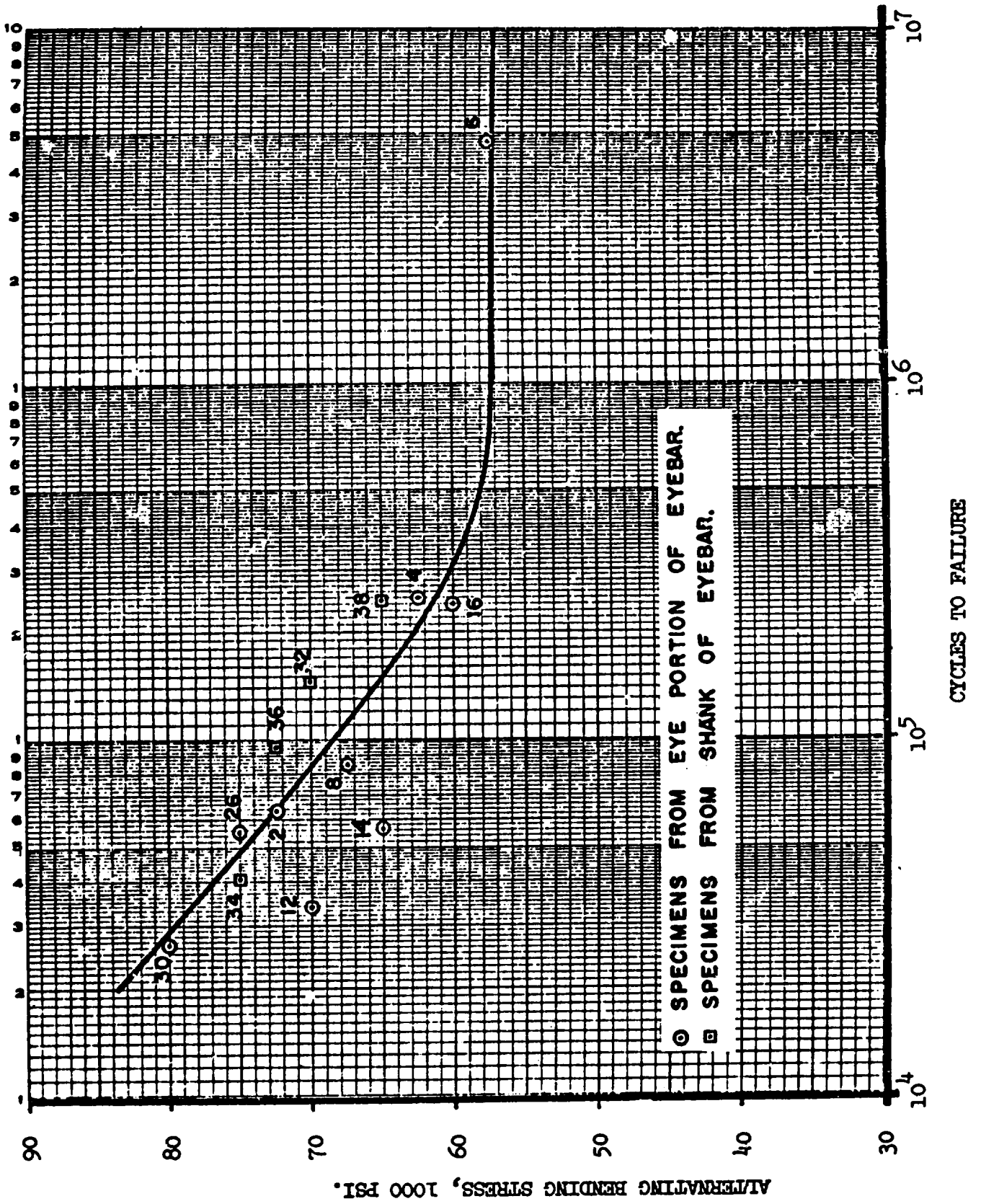


Figure 31a - Results of Rotating Beam Fatigue Specimens Tested by W. L. Starkey

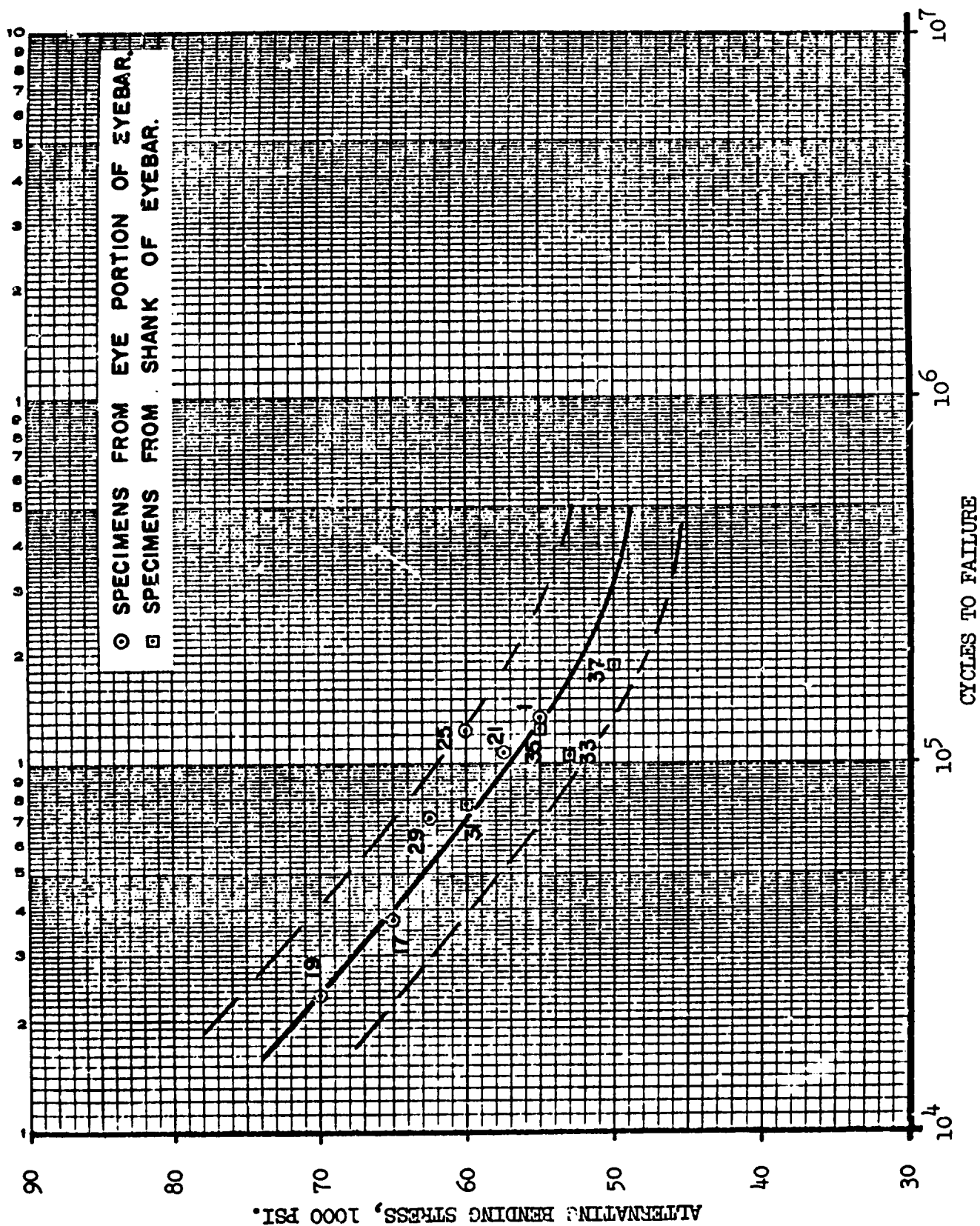


Figure 31b - Results of Fretting Fatigue Specimens Tested by W. L. Starkey

2.62 on the right side, measured at a total load of 600,000 lbs. in the bar. Considerable variation was noted at different load levels and at the opposite faces of the eyebar, indicating some departure from ideal geometry of pin fit. The range of stress concentration factors varied from a low of 2.33 to a high of 2.93, all based on the nominal stress in the shank of the eyebar.

D. STATUS OF BRIDGE INSPECTION AND MAINTENANCE

The Federal-Aid-Highway Act of 1968 required the Secretary of Transportation to establish standards to provide for the proper safety inspection of bridges in the Federal-Aid-Highway system, and to establish a program designed to train employees of the Federal government and of state governments to carry out such inspections.

In March 1968, the "Informational Guide for Inspection of Highway Bridges" (hereinafter referred to as the Guide), developed by the Bureau of Public Roads in cooperation with the American Association of State Highway Officials, was distributed to all states, to all counties, and to 2,400 selected cities in the United States. The Guide requested that an inventory of all highway bridges be furnished in two lists, for use in a two-part program for bridge inspection by each jurisdiction. The basic division is for bridges constructed prior to 1935 and those constructed later. Bridges of certain critical categories are included with those constructed before 1935. The Guide recommended that each authority undertake an immediate action program to inspect all bridges in the first category not later than November 1, 1968. With respect to the second category, it was recommended that those bridges be inspected not later than January 1970.

In January 1969, Committee 3, National Study to Assure Bridge Safety, of the President's Task Force on Bridge Safety, issued its report, including a compilation of bridge information submitted by states, counties, and certain cities. Information in that report showed that 34 states met the November 1, 1968, deadline, and that 43 states planned to meet the January 1970 deadline. The report also stated that 17 states had previously established bridge inspection programs, and that the other 34 states had initiated or revised their inspection programs. As of October 15, 1970, almost all states had completed inspection programs for all highway bridges under their jurisdiction.

In its interim report in October 1968, the Safety Board recommended that the Department of Transportation make available the product of the Federal-Aid-Highway Act of 1968 and the Guide to the owners of approximately 330,000 bridges and related structures not on the Federal-Aid-Highway System. Those bridges are owned, inspected, and maintained entirely by state, county, or city authorities, or by private concerns. As a result of the detailed inventory monitored by the Federal Highway Administration in 1968, the number of bridges not on the Federal-Aid System was revised upward to total approximately 398,000 of the overall total of 563,500 highway bridges in the United States.

The Committee 3 Report states that it is particularly noteworthy that 343,000 of the total of 373,000 bridges on county secondary roads, rural roads, and city streets were built prior to 1935. The burden of any corrective actions required will fall almost entirely on the state or local governments.

The Federal Highway Administration has disseminated or made available copies of the Guide to the owners of all highway bridges in the United States.

With respect to the bridge safety requirements of the Federal-Aid-Highway Act of 1968, the Department of Transportation has taken the following action:

1. Issued the Guide, which contains bridge inspection information, to the owners of most highway bridges.
2. Issued the Committee 3 Report in January 1969 containing a bridge inventory, status of state and local inspection programs, and the status of railroad, toll, and Federally owned bridge safety programs.
3. Issued a Bridge Inspector's Training Manual in July 1970.
4. Issued the "National Bridge Inspection Standards" as proposed rulemaking on September 24, 1970.
5. Conducted training symposiums in all of the nine Federal Highway Administration Regions for state bridge maintenance personnel and Federal employees assigned to bridge inspection responsibilities. In addition, the American Association of State Highway Officials issued in July 1970 its "Manual for Maintenance Inspection of Bridges."

The Safety Board has been advised by the Department of Transportation that the widest possible distribution will be made of the manuals, standards, and regulations developed in compliance with the Federal-Aid-Highway Act of 1968.

IV. ANALYSIS

This section will interpret the field and laboratory investigations with respect to the following questions:

(1) Did the structural steels of which the Point Pleasant Bridge was constructed meet the specification requirements, and was the particular steel in members found to contain critical fractures in any way unusual?

(2) What were the actual stress levels in critical locations as opposed to the conventional primary stress analysis based on the assumption that the structure is a pin connected, linear elastic system?

(3) Was the brittle fracture in eyebar No. 330 the event which initiated the collapse, and have all other possibilities been eliminated?

(4) Is the sequence of collapse based upon the assumption that eyebar No. 330 was the initial fracture consistent with the observed types of damage, the positions in which the wreckage fell, and the testimony of witnesses?

(5) What was the mechanism by which the crack in eyebar No. 330 grew to critical size?

(6) Were the assumptions made in the design of the bridge consistent with the best practice in 1926, and what are the implications of these assumptions in light of today's knowledge?

(7) What questions and observations does this investigation raise with respect to the safety of other bridges?

A. The Properties of the Steels in the Point Pleasant Bridge

Two types of steel were used in the main superstructure elements of the Point Pleasant Bridge. The trusses, hangers, towers, and floor system members were fabricated from the common carbon structural steel of that era, manufactured under A.S.T.M. specification A7-24. The eyebars of the chain were made from a special steel of the U. S. Steel Corporation which had been developed a few years earlier and had been used in the eyebars of one other bridge at Florianopolis, Brazil. This steel was basically a heat treated "1060" carbon steel. The eyebars were tested for compliance with the manufacturer's specification as approved by the designers.

1. A summary and comparison of the chemical compositions of the steel taken from portions of trusses, hangers and chain bent posts as obtained by the several laboratories is given in Table 2, along with the limits placed upon these elements in the ASTM specifications, where applicable. It is to be noted that the ASTM specifications for A7-24 steel placed only upper limits on the two elements sulfur and phosphorous, and that all samples tested by both NBS and U. S. Steel met this requirement.

2. The results of tension tests for the steel taken from trusses and chain bent posts are given in Table 3, together with the limiting values of those properties which were listed in the ASTM A7-24 specification, and some typical values obtained by others for steels rolled in the same era to these specifications. The following features of the ASTM A7-24 requirements should be noted:

(1) An acceptable range of tensile strengths was specified; namely, 55,000-65,000 psi.

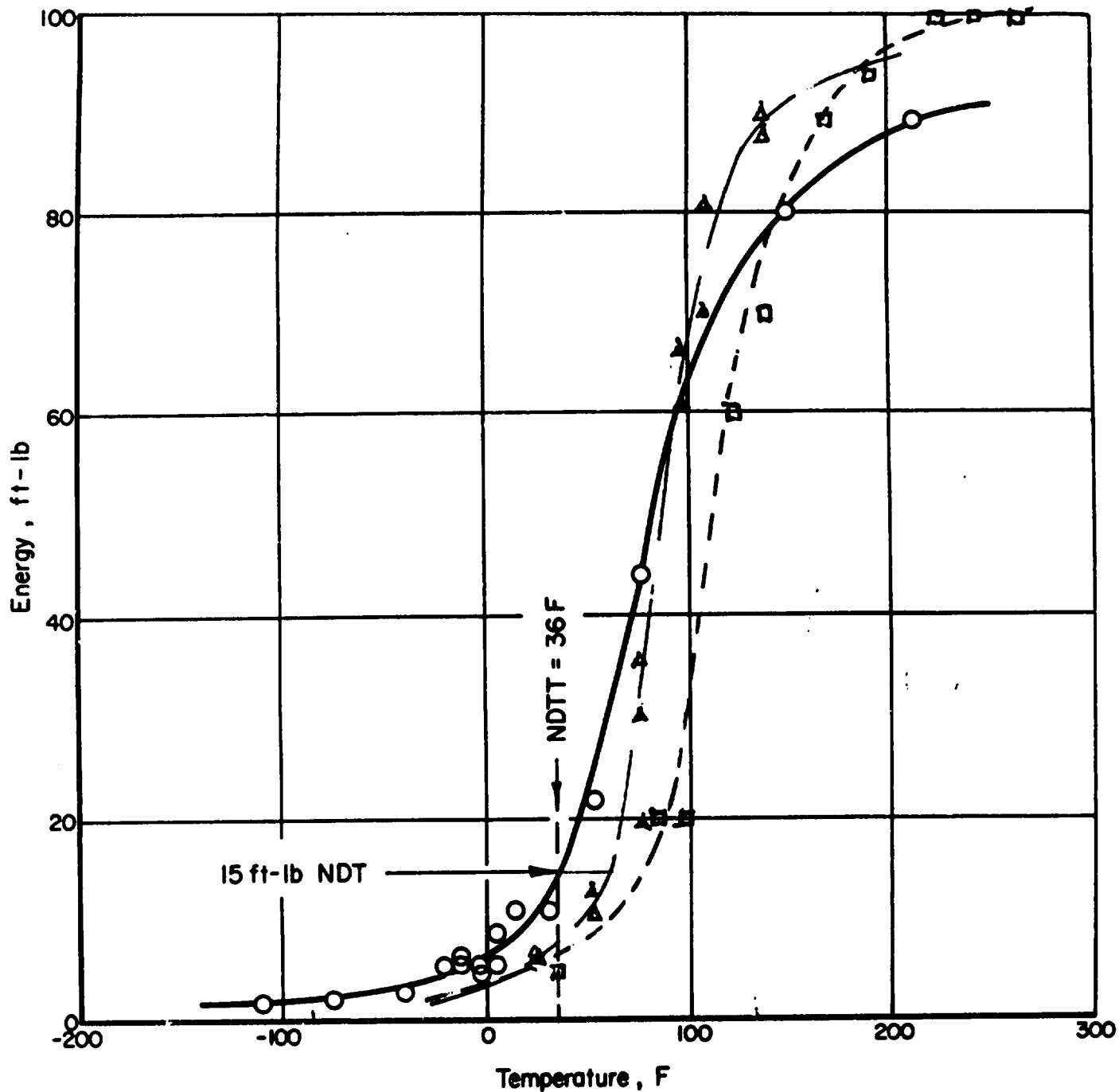
(2) The yield point, as determined by "drop of beam" technique was required to be at least 50 percent of the tensile strength, but not less than 30,000 psi.

(3) Percent elongation was specified to be not less than 22 percent measured over a 2" gage length.

It is apparent that the data from both laboratories is in good agreement and indicates that the steel is within the specification requirements.

No requirement for fracture toughness was included in the A7-24 specification, but three of the participating laboratories ran series of Charpy impact tests to obtain such data on this steel. These results showed appreciable variability, probably due to the different locations and thicknesses from which the samples were taken. A comparison of some of the transition temperature curves is given in Figure 32. The corresponding "15 foot pound transition temperatures" are shown in Table 4.

Regardless of the differences in the data from the various laboratories, it is apparent that the A7-24 steel in this structure, when at the 32°F. temperature which existed at the time of collapse, was operating below its transition temperature. At this temperature, all of the laboratories obtained Charpy values below 10 foot pounds, with an average of about 7 foot pounds. This would indicate that the steel at this temperature had low energy absorption capacity for loads applied at high strain rates compared to that exhibited at room temperature or above. The instrumented Charpy tests conducted by Battelle



- Battelle Mem. Inst., Chain bent post LO-UO, N (solid curve)
- Nat'l. Bur. Stds., Chain bent post, longitudinal, LO-UO, (dotted curve)
- △ U. S. Steel Lab., Chain bent post, longitudinal, L58-U58N (dashed curve)

Figure 32 - Comparison of Charpy Impact Data for A7-24 Type Steel from Chain Bent Posts Obtained by Participating Laboratories

showed that high strain rates in the presence of a mild notch could produce brittle fracture at temperatures of about 0 degrees Fahrenheit, as compared to -230 degrees Fahrenheit for the same specimen configuration with slow loading rates. In spite of this, the material showed reasonable resistance at slow load rates in the presence of a sharp crack at room temperature, as evidenced by the ductile fracture in the surface-flawed specimen tested at Battelle in an attempt to obtain the critical stress intensity factor. A repeat test of the same type at 0 degrees Fahrenheit showed essentially the same result.

3. Chemical analyses were conducted on samples of the eyebar steel by both the National Bureau of Standards and the U. S. Steel laboratories. A summary of the results is presented in Table 5. It will be seen that these results are in excellent agreement. The carbon content was appropriate to "1060 carbon steel," and the control of sulfur and phosphorous was adequate. The analysis of the C13 end of eyebar No. 330 shows no significant differences compared to other specimens, or compared to mill tests on sample eyebars made in 1927.

4. The tests to determine mechanical properties of the eyebar steel were extensive due to the fact that metallurgical examination showed that there was a considerable variation in structure between the surface and the interior of the eyebar. This material was heat treated by heating to 850°-900°C, quenching in water, and then heating at 600°-650°C for 2 hours. The nature of the heat treatment process produced these variations due to the difference in cooling rates and hardenability of the steel during quenching. The outer material cooled most rapidly and formed martensite, which became mixed with slack quenched products as the depth increased, and changed to primarily pearlite and ferrite in the interior. These observations were made by NBS, U. S. Steel, and the Battelle laboratories. These laboratories also noted that the outer layer of martensite was decarburized near the surface of the bar, usually for a depth of about 0.1 to 0.2 inches, but to less depth in the pinhole surfaces where material had been removed by machining. Some spheroidization of the carbides was noted by both NBS and Battelle. Many checks of hardness were made to maintain a careful control of the specimens used for mechanical tests, and care was taken to separate the specimens taken from the different layers. In the specimen plan established for checking the properties of the eyebar steel, arrangements were made to ship adjacent specimens to different laboratories in order to permit reliable comparisons (see Figure 5a through 5c).

A comparison of the principal mechanical properties as found by the various laboratories is given in Table 6. For the results of NBS and U. S. Steel laboratories, where the properties of the outer layers were measured separately from those of the inner layers, there is excellent agreement. It will also be noted that the estimated effective values of yield and tensile strength for the entire bar computed by

NBS by taking a weighted average (two parts outer layer plus one part inner layer divided by three) agree well with the FHWA specimens which extended through the full thickness. The data of NBS and U. S. Steel on the outer layers agree quite well with the results of the Battelle specimens from this layer for yield strength, but the Battelle specimens show somewhat lower tensile strength.

The data for steel taken from eyebar No. 330 shows no significant difference with respect to the data for other bars. The values for all bars tested, when weighted averages are taken to add properties for inner and outer layers, fall within the specification requirement as to ultimate strength (105,000 psi), and the elastic limit value of 75,000 psi was satisfied.

5. It is difficult to compare the data on fatigue characteristics of this material obtained by the Battelle laboratories in their crack growth studies with either that obtained by FHWA in tension tests to failure of full thickness specimens or to those obtained by Professor Starkey on small rotating beam specimens. The latter two sets of data may be compared with each other more readily by reinspection of Figure 26 (FHWA) and Figure 31a (Starkey). The FHWA tests, in general, covered a lower range of stress (closer to that which existed in the structure) with a maximum range of 66,000 psi and a minimum range of 42,000 psi. Starkey's specimens used full reversals of stress varying from 80,000 psi to 57,000 psi, so that there is actually no overlap with the FHWA work. At 60,000 psi stress range, the FHWA curve is displaced considerably to the left (toward shorter life), indicating a life of 160,000 cycles in comparison to the 240,000 cycles indicated by Starkey's data for a full alternating stress of 60,000 psi. This is probably due to the fact that Starkey's specimens were polished, whereas the FHWA specimens had the natural exterior surface of the eyebar on two faces. These natural surfaces contained corrosion pits and surface imperfections, so that displacement toward shorter life in a manner similar to Starkey's fretting specimens was to be expected (See Figure 31b). Below a stress range of 60,000 psi, Starkey assumed that an endurance limit existed for this material, since he obtained an extreme life of nearly five million cycles for one polished specimen at a range of 57,000 psi. The FHWA data and Starkey's data for pitted specimens do not exhibit such a tendency. If Starkey's data for the upper part of his stress range were extended in a straight line down to an alternating stress of 43,000 psi, the indicated life would be about 1,600,000 cycles. The FHWA specimens for a range of stress of 43,000 psi, indicate a life of about 1,400,000 cycles with some possibility of an endurance limit just below this level.

A comparison of the fatigue crack growth rates obtained by Battelle with the FHWA fatigue data is difficult for the following reasons:

(a) The Battelle surface flaw specimens were so constructed that the initial flaw was on the side cut from the interior of the eyebar, where the structure is pearlitic and softer than the surface martensite, whereas the FHWA cracks initiated in the surface material.

(b) No crack growth rates were measured in the FHWA tests.

B. Actual Stress Levels in Various Components of the Structure as Compared to Primary Stress Analysis

The stress analysis conducted by the designers of the Point Pleasant Bridge, as was customary in that era, was a linear elastic analysis for primary stresses only. The term "linear elastic" implies that all members were assumed to function in such a way that deformation is directly proportional to load. This condition is satisfied if all members remain within the elastic limit and if the deformations in the structure under load do not make significant changes in the equations of equilibrium. The first of these conditions is almost exactly satisfied, except for very minor localized deformations in the joints. The second condition is not satisfied in flexible suspension bridges due to the fact that small vertical displacements change the moment arm of the large forces in the eyebar chain to produce non-linear effects.

The term "analysis for primary stresses only" implies that all joints in the truss as well as the real pin connections in the chain, are free to rotate as load is applied, thus producing only tension or compression in the members of the chain and stiffening truss system. This assumption is commonly made in the analysis of trussed structures even today, although it is well known that the rigidity of the actual joints in the trusses and the friction in the pin connections of the eyebar chain prevent free rotation of the ends of the connecting elements, introducing bending stresses in addition to the primary tension or compression.

Finally, the original stress analysis included a 30 percent allowance in members of the floor system for dynamic stresses due to moving vehicles, but it assumed that the loadings used in the design of the stiffening trusses and chains were adequate to include any dynamic effects which might be present in these elements.

A number of studies were conducted in order to assess the significance of several refinements in the stress analysis as follows:

1. The field studies of the essentially identical bridge at St. Marys, West Virginia, were used to obtain information which, together with analytical studies, would permit an assessment of the

actual level of stress in certain critical members in the system. These studies were reported in Section III and are documented in Reference 16.

Secondary stresses due to bending moments introduced in elements by joint rigidity were checked at the connection of the chain bent post to the chain bent girder, at the lower end of a typical vertical truss member, in gusset plate U7N, and in the eyebar head at joint C11. The stresses associated with the measured strains at these locations due to joint rigidity are not believed to have a significant influence on the safety of the structure, since they were well within the 10-15 percent of primary stress which is assumed in setting the allowable stress levels for primary stress.

Significant dynamic bending stresses were found in the hanger system, but these were also a small fraction of the total dead load plus live load stress for which the hangers were designed. The eyebar chains also showed significant dynamic strain effects for a rapidly moving test vehicle as compared to the strains produced by the same vehicle moving at a slow crawl speed. These results, however, are for a single moving vehicle. With a large number of vehicles on the span, the ratio of resultant dynamic effects to the static live load stress would decrease, since it would not be likely that all of the dynamic vehicle effects would be in phase.

2. A second possibility with respect to dynamic stresses exists in the occasional excitation of the structure by wind. Prior to the public hearing of May 1968, computations were performed to determine the natural mode shapes and frequencies of the Point Pleasant Bridge. These were checked experimentally by mechanical excitation of the St. Marys Bridge and were found to be in reasonable agreement with the computations. The energy absorption capabilities of the structure while undergoing oscillations were also determined experimentally for each mode, and were found to be somewhat higher than usual for a suspension bridge of this span length. This was probably due to friction generated in the pin joints of the chain, which did show some movements when moving loads were in the center span. On a basis of this evidence, Mr. Vincent expressed his expert opinion at the hearings to the effect that aeroelastic excitation of the Point Pleasant Bridge for the condition existing at the site at the time of collapse was highly improbable. It was noted that the wind velocity at the time was only about six miles per hour and that the wind was blowing parallel to the longitudinal axis of the structure.

This did not preclude, however, the possibility that winds blowing transverse to the axis of the structure at various times during its history could have excited oscillations which might have contributed to a reduction of the life expectancy by producing cyclic loadings in the eyebar chain.

To check this possibility, additional computations were made to examine the susceptibility of this structure to aeroelastic excitation and to assess the magnitude of stresses in the eyebar chain which might have been produced during such oscillations, assuming that a suitable wind was available as an excitation agent. The conclusions reached in this analysis are to the effect that the relationships between the natural frequencies of the structure, the frequency of possible exciting aerodynamic forces, and the energy absorption characteristics of the structure make such excitations improbable, and that even if they were excited, the high energy absorptions would limit them to small amplitudes such that stress level in the eyebar chain would be insignificant.

This conclusion is consistent with history of the structure since there are no reports or records of any instances in which the structure had developed large amplitude oscillations of the type required, which would have probably resulted in at least the temporary closing of the structure. Persons using the bridge have commented to the effect that it "vibrated quite a lot." Witnesses who were on the structure at the time of its collapse were in some disagreement as to whether the vibrations then were any different from those they had felt previously. Among those who were commuters using the bridge on a daily basis, most indicated that the bridge always vibrated as much as they experienced it doing the day of the collapse. An analysis of the witnesses' testimony indicates that these were probably short period vibrations (0.1 to 0.3 seconds per cycle) and not of the longer periods associated with general excitation of the deck structure.

3. Some of the laboratory work was directed at obtaining a reliable estimate of the actual level of stress at the edge of the hole in a typical eyebar in a location where the fracture of eyebar No. 330 initiated on a plane through the center of the hole perpendicular to the axis of the bar. It was well known at the time of the design of the Point Pleasant Bridge that stress concentrations existed at such a location. Theoretical solutions from the theory of elasticity and experimental solutions by photoelastic techniques had been obtained (References 32, 33, and 34), in which it was found that the stress at this point would be about 2.77 times the nominal stress in the shank of the bar.

The actual stress level at the critical location would be different from that found by this solution for the following reasons:

(a) The geometry of the head assumed in the references cited was somewhat different from that of the Point Pleasant Bridge eyebars.

(b) The special geometry of the hole, which in the Point Pleasant Bridge eyebars was bored 0.005 inches larger than the nominal pin diameter on the bearing

side and 0.0312 inches (1/32) larger than the pin on the non-bearing side, with the center for this side of the hole offset 1/8 inch.

- (c) The sensitivity of the results to pin fit.
- (d) Pin deformation, especially bending, tending to make stresses on one face larger than the other.
- (e) Residual stresses in the eye prior to loading.
- (f) Stresses under load which exceeded the yield strength, when considered together with the presence of the residual stresses.

The work at the Battelle laboratory demonstrated that residual stresses due to the heat treatment process could be as much as 20,000 psi. In general, there were compressive stresses near the bar surfaces and tensile stresses in the interior. This pattern was altered at the pin-hole due to the removal of material after the heat treatment by the final boring of the hole, probably resulting in some relief of the surface compression.

Upon erection of the eyebar in the structure, the gradual application of dead load would raise the stresses across the section of the eye in a pattern very close to that indicated by the elastic theory, with the stress at the edge of the hole approximately 2.8 times the nominal. Since the nominal dead load stress in the shank of eyebar No. 330 is 36,000 psi, the unit stress at the edge of the hole exceeded the yield strength when between 70 and 90 percent of dead load had been applied, depending on the level of residual compression which existed at this location as a result of heat treatment. In any event, the first time the shank of the bar came up to full allowable stress of 50,000 psi due to the application of full live load with unfavorable temperature conditions, there must have been a considerable depth of material at the edge of the hole stressed to yielding. The stress level in this material would still probably be less than the yield strength of the material measured at 0.2% offset, since the strain pattern across the section could not have changed radically. Stresses on the order of 85,000 psi therefore appear likely, in spite of the fact that pin bending might have caused higher strains on one face than the other.

These general observations are confirmed by the FHWA tests on model eyebars cut from the interior layers of the actual eyebars, which would have been essentially free of residual stresses, and by the full scale bar tested at Lehigh University which contained residual stresses due to the relief of loads which had been on the bar in service. The FHWA model tests gave somewhat lower average stress concentration factors, since the material around the hole had not been strain hardened by prior

loading. In both cases, the experimentally determined stress concentration factors were high enough to indicate yielding at the edge of the hole under the action of dead load stress alone. It is therefore likely that the material at this location was cold worked by having been strained well in excess of the yield strain sometime during the life of the structure, with subsequent "elastic" behavior up to this level and an increased susceptibility to either stress-corrosion or corrosion fatigue. The work of the Battelle laboratory confirms that there were substantial differences in residual stress between the two faces of the bar.

The range of stress at the edge of the hole was probably governed by a stress concentration factor essentially that of the elastic case, 2.77. As discussed in Reference 2, the load history of the bridge is not sufficiently well established to compute the number of cycles of various percentages of full live load stress. The typical loading conditions to produce various percentages of full live load stress in the north chain are as follows:

- 100% Design stress - both lanes, maximum load full length of bridge
- 75% Design load - north lane, maximum load full length of bridge
- 50% Design load - both lanes, maximum load west end to center
- 37-1/2% Design load - north lane, maximum load west end to center
- 20% Design stress - north lane, mixed truck and auto loads, west end to center
- 40% Design stress - Actual load at time of collapse

The interim report (Reference 2) showed that the typical traffic in 1964 was a mixture containing only about 16 percent heavy vehicles. Significant percentages of full live load design stress could therefore have been produced only when traffic was halted and vehicles bunched to the extent that actual loadings approached the design load. Under these conditions, the dynamic effects of live load are probably negligible. It would appear reasonable to assume that the loading at the time of collapse was an upper bound to the peak live load which might have occurred on the structure not more than 20 and 30 times per day, or roughly 300,000 to 450,000 times during the 40 year life of the structure. The stress range would be about $2.77 \times 5,000$ psi. or 13,350 psi. An ordinary fatigue failure is therefore not likely, since a fatigue life of at least 1×10^9 cycles is indicated for such a stress range.

C. The Mechanism of Collapse as Determined by the Process of Elimination

Referring again to the logic diagram of Figure 3, it is apparent that all but one possible path in this diagram has been eliminated. The items not previously eliminated at the first level are (1) dynamic

effects of live load, (2) secondary stresses, and (3) fatigue from wind induced oscillations leading to fatigue. The extensive experiments on the St. Marys Bridge have shown the first two to be incapable of producing significant stresses in critical members. Computations of the critical flutter velocity and the lack of reports of wind-induced long period oscillations eliminated the latter.

1. On the superstructure defect path, all fractures in possible critical locations in the stiffening truss were found to have been caused by high strain rates, indicating that they occurred subsequent to the initiation of collapse. The fracture in L12N-L13N, although it contained evidence of a small pre-existent crack, also falls in this category and therefore could not have been the initial fracture.

There were three failures in the hanger system which might have been initiating fractures. The tearing out of the hanger connection at U13N has been established to have occurred during the collapse after some rotation of the hanger with respect to its proper vertical position. It is believed to have been pulled out when the hanger, still connected to the upper pin C13N and the pair of eyebars extending from C13N to the Ohio tower, acted with these eyebars as a linkage such that the fall of the north leg of the tower pulled them into a straight line and ripped the connection from the truss. The two hangers at panel points 17 and 19 of the north truss contained cleavage fractures. Paint was found on the fracture surface at the upper end of hanger 17N suggesting the possibility of a rather large pre-existent crack. The nature of the fracture and the deformations of the member, however, established that this fracture occurred under high strain rates and in conjunction with a twisting moment on the member. Therefore, this fracture must also be eliminated as possible "trigger" of the collapse. The fracture in hanger 19N was also found to be associated with bending and twisting.

This leads to the final path of the logic diagram on Figure 3. There are several types of evidence which eliminate the possibility that eyebar No. 33 slipped off or "walked off" the end of pin C13N. The metallurgical examination of the burr at the outboard edge of the hole in this eyebar failed to show any evidence of progressive terraces which are characteristic of "walking" action. The fracture of eyebar No. 330 shows little evidence of any bending moment perpendicular to the plane of the bar, indicating that the pin could not have been rotating with respect to this plane at the instant of failure. Finally, the results of the FHWA model test in which the brittle fracture in eyebar No. 330 was simulated produced fractures and permanent deformations remarkably similar to those found in prototype parts, whereas the attempt to simulate the "walk off" action, even with the pin canted at about one half degree, failed.

2. The laboratory work at NBS located and measured the pre-existent crack in eyebar No. 330. Fracture mechanics work at Battelle

established that the stress level at which this was a critical size flaw was just about equal to the yield strength for this material, and a combination of stress analysis, model tests at FHWA, and full scale eyebar tests at Lehigh University showed that such levels probably existed at this location at the time of collapse. The fracture of a full scale eye at Battelle at 32 degrees Fahrenheit established that a cleavage fracture with no ductile zone could be produced in this material with slow "static" loading rates.

3. The questions of what initiated the crack in this eyebar and what mechanism was dominant in its growth to critical size are not completely resolved. There is general agreement among members of the working group that the crack initiated in a small corrosion pit on the pinhole surface. Whether or not this pit formation was accelerated by mechanical fretting is uncertain. Although Professor Starkey found evidence of fretting on some pins and at some points on the hole surfaces of eyebar No. 330, a positive identification of fretting debris with the crack in the plane of fracture was not possible due to the exposure of the fracture before laboratory examination. The most favorable conditions for the development of fretting action were at the same location as the most favorable location for the development of either stress-corrosion or corrosion-fatigue; namely, at the point on the hole surface on a plane through the center of the hole normal to the axis of the bar, referred to as the "90 degree" position. This was favorable for fretting action because at this point the greatest relative displacement of eyebar hole and pin surface took place due to elastic strains, combined with a reasonably high bearing pressure. It was also favorable for stress corrosion because of the geometry of the hole, which provided a tapered capillary space at this point which could collect and concentrate contaminants dissolved in rain water. It is believed that fretting was a factor in the initiation of these pits.

The mechanism of growth of the pits to cracks of critical size was first thought to have been clearly identified as a stress-corrosion action on a basis of the early NBS work reported in February 1969 (Reference 17), although Professor Starkey had suggested corrosion-fatigue in his report of February 28, 1969 (Reference 29), possibly associated with further fretting action. Subsequent work at Battelle supported the assumption of stress-corrosion, but the U. S. Steel laboratory found evidence of transgranular fracture, indicating that corrosion fatigue may have been involved.

To resolve these questions, a task group was appointed by the Chairman to open a fresh crack in a piece taken from eyebar C9-C11 (south bar of north chain) without the use of cutting oils to avoid the possibility of contamination. The laboratory work of that task group, which included representatives of NBS, U. S. Steel, Battelle, and Modjeski

and Masters, has been described in Section III C of this report. The final paragraph of that report reads as follows:

"In summary, it was agreed that the small oxide-covered crack which led to the rapid fracture of eyebar No. 330, similar nearby secondary cracks, and similar cracks in other eyebars were produced by a corrosion process. There is supporting evidence that either stress-corrosion cracking or corrosion-fatigue could be this corrosion process although the limited data obtained to date are not sufficient to draw a definite conclusion. In view of the fact that no further eyebars with cracks are available, fracture studies to more clearly establish the mechanism of the crack propagation are not possible."

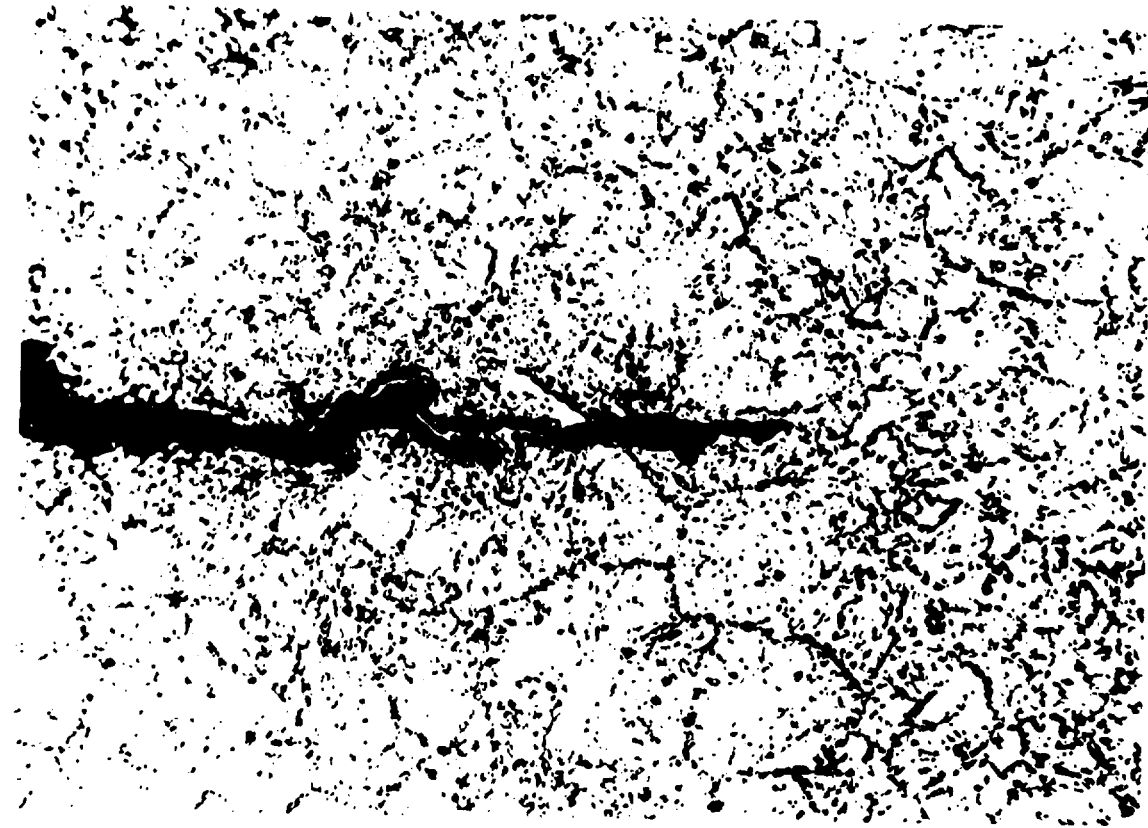
Subsequent to this report, the U. S. Steel laboratory used a special picric acid etch to bring out the grain boundaries more clearly in a portion of the fracture in eyebar No. 330. An example of the result is shown in Figure 33a and 33b. In the right photograph, the appearance of the specimen after etch is shown. In the left photograph, the grain boundaries detected by the investigator have been marked on an overlay. This crack is clearly transgranular rather than intergranular, favoring the mechanism of corrosion-fatigue.

The evidence supporting stress corrosion cracking is as follows:

- (a) Continuous high stress intensity at or about the yield strength of the material.
- (b) Probable concentration of corrosive agents such as hydrogen sulfide or salts in a confined space, as indicated by the presence of the elements sulfur and chlorine on the crack face, particularly near the mouth of the crack.
- (c) Some intergranular cracking is present.
- (d) The material showed susceptibility to H₂S stress-corrosion cracking under concentrated, controlled conditions at stress levels as low as 15,000 psi.
- (e) Range of stress (live load) was small, probably about 15,000 psi.

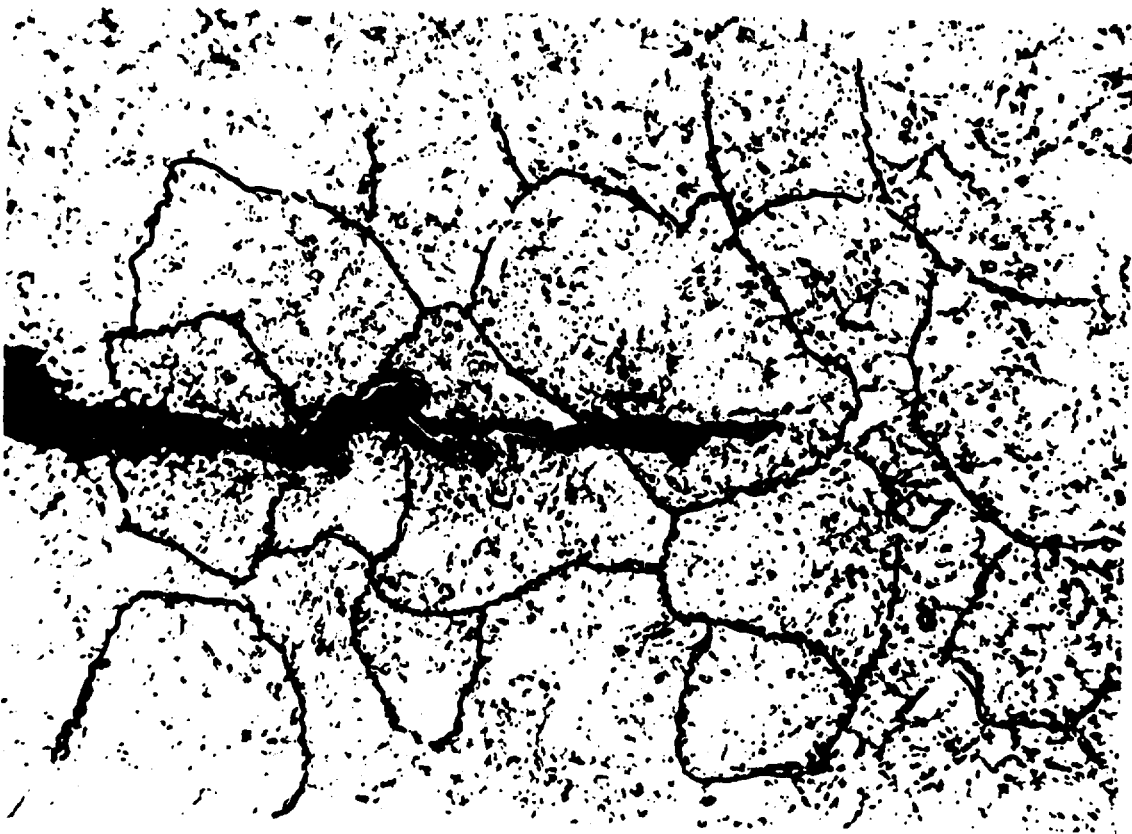
The evidence supporting corrosion-fatigue is as follows:

- (a) Some cracks in eyebar No. 330 are definitely transgranular.



(b) Crack Appearance after Extended Picral Etch
(x 500)

NOT REPRODUCIBLE



(a) Probable Grain Boundary Lines Superimposed

Figure 33 - Relationship of Crack Propagation of Secondary Crack in Eyebar No. 330 to Grain Boundaries
(U. S. Steel Photo)

(b) The material was cold worked near the hole surface, increasing its susceptibility to corrosion-fatigue, probably to a greater degree than its susceptibility to stress-corrosion cracking.

(c) Contaminant concentrations in the field were low relative to those used in the laboratory to establish stress-corrosion susceptibility.

(d) A variable stress level was present, although it was small.

If corrosion fatigue was responsible, it is logical to ask why such cracks did not develop first in the eyebars between U0 and U7 of the side span, where the range of live load stress contributing to fatigue was much larger and the dead load stress related to stress-corrosion cracking was smaller. The influence lines (see Figure 34) for these members have negative segments for loads within the side span, due to their participation in the stiffening truss. The member loads are shown in Table 7.

It is also interesting to examine the probable frequency with which these maximum design live load stress ranges will be reached. As noted previously, the probability of 100 percent of design stress is quite remote. The live load at the time of collapse in eyebar C11-C13 was only 237.3 kips, or about 41 percent of design live load. This was due to a load extending from the west end of the structure to just beyond the center of the main span. The load in bar U5-U7 at the instant of collapse was only 142.5 kips, or about 17 percent of full live load tension. For this bar, however, the range of stress was greater than in C11-C13, since while the loads were accumulating only on the Ohio side span, the stress was of opposite sign. The total load in the side span was 125.1 kips or 330 lbs/ft., which is 47 percent of design live load and would have produced a compressive load in U5-U7 of about 200 kips. Thus, the load range for this bar was 342 kips.

Loadings which did not extend very far into the center span produced even greater differences in stress range. Moreover, trains of vehicles which move continuously across the structure while maintaining a total length about equal to the length of the main span would produce approximately 85 percent of maximum range (495 kips) in C11-C13, but 96 percent of maximum range (120 kips) in U5-U7. Thus it would appear that the general range of stress in U5-U7 would be about twice that of C11-C13 for any given probability of occurrence. This would reduce the fatigue life by a factor of ten or more, or in other words, make the occurrence of a fatigue fracture in U5-U7 ten times more probable.

It therefore appears that the stress-corrosion was the dominant mechanism, in spite of the fact that there is evidence

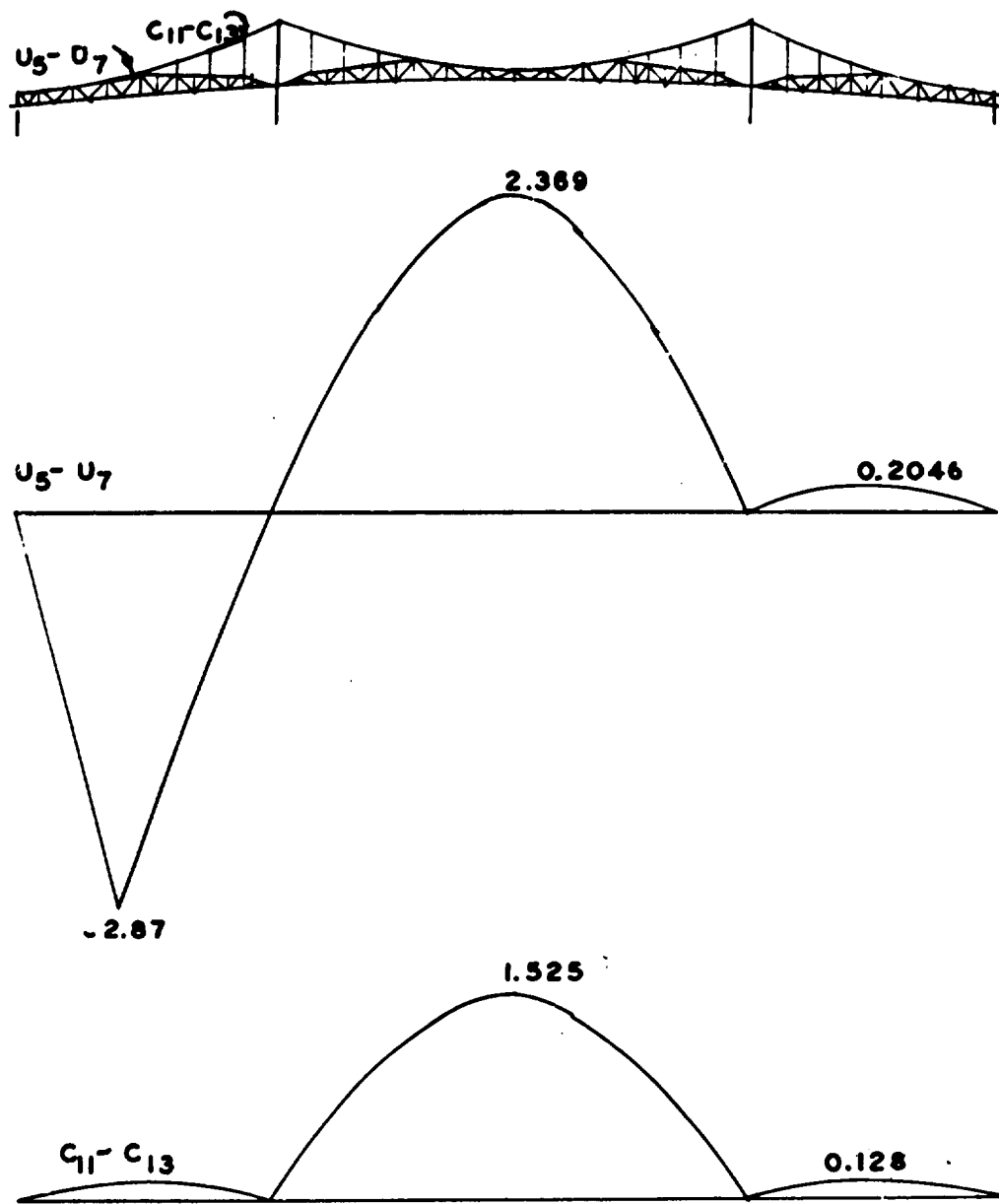


Fig. 34 INFLUENCE LINES FOR $U_5 - U_7$, $C_{11} - C_{13}$

of transgranular crack propagation. It is possible that the minor fatigue action upset the normal preference of the stress-corrosion mechanism for attack along the grain boundaries by creating localized slip planes also susceptible to such attack, but this might be considered a speculation.

D. Compatibility of Established Mechanism of Failure with Observed Facts and Witness Testimony

The arguments in favor of considering the fracture in eyebar No. 330 as the event which initiated the collapse have thus far been derived from fractographic and metallurgical evidence, together with analytical determination of stress levels and conditions at the time of collapse. Other fractures have been eliminated as initiating events by similar evidence. There remains the question as to whether a failure sequence beginning with the fracture in eyebar No. 330 is compatible with facts derived from the general nature of damage observed in the wreckage, the position in which the wreckage fell, and the observations of witnesses.

This section describes what is believed to be the sequence of events during the collapse of the Point Pleasant Bridge, cites those observed facts which support this sequence, and interprets the statements of witnesses in relation to this assumed sequence. The detailed studies of distortions, the directions of loadings which appear to have caused these distortions, the fracture of various connections and the scars and other impact damage in the structure upon which this analysis is based come from many sources, but most extensively from the reports of R. A. Hechtman and Associates (References 8 through 14) and the field notes on the examination of wreckage prepared by the J. E. Greiner Company (Reference 35).

1. It is helpful first to consider the deformations which existed in the structure just prior to collapse, as developed in the computer analysis prepared by the Bridge Design Review and History working group. Using the data on distortions in the structures produced by live load at the time of the collapse and a temperature change for a 36°F. drop from 68°F., the following conditions appear to have existed. The Ohio tower was essentially vertical due to the fact that the westward movement of its top produced by thermal contraction of the chain was almost exactly compensated for by the eastward movement produced by the live loading. The West Virginia tower was displaced slightly to the west at its top, probably on the order of one or two inches. The Ohio side span was deflected vertically at panel point 7 about 0.11" (0.71" downward due to loading and 0.60" upward due to temperature). This distortion of the side span produced a slight westward movement of the pin at panel point 0 in the slot of the chain bent post. Computations show a westward movement of 0.53" due to loading, but because of a 0.34" eastward movement as a result of the temperature drop, the net movement is

only 0.19" to the west. This leaves a clearance of 0.81" at this point. The main span was deflected vertically downward approximately 2.93" at midspan. The West Virginia side span was deflected vertically upwards. The amount of this deflection was not given by the output of the computer analysis but is estimated to have been on the order of three inches. Similar consideration of the combined effects of loading and temperature shows that there was a clearance of 5.49" in the expansion joint at the Ohio tower and 12.24" in the expansion joint at the West Virginia tower.

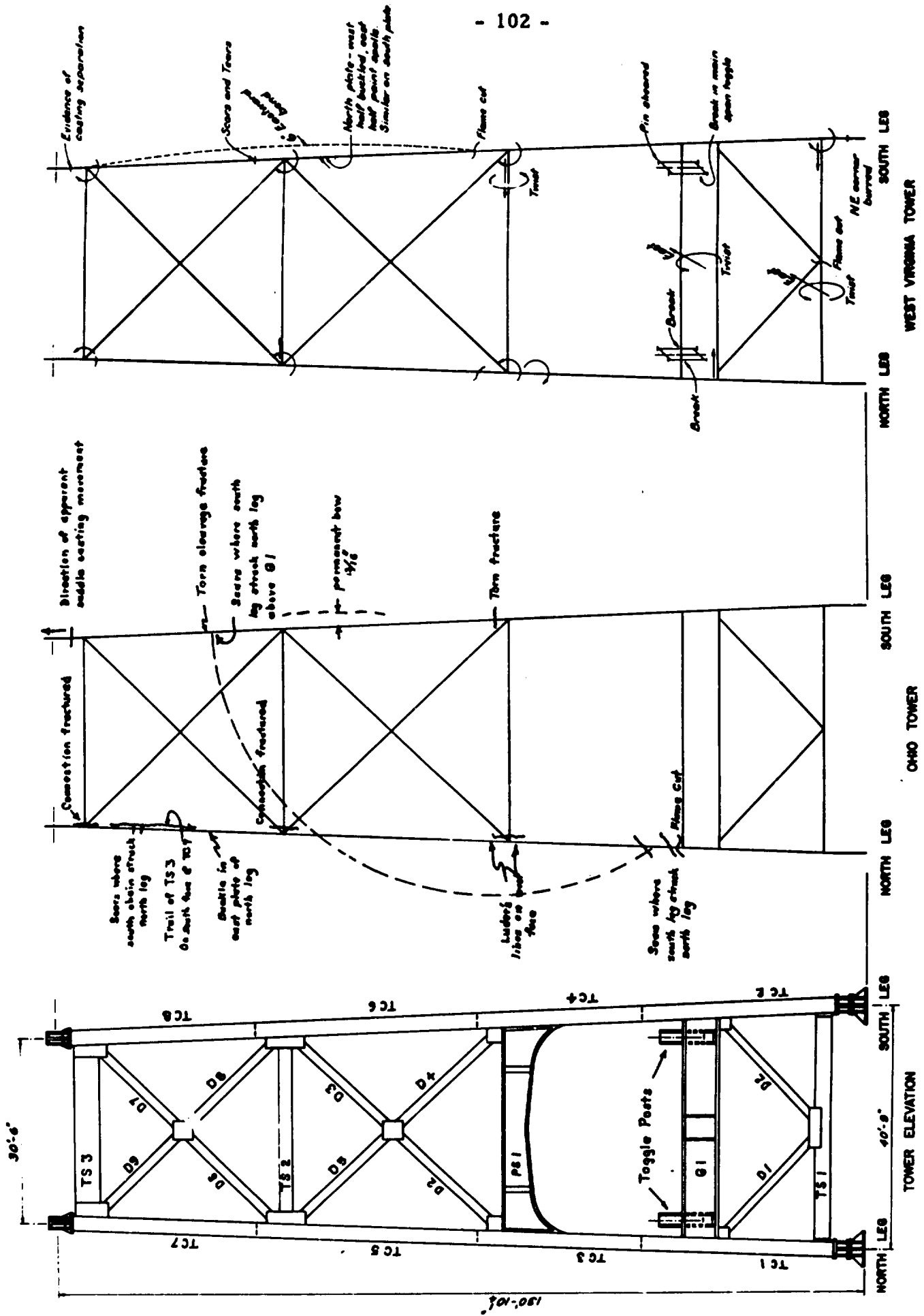
2. The discussion of the sequence of collapse will be arbitrarily divided into seven steps. Time will be reckoned from the instant at which the brittle fracture in the lower limb of the C13N head of eyebar No. 330 occurred. The estimates of time are based on the computed rate of free fall for those portions of the structure which lost essentially all support after the final separation of eyebar No. 330. Evidence found on tower wreckage is summarized in Fig. 35, and damage to trusses is documented in Appendix A.

Step 1

Time = 1.0 seconds

Results of the scale model tests of the eyebar joint at C13 indicated that this joint did not become unstable at the instant when the lower limb of eyebar No. 330 fractured. Some short period of time, on the order of a second, was required to complete the rupture of eyebar No. 330 through the upper limb of its C13 head. This process required 1.2 seconds in the model test. Similitude relationships indicate a somewhat longer time at prototype scale, but this analysis assumes that the prototype time was also about one second, in view of the fact that the prototype chain probably maintained its full load to a greater degree than did the model. During this one second of time, there was an extension of about three inches in the effective length of the chain. It is assumed that the north leg of the Ohio tower moved slightly to the east, permitting one third of this extension to be accommodated in the main span and two thirds of it to be accommodated in the Ohio side span. The resulting vertical deflections, computed from chain length/sag relationships, indicate a vertical deflection of about two inches in the center of the main span and six inches in the center of the side span.

This deflection in the north truss of the Ohio side span had two immediate consequences. First of all, it instituted a rapid increase in the tension stress of the lower chord members of the north truss, which momentarily carried a portion of the load by simple truss action between panel points 0 and 15. It was able to do so at this stage, since there was still enough tension in the upper chord members from U1N to U7N to compensate for tendencier to compression in these members. Secondly, this deflection was large enough to result in a



FRACTURES AND OTHER STRUCTURAL DAMAGE ON TOWERS

FIGURE 38

TOWER ELEVATION

NORTH LEG

SOUTH LEG

NORTH LEG

SOUTH LEG

NORTH LEG

SOUTH LEG

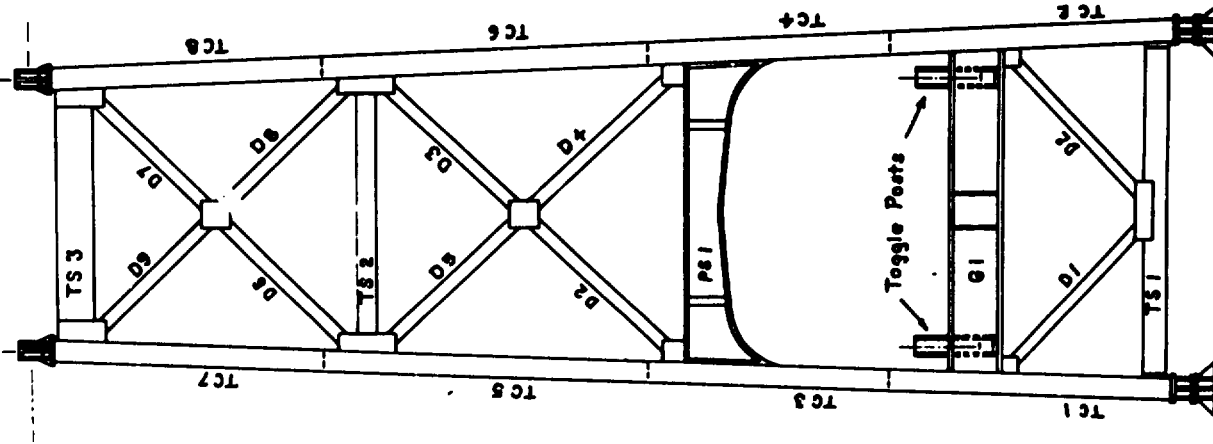
WEST VIRGINIA TOWER

OHIO TOWER

30'-6"

150'-10 1/2"

40'-9"



westerly movement of several inches of the pin at panel point 0. Since this is more movement than the clearance in the slotted hole can accommodate, there was an immediate abnormal loading of the chain bent post, producing a maximum bending moment on the reduced net section through the pin. Computations of the strength of this post under such loading conditions indicate that extreme fibers of this cross section would reach yield strength stress levels for a loading of about 20 kips on the pin. The actual separation of the post at this cross section shows very little evidence of yield except in the west splice plate and in the splice angles connected to the northeast corner. It is therefore believed that the rapid loading produced the observed cleavage fractures in some of the thicker sections such as the west channel flanges of this post at this early stage of the collapse. However, the post probably remained attached at this stage by at least the west splice plate and the east splice angles, because the loading was displacement limited.

Step 2

Time = 1.2 seconds

At this point in time, the final fracture of the upper limb of the C13 eye of eyebar No. 330 permitted the pin at C13N to rotate about a vertical axis, so that eyebar No. 33 slid off the south end of this pin. A burr on the northeast side of the pin hole in this eyebar was formed in the process (see Figure 9). In the model test, the eyebar corresponding to No. 33 was given a considerable impulse to the south at its C13 end as a result of this action, but did not come loose at joint C11. In the prototype structure, the retaining bolt at C11N was apparently broken, since the eyebar came completely free and was found on the ground with its C11N eye at about panel point 9 and its C13N eye just below the water edge. The elastic energy released in the failure of joint C13N could impart sufficient velocity to this eyebar to account for its westward movement, but it remains a mystery as to how it reached its final position in such a manner that portions of the deck system, one vehicle, and the north truss lay on top of it. It is possible that it fell in such a way that it punctured through the deck and then slid to its final position.

The separation of joint C13N completely released the tension in the eyebar chain as far as joint U7N. Beyond this point, the relief of the tension was not complete, since the shortening of the eyebars caused them to pick up load as this shortening produced distortions and westward movement of the truss. The total elastic energy available in the eyebar chain from point U7N to the anchorage was about one half million foot pounds. If this had all been transferred into kinetic energy of motion of the side span, it would have produced a velocity of approximately 6 foot per second. However, neither the north truss nor the floor system was free to move without restraint, since they were attached to the south truss. The wind bracing system and deck slab insured that the two trusses moved very nearly the

same amount, differing only by the elastic distortions in these systems. The south truss, in turn, was restrained by the south chain, which at this stage of the collapse could still resist westward movement much as an elastic spring, although such westward displacements were resisted primarily by the distortion of the shape of the chain in the side and center spans.

The sequence of events is believed to have been approximately as follows. The sudden release of tension in the north eyebar chain, traveling as a rarefaction wave at acoustic velocity (about 14000 ft./sec.) from C11N through U7N, the top of the chain bent post, and then to the anchorage, reached that point in about 0.024 seconds. The first part of the path, from C11N to U7N, offered essentially no restraint. The possibility that the chain pulled free of gusset plate U7N as the wave reached that point was rejected in that there is clear evidence that the eyebars from U7 to C9 remained attached long enough to indent the stay plate on U7-U8 (see Reference 35, installment 1, page 2, 51, 57 and Reference 5, Exhibit 4J-3).

As the wave traveled from U7N to U5N, the eyebar pair shortened about one inch, which resulted in the distortion of the truss in the triangle U5N-L6N-U7N, with high secondary bending stresses and possible partial fractures at L6N. This process was repeated for the pairs of eyebars U5N-U3N, U3N-U1N and U0N-U1N, with resulting bending distortions and downward deflection of L4N and L2N and pin rotation at L0N. The rate of progression of the wave was slower than the acoustic velocity and the relief of tension incomplete because of elastic restraints developed and momentum transferred to the truss. The shortening of the eyebars between the top of the chain bent post and the anchorage could not be accommodated by mere distortion of the truss, but only by a movement of the entire truss and deck system to the west. The forces required to initiate this motion resulted in a slower rate of progression of the rarefaction wave, and the establishment of some tension in elements from U0 to U7. The chain bent post above the pin at L0 was held essentially vertical by its attachment to the diagonal L0-U1 and the eyebar U0-U1, so that the westward movement of L0 resulted in severe bending of the post at this point, with westward tilting of the chain bent cross frame girder below the deck. Both north and south chain bent posts were involved in this motion, due to the lateral bracing and floor system. A motion of about 2 1/2" at the top of the chain bent post was sufficient to relieve the tension in the eyebar chain extending from this point to the anchorage, but the motion continued as a result of the momentum transferred to the whole side span system. Assuming that 50 percent of the original energy in the north chain were so transferred, it was moving westward at about four feet per second. This motion continued until restrained by the buildup of tension in the south chain east of the chain bent post, and the collision of the chain bent frame with the approach span girders.

This collision on the south end of the chain bent frame involved contact between the cross frame girder and the outstanding leg of the easternmost stiffener on the south face of the south approach girder. The south chain bent post did not collide with the approach deck slab, but merely scrapped along its edge. At the north end of the frame, however, the action was somewhat different. Here the chain bent cross frame girder collided with the stiffener on the approach girder, but the chain bent post also collided with the edge of the approach deck slab with considerable force. The fracture of the north chain bent post was apparently completed at this instant, except for the northeast splice angle. In the extreme position of the post, the top was about 18" west of its normal position, allowing the eyebars west of this point to drop at an abnormal angle, indenting the cover plate on the west side of the post at the top (see Reference 35, installment 1, p. 27).

At the same time that these events were in progress, the portion of the north truss east of panel point 7 was in essentially free fall, restrained only by the limited ability of this truss to carry loads by simple span action between L0 and L15. It is assumed that enough tension remained in the elements from U1N to U7N to counteract tendencies to compression. There was an initial rapid buildup of tension in the lower chord as a result of this action, terminated by the shearing of the toggle link at L15N due to the westward movement of the truss. Some of the cleavage fractures observed in this lower chord may have occurred at this time.

At the same time the main span of the north truss continued to fall. In this span, a secondary mechanism for supporting loads by simple span action of the truss between towers was not available, since the upper chord in the middle portion of the span consisted of the eyebar chain. Without the original chain tension, these eyebars could take very little load in compression before they began to buckle. The main span north truss therefore dropped in essentially free fall, inhibited only by the slight restraint offered by these eyebars prior to buckling, and the inertia forces associated with the eastward inclination of the north leg of the Ohio tower. The latter has been computed and was found to be very small compared to initial chain tension.

Step 3

Time = 1.5 seconds

The north truss of the Ohio side span began a general disintegration east of panel point 8. The north chain bent post was fractured but still holding by the splice angle at its northeast corner. The portion of the deck between panel points 9 and 15 was in free fall. The western half of this span of the north truss was now beginning to move eastward, due to the restoring forces exerted by the south chain.

At about this time (see Reference 14), the bracing attached to the top of the north leg of the Ohio tower separated. The combined effect of the northward and eastward loadings of the south leg due to the eastward movement of the north leg (about two feet at the top at this time), and the now unbraced eccentric load exerted by the south chain on the top of this leg, produced a bending and a fracture of the south leg just above the portal bracing. This initiated a northerly movement of the south chain, the fractured upper portion of the leg pivoting just above the portal bracing.

The north side of the main span continued in essentially free fall, but the portions east of about panel point 30 now developed a secondary mechanism of load support. A deflection of approximately five feet at panel point 30 eliminated the clearance which existed at the expansion joint in the deck at the West Virginia tower. This permitted the north truss and the chain connected from panel point 35 to the top of the West Virginia tower to act as a "tied cantilever." As displacements continued, this cantilever action gradually picked up load, and at the same time lifted the north edge of the West Virginia side span because of the restoration of tension in the chain and then its increase beyond the normal value due to the dynamic application of load. The computed static tension in the chain at the top of the tower for such action is 1909 kips, which is very close to the normal tension at this point (dead load plus collapse live load).

Step 4

Time = 1.7 seconds

At about this time, the top of the south leg of the Ohio tower was some 15 feet north of its original position but had undergone only very small eastward movement. This action exerted a northward component on all elements in the Ohio side span and the main span through the south truss. It also produced a bending moment around the east-west axis in the south Ohio chain bent post at a relatively slow rate of loading.

Meanwhile, the north truss continued to fall but was pushed to the north because of lateral loadings transmitted to it through the floor system which was still attached to the south truss. The estimated deflections of the north truss at this step are as follows:

Panel Point 7.....	8 ft., downward
Portions between Panel Points 8 and 13.....	10-12 ft., downward
Main Span Portions West of Panel Point 30.....	8 ft., downward
West Virginia Side Span Panel Point 51.....	3 ft., upward

Step 5

Time = 2.0 seconds

At this time (1.0 seconds since the final separation of the chain at C13N) the center of the main span had fallen approximately 16 feet at

its north edge. The top of the north leg of the Ohio tower was about eight feet east of its normal position. The north truss was generally disintegrated between panel points 21 and 30. The portion of the north truss between panel points 15 and 20 had begun to tear loose from the chain due to the loss of support at the toggle link at panel point 15. The portion of the truss east of panel point 30 was momentarily restrained by its cantilever action from the West Virginia tower and was deflected downward at its west end by perhaps five or six feet.

The top of the south leg of the Ohio tower was now about 30 feet north of its normal position. The south chain was still intact and was exerting strong northward components on the south Ohio chain bent post, the south truss in the Ohio side span and the main span, and the south leg of the West Virginia tower. The effect of this latter component produced a permanent bend in the upper portion of the south leg of the West Virginia tower, the axis of the bending moment observed in the permanent distortion above the portal bracing being approximately along a northeast/southwest line. The northward component exerted at the upper chord level of the central portion of the south truss in the main span caused further rotation of the deck system in this portion in a counterclockwise direction (viewed from the west).

The northerly edge of the West Virginia side span was still being pulled upward by the increase in cantilever moment exerted by the north truss in the main span. The south edge was beginning to fall due to the reduction in eastwest tension in the south chain.

In the Ohio side span, the vertical deflection at panel point 7 of the north truss had reached about 16 feet. The combination of the eastward motion of the west half of the span and the rotation about L0 due to the vertical deflection has again tightened the portion of the north chain between the north chain bent post and the anchorage. It is believed that very little cantilever moment was achieved, due to the fact that the chain bent post was already nearly completely separated at point L0. It is likely that the resultant shock, combined with the northerly components of lateral force being exerted on the north truss through the floor system and the northward twist of the span, resulted in the final separation of the post with sufficient westward velocity to account for its final resting place. Since there is evidence (Reference 35, installment 1, p. 36) that the bottom of joint L0 struck something during the collapse, and the northeast corner of the coping on the chain bent pier is damaged, it is speculated that L0-L2 caught and pivoted at this point, throwing joint L2 farther to the north. It is believed that the rupture of the gusset plate at panel point U7N also took place at this time due to this shock, which also completed some of the partial fractures at L2, L4 and L6N.

The south chain bent post of the Ohio side span must have completed its plastic bending failure to the north at about this same time, since it struck the deck before the deck slab fell away. (Reference 35, installment 1, p. 21).

Joint L13N had fallen about ten or twelve feet at this time, and joint U13N had followed this vertical motion but had also moved three or four feet northward due to the rotation of the deck at this point. As the top of the north leg of the Ohio tower continues to move eastward, the linkage formed by the hanger U13N-C13N, pin C13N and eyebars C13N-C15N pulled into a straight line, wrenching hanger connection U13N from the truss. The direction of pull, relative to the original position of the truss, was eastward and slightly to the south of the vertical.

The portions of the deck between panel points L9 and L11 had now fallen about 16 feet at its northerly edge. The resulting counterclockwise rotation of the deck, viewed from the west, was accelerated by the northerly movement of the south chain. The portion of the deck from about L6 to L10 dropped enough so that what had been the northerly end of the floor beams made contact with the ground. The shock of this ground contact probably fractured the connections of the floor beams to the south truss, allowing the south ends to drop to the ground, each floor beam rotating about its ground contact point. This resulted in this portion of the floor system coming to rest considerably south of its original position. The portion of the Ohio side span floor system between L3 and L5 apparently sagged to the ground with but little counterclockwise rotation viewed from the west. It was, however, thrown to the north as a result of its attachment to the south chain during the initial part of its fall. Joints L1, L2 and L3 were thrown even farther north, apparently because of the pivoting of L0-L1 at the pier.

In the main span, the south truss between the Ohio tower and panel point 21 broke loose from the chain by fractures in the hangers, permitting the south side of the deck to follow the north side in this portion with only slight counterclockwise rotation viewed from the west. The center portion of the south truss in the main span apparently remained attached to the chain during this phase of the collapse and produced further counterclockwise rotation in the deck.

Step 6

Time = 4.0 seconds

The collapse of the Ohio side span was virtually complete. During step 6, the upper portion of the south leg of the Ohio tower continued to rotate to the north, dragging the south chain and the portions of the trusses still attached farther to the north. The north chain,

by a combination of this general northward movement and its own northward movement due to the counterclockwise rotation of the deck, struck the crotch of a tree just west of panel point 9, and about 10 feet north of its final resting place.

In the main span the loss of support from the south chain and the displacement of this chain to the north prevented the development of effective cantilever action from the West Virginia tower. When the south leg of the Ohio tower had rotated approximately 50 degrees to the north, the south chain contacted the north tower leg or bracing and a series of multiple fractures occurred in the south chain just east of panel point 17. This was apparently followed by additional multiple fractures in the eyebars of the south chain just west and east of the West Virginia tower. This resulted in a complete loss of support for the south side of the main span which might otherwise have cantilevered from the West Virginia tower. The consequent overloading of the north truss east of panel point 30 produced multiple cleavage fractures in the north chain just west of the West Virginia tower. The entire east half of the main span was now free to fall with but little rotation. Apparently additional multiple cleavage fractures occurred in the lower chord of both trusses as the west end of this portion fell to the water, with the result that only the three panels closest to the West Virginia tower remained intact.

Step 7

Time = 6 to 10 seconds

With the loss of the south chain just east of the West Virginia tower, the south side of the West Virginia side span was free to fall. The north side of this span was in a lifted position at this instant. With the sudden loss of the north chain just west of the West Virginia tower, the tower began rotating toward West Virginia, ramming the West Virginia side span violently against the West Virginia approach span girders. This resulted in the shearing of the pins in the toggle links at the West Virginia tower, and the rupture of both West Virginia chain bent posts at the level of their connection to the lower chord. The north chain in the West Virginia side span was now also ineffective. The westerly portion of this chain apparently remained attached to the north leg of the tower long enough to impart a considerable clockwise rotation to the deck before it parted. This portion of the deck, and the north stiffening truss, came to rest in the water with the north face of the truss upward. It appears that the West Virginia tower was the last part to fall into the water. It fell toward West Virginia and slightly downstream of its normal position, portions of the portal bracing landing on top of what had been the north edge of the deck system.

Meanwhile at the Ohio end, the northward rotation of the south tower leg had reached its maximum extent so that the saddle was perhaps

65 or 70 feet north of its original position. This caused a general racking of the Ohio tower, and carried the south chain at panel point 9 to the north close to a tree some eight or ten feet north of its final resting place. The completion of the rotation of this portion of the Ohio tower south leg below the horizontal position apparently returned the south chain part way toward its original position. Additional fractures occurred in the south leg as it struck the north leg again (Reference 14) and dislodged the saddle, which was now in an almost inverted position, depositing it on the ledge at the north end of the Ohio tower pier footing. Further evidence of this return motion of the south chain was observed in the vicinity of panel point 7, where it was obvious that it had been moving to the south in its final motion, scraping a considerable amount of earth ahead of it.

3. The testimony of witnesses who observed the fall of the bridge from a distance is generally in accord with the sequence of collapse discussed above with but a few exceptions:

Wesley F. Wears, who was at the City Ice and Fuel Company dock about a quarter mile downstream on the West Virginia side, stated in part: "... I turned around and looked and saw the Ohio towers falling. The tower legs seemed to twist counterclockwise (when viewed from the top) and fall upstream and towards the center of the river. The center span of the bridge broke in the middle and fell straight down. It looked as though the cars on the center span all fell with the bridge and looked like they were falling in a funnel - some falling backward, some falling forward. I didn't see any vehicles fall off the bridge - just fall with the bridge. After the center span fell, the West Virginia towers and span fell.....the bridge was all down in a matter of five seconds as I estimate it".....
"None of the Ohio tower structure seemed to change shape or bend as they fell." (See file of written witness statements)

James Neil Britton, who was also at the City Ice and Fuel dock, testified at the public hearing in May of 1968 (see pages 162-169 of transcript) in part as follows:
"As I was sitting there idly counting traffic, I noticed the towers, which would be the Ohio towers, begin to twist in a clockwise motion approximately one-eighth or a quarter turn before they actually seemed to turn loose and the floor of the bridge break, and then the Ohio span over here collapsed, and in a simultaneous motion it worked its way back to the channel span

here with part of the bridge turning upside down and over next to Pier 4 here which could be on the West Virginia side. The bridge seemed to break in two and fall straight down ..." and then "this part here, which is the channel span of the bridge, seemed to turn completely upside down, partially, over to about where the center of the span would be (panel 30) and then on farther back (panel 38 or 40 in the record), it seemed to break in two and fall straight down at this point. I would say within fifty or seventy five feet of the towers here on the West Virginia side it broke in two and fell straight down" "It dropped straight down with this portion of the roadbed here still clinging to the pier here." (It is to be noted that under subsequent questioning as to which way the Ohio tower rotated, Mr. Britton confirmed that he did indeed mean clockwise as viewed from above.)

The break in the main span just west of the West Virginia tower observed by Mr. Britton could have occurred after failure of the "cantilever" effect, since if a length of some 300 feet started to fall with its east end supported at the tower, the inertia forces do produce a maximum moment at about the one third point.

Other eyewitnesses were either at the intersection west of the Ohio end of the bridge or at the traffic signal at 6th and Main Streets in Point Pleasant at the east end. Neither of these positions affords a view of the entire length of the structure. The testimony of these witnesses is, however, in general agreement on the sequence of collapse.

One witness who was at 6th and Main Streets in Point Pleasant said (written statement by Miss Lyda Smith) in part, "I saw the 'girders' from the Silver Bridge start to fall upstream slowly. Then the cement floor of the bridge (West Virginia side span) started to hove up in the middle and then there was a flash of light overhead on the electric wires." "the bridge flooring beyond the approach broke up into large cakes and buckled up." This is confirmed by one other witness (Stephen K. Darst, transcript pp. 149 et. seq.), who also noticed that the north eyebar chain in the West Virginia side span swayed north and south several times, followed by the south eyebar chain in a similar motion just before the collapse of this part of the structure.

A summary of the experience of the survivors from vehicles which were on the bridge at this time of collapse is presented in Figure 36. With respect to vibration experienced before the collapse, there are inconsistencies. Those near the Ohio end reported both vertical and horizontal motions of the eyebar chain between the chain bent post

and the anchorage. Those within the Ohio side span and the main span reported feeling vibrations, especially from side to side, although some who had used the bridge frequently did not think they were unusual until just before the collapse. The witness in Vehicle No. 38, who had started out onto the West Virginia side span, felt it was shaking so badly she stopped and backed off to the approach span, saving herself and others. This, however, was after the collapse had begun. Many agreed that the vibrations became really noticeable after the two east bound dump trucks passed them or approached them. These trucks were moving at between 10 and 15 mph, and would have taken about 35 to 50 seconds to reach their position at the time of collapse after entering the suspended portion of the structure at the Ohio chain bent. It is the belief of the Board that most of the unusual vibrations noted were due to the passage of these trucks. They were felt by the people in the west bound vehicles because they were standing still on the bridge. Many of them would not have had this experience before on this bridge, since the traffic only occasionally backed up far enough to place standing vehicles out on the span. Some of the more violent lateral motions were undoubtedly associated with the early stages of collapse.

The loud cracking and popping noises, presumably due to fractures, were reported most frequently in the vicinity of the chain bent post, panel point 7, and all the way over at panel point 39 (this one after lateral motion began). These are possibly associated with the fracture of the chain bent post, the gusset plate at U7N and fractures of eyebars in the main span. The duration of noise during the collapse is variously reported 8 or 10 to as much as 60 seconds.

The directions in which various survivors felt that their vehicles fell is consistent with the sequence of collapse developed above. Those closest to the Ohio chain bent post went down gently and rear end first. Those farther out on the Ohio side span rolled to the north. Those in the main span west of the center fell on the north side first and rear end first. At the center the fall was to the right or north side for west bound vehicles. The survivor of Vehicle No. 37 (F. Wamsley) reported a fall to the left (also north side for an east bound vehicle) and then straight down. There is some question about the position of this vehicle just at the instant of collapse. Wamsley recalls no cars ahead of him, a recollection supported by Charlene Wood who remembered a "truck coming toward her." It is at variance with the recollection of several other witnesses in the west bound traffic who recall the two dump trucks "close together" or "one car in between." In any event, the divers found both trucks on the bottom near the center of the main span, and four passenger autos within about 100 feet of the West Virginia tower. A position of Vehicle No. 37 at about panel point 33 would be more consistent, and would also have produced slightly higher stress in critical eyebar No. 330.

People from vehicles in the vicinity of panel points 3 and 4 reported an experience of a short drop, then a hesitation before complete fall. This is compatible with the collapse sequence. Those who were on the west end of the main span reported a momentary hesitation after a fall of the upstream side of about three feet, but only momentary. This could possibly be due to the gradual fall of these elements followed by free fall after the fracture of hangers at panel points 17, 19 and 21.

Out in the middle of the main span, at about panel point 28 or 30, a witness was able to get out of the back seat of a two door car between the time it dropped the first three feet and the final fall. This is possibly due to the fact that this portion held for several seconds due to cantilever action of the north truss.

E. Status of Bridge Design Practice in 1926

Adequate interpretation of the evidence developed in this investigation requires a consideration of the status of professional knowledge of the principles of bridge design which existed at the time of the design and erection of the Point Pleasant Bridge in 1926 and 1927. This portion of the report discusses some of the basic assumptions and concepts which were in general use and widely accepted at the time of the design of the Point Pleasant Bridge.

1. In the design of large structures, as in the design of most systems, there is no such thing as absolute safety. Even when the completed structure is subjected to a so-called "proof loading," one cannot be certain that he has eliminated all possibility that some rare combination of loading and/or environmental conditions may cause a failure. What the designer attempts to do is to reduce the probability of failure to an extremely remote one by setting the loads to be carried by the elements of the structure to some fraction of their actual strength. The ratio of this computed load on the member to its actual strength is sometimes referred to as the safety factor, and the design specification for any particular structure attempts to maintain this factor more or less uniform for all elements in the structure. What constitutes a proper factor of safety for each class of structure has evolved largely through experience and judgment although in recent years attempts have been made to derive such factors of safety on a rational basis.

In order to select an adequate factor of safety, one must consider the fact that his estimates of the loads to be imposed upon the structure and the estimates of the strength of the individual components are both subject to a range of error. The errors in estimating the strength of the members are caused by variations in the manufacture of the materials and fabrication and erection tolerances. The latter affect both the cross section areas provided and the geometric lines along which the loads are applied to the members. The

loadings imposed are subject to errors arising from several sources. One can calculate with great precision that portion of the load which is produced by the weight of the structure itself (probably within one to two percent error), but the loads imposed by external loads of traffic and the environment cannot be determined with the same precision.

There is obvious difficulty in estimating what types of heavy vehicles we will be moving on our highways in the year 2010, which is the same 40 year projection into the future that was faced by the designers of the Point Pleasant Bridge in 1927. Besides the difficulty of projecting the loads likely to be produced by individual vehicles in the future, there is a problem of what combinations of these heavy vehicles are likely to occur on the structure where the influence of more than one vehicle is involved in the stress computations. For example, the maximum stress in the eyebar chain due to traffic was produced when both lanes of the structure were loaded over the full length of the suspended portion of the structure. It is highly improbable that this full length would be occupied entirely by vehicles of the maximum weight for which individual local elements of the deck were designed. It is even more improbable that this event could occur simultaneously with a temperature condition producing maximum stress and with maximum stresses due to a wind blowing at right angles to the structure.

The designer, therefore, must use careful judgment in deciding which influences should be assumed to occur simultaneously and must make appropriate reductions in the factor of safety for highly improbable conditions. One further matter is involved in the establishment of the actual factor of safety; namely, the precision with which the stress analysis is conducted. The greater the refinement of the stress analysis and the accuracy of estimating such factors as dynamic effects of moving loads, the lower need be the nominal factor of safety to achieve a given level of improbability of failure.

Systematic procedures by which all of these factors had been incorporated into highway bridge design practice were fairly well established by 1926. A nationally recognized design specification appeared in 1923, when the first edition of such a specification was issued by the American Association of State Highway Officials. A similar specification for railroad bridges had been issued in 1910 by the American Railway Engineering Association. The basic procedure consists essentially of four elements:

- (a) An allowable working stress for basic tension members is stipulated, usually in terms of a percentage of the elastic limit stress for the material to be used (more recently in terms of the

yield point or yield strength of the material).

(b) The establishment of standard loadings for those loads which will act on the structure in addition to its own weight. An attempt is made in the establishment of these loads to project likely trends for traffic loadings into the future, and to estimate the extreme environmental loadings such as those due to wind which have a 50 percent probability of occurrence within the proposed lifetime of the structure.

(c) The refinement with which the stress analysis is to be conducted is either implied or stipulated and the basis upon which the strength of members other than tension members is to be computed is prescribed.

(d) The materials quality control which is believed consistent with the other considerations is stipulated, as well as the fabrication and erection tolerances which control the degree to which the behavior of the members correspond to the design assumptions.

As an example of the above, the 1931 edition of the American Association of State Highway Officials Specification for the design of highway bridges stipulated a basic allowable tensile stress of 16,000 pounds/sq. in. for A7 carbon steel members for which the prescribed minimum yield point was 30,000 psi., giving a nominal factor of safety of 1.87 against yielding. A somewhat higher unit stress of 24,000 psi. was permitted for members subject to dead load only.* Three classes of loadings were specified for traffic. The heaviest class was designated as H20 and consisted of a two axle 20 ton truck followed by and proceeded by 15 ton trucks at 30 feet spacing. For elements in the structure requiring the loading of more than 60 feet of length, simplified loadings consisting of 640 pounds/linear foot/lane were permitted together with single concentrated loads of 18,000 pounds where bending moments in the member were being computed, or 26,000 pounds where the shearing stresses were being computed. The introduction to this specification stipulates it is intended for structures not in excess of 400 feet in length. This specification reflected the practice of making reductions in the load as the improbability of the load pattern increased. Section 5.2.10 of the specification permitted load reductions of up to 25 percent on roadways carrying four lanes of traffic when the occupancy of all four lanes was required to produce maximum stress in the member.

*Members carrying combined dead load and live load were proportioned for the sum of the areas required for each of the prescribed unit stresses, subject to the overload provision that a 100% increase in live load not produce unit stresses in excess of those permitted for dead load.

The specifications further provided for quality control requirements for the type of steel stipulated. It provided that the computation of stresses could be performed on the assumption that the structure was linearly elastic, and stipulated the combinations of dead load, live load, dynamic and other forces which were to be considered in the design.

Prior to the issue of the AASHO Specification of 1923, highway bridge designers were more or less dependent on their own judgment in matters which were later codified in the specifications. Some well recognized guides existed in related fields such as the specifications for the design for steel buildings by the American Institute of Steel Construction which was first issued in 1923, and the specifications for Steel Railway Bridges first issued by the American Railway Engineering Association in 1910.

2. The element of judgment was especially important for the designers of long span bridges, since none of the existing codes or specifications were intended to be applicable to such structures. As a matter of fact, no nationally recognized code for the design of long span bridges exists even today. There are three considerations that place the design of long span bridge structures in a special class:

(a) The refinement with which the stress analysis is performed is of great importance since these structures often may not conform very well to the assumption that they are linear and elastic in their response.

(b) The probability of obtaining maximum live load over the full length of the structure is remote compared to the probability of a similar situation on a shorter span.

(c) The proportion of the total stress in the main supporting members, such as the cables or eyebar chain of a suspension bridge, due to the weight of the structure itself is much greater than it is for short span structures, frequently accounting for 70-90 percent of the total load in such members.

The first of these special considerations requires that stress computations for long span structures be carried out with greater care and that the indicated results from the assumptions of linear elastic behavior be carefully examined for their validity and revised, if necessary, by more refined methods which take into account the effects of distortion in the structure upon its internal equilibrium. In the case of the Point Pleasant Bridge Design, the stress analysis was

carried out by a linear elastic procedure involving the consideration of the elastic energy within the system. As noted in a previous section of this report, this original analysis has now been thoroughly checked by two independent groups and has been found accurate with a few very minor deviations. There is no record to establish whether the designers reexamined these results to consider the effects of distortion by applying the so-called "deflection theory" to the analysis. For suspension bridges, however, the more exact deflection theory will indicate lower stresses in the stiffening truss than will the linear elastic theory, so that the use of linear theory tended to increase rather than decrease the factor of safety in the structure. A simple check of one loading case at one point in the center of the main span indicates that the more refined analysis would have reduced the stiffening truss chord stress by approximately 16 percent.

Both the second and third considerations make it feasible to raise the allowable design stresses above those commonly used for short span structures. This practice was and is common for stiffening trusses and main supporting elements of suspension bridges.

The designers of the eyebar chain alternate for the Point Pleasant Bridge selected an allowable stress for the eyebar chain of 50,000 psi. This was approved by the consultants. This material was to be manufactured so as to produce a minimum elastic limit of 75,000 pounds/sq. in. This provides a nominal factor of safety on the elastic limit of 1.50. Such a factor of safety appeared reasonable, in the judgment of the designers, in view of the fact that approximately 75 percent of the stress in the eyebar chain elements was due to the weight of the structure which could be quite precisely calculated.

It is interesting to compare this factor of safety for the main supporting chain with those of other bridges designed during the same era. In the design of the Florianopolis bridge in Brazil, D. B. Steinman used an allowable stress of 46,500 psi. for an eyebar chain composed of essentially identical material. This would yield a factor of safety on the elastic limit of 1.61. The Florianopolis bridge, however, was designed to carry both highway and rail loadings, resulting in the dead load stress being a slightly lower fraction of the total stress in the chain (approximately 70 percent). The typical factor of safety used in the design of wire cable bridges at the same period was from 1.6 to 1.7 based on the yield strength.

Similar increases in the allowable stresses in the stiffening truss over and above those common in short span bridges were customary for long span structures. In the design of the Point Pleasant Bridge an allowable stress of 24,000 pounds/sq. in. in tension was used in a material (A7-24 carbon structural steel) for which the stipulated minimum yield point was 30,000 psi. This corresponds to a safety factor of 1.25 on the yield point. Steinman in the design of the Florianopolis bridge used a basic allowable stress of

18,500 psi. for a stiffening truss composed of the same material. The actual computed maximum stress for the Florianopolis bridge was 14,500 psi. when the deflection theory was used to correct the computations performed by the linear elastic assumption.

This comparison is, however, meaningless without consideration of the live loads which were used in the design. The designers of the Point Pleasant Bridge used a live load of 14,000 pounds/linear ft. of bridge plus a 42,000 lb. concentrated load for stiffening trusses, towers, and cables. This is in excess of the 640 lbs./ft./lane for a modern H20 loading on two lanes (as the structure was actually used), and no reduction was taken for the improbability of obtaining such loads over the long loaded lengths required for maximum chain loads or maximum stiffening truss bending moments. Steinman used a live load of 2200 pounds/linear ft. for two lanes of highway loading plus one lane of light railway loading down the center lane of the structure. A reduction of this live load was used for the design of the chains (1850 lbs./linear ft.) in view of the improbability of obtaining maximum loads over the full length of the structure. While the selection of the design stress for the stiffening trusses for the Point Pleasant Bridge appears to be somewhat high, it should be noted that the consideration of the deflection theory reduces actual stresses by approximately 16 percent below those indicated by the linear analysis on which the design was actually based. Moreover, yielding of the stiffening truss in a suspension bridge does not produce a collapse, since the truss is not required for equilibrium. Such yielding would lead to large deflections so that the cable could distort to provide a new stable equilibrium. This condition, could not, of course, be tolerated except in emergency conditions, for repetitions of such events would quickly lead to serious damage. There is no evidence to indicate that the failure of the Point Pleasant Bridge initiated in the stiffening trusses.

3. The problem of stress concentration was well recognized at the time of the design of the Point Pleasant Bridge. Both theoretical and experimental solutions for typical cases in machine design and structural engineering were available. The classic solution for the stresses at the edge of a circular hole in an infinitely wide plate subjected to uniaxial tension was known to give stress concentration factors approaching 3. There was, however, a general assumption that such effects could be ignored except when highly brittle materials were used or in cases where fatigue might occur. Castings of such materials as iron were provided with generous fillets, and machine parts subjected to repetitive loads were designed for conservative unit stress and detailed to avoid sharp discontinuities where possible.

The structural engineering profession of that era assumed that these effects, which were present around every rivet hole and every abrupt change of section, could be ignored if:

- (a) The loadings to be applied were essentially static.
- (b) Appropriate reductions of allowable stress were made when large ranges of stress due to repetitive loading were involved, especially when reversal of stress was involved.

The first assumption was based upon the experimental evidence from tests of such items as riveted joints, where local overstress and yielding resulted in redistribution of stress and had little effect on the ultimate load. The whole theory of design of riveted connections depended upon this concept. A similar concept applied to the design of eyebars, where static tests also showed that a properly proportional head could develop the strength of the shank of the eyebar in spite of the stress concentrations at early stages of loading.

The "appropriate reductions of allowable stress" for elements subjected to repetitive loadings were determined either by experience or by laboratory tests, which showed that most structural metals then in use exhibited an "endurance limit" stress level, below which it was immune to fatigue failure.

These general assumptions are still in use today for such structures as bridges and buildings of ordinary structural steels. Somewhat more refined techniques are used in the design of pressure vessels, or structures of high strength alloys or nonferrous metals.

Relatively little was known of the stress-corrosion-cracking mechanism with respect to the common structural steels used in bridges of that era, or the role of hydrogen-stress cracking or corrosion-fatigue for these materials. Such fatigue mechanisms were beginning to be understood in the high alloy steels and nonferrous metals, but even here the quantitative data was limited. References 36 and 37 give some indication of the status of knowledge in the early 1930's, some five years after the design of the Point Pleasant Bridge. The state of knowledge at that time with respect to stress-corrosion of mild steels is reflected in References 38 and 39, which deal mostly with the benefits of deoxidation or "killing" of steel to inhibit intergranular stress-corrosion.

Even today there is little data available for many of the steels which have been used in bridge building over the past fifty years or are in common use at the present time to make reliable quantitative crack growth predictions, where such growth is due to either stress-corrosion cracking or corrosion-fatigue. Nor are there reliable data as to what constitutes critical crack size for brittle fracture. Since many of the materials in question possess considerable ductility, it is even doubtful that the discipline of linear fracture mechanics will be adequate for the determination of such critical crack sizes, and new advances to extend these concepts will be required before sufficient insight will be obtained to interpret flaws in these materials.

V. CONCLUSIONS

(Listed after conclusions are page numbers in this report which contain facts leading to conclusions.)

The field and laboratory work conducted in this investigation, together with the results obtained by the Bridge Design Review and History and the Witness Groups, support the following conclusions:

A. With Respect to the Sequence of Events in the Collapse of the Point Pleasant Bridge:

1. The total collapse of the structure required the failure of some element in the supporting chains or towers. The directions in which the towers fell indicate that this failure was at the Ohio tower or west of this point in the Ohio side span, and in the north chain or its supporting elements. (93, 94, 95, 96)

2. Examination of the Ohio tower wreckage showed no failure in the north leg and the laboratory examination of the fractures in the Ohio north chain bent post and gusset plate U7N showed these fractures to have occurred from excessive or abnormal loads beyond those which were possible from the loading on the structure just prior to collapse. The only remaining failure in the chain or its supporting elements in the Ohio side span which could have led to collapse is a failure of some element in the chain itself. (20, 93, 94, 95; 96)

3. The joint at C13N, the first joint in the north chain west of the Ohio tower, began to separate because of the brittle fracture in eyebar No. 330 (the northerly bar of the pair in the north chain connecting pins at joints C11N and C13N. Subsequent to this fracture, eyebar No. 33 (the southerly bar of this pair) slid off the south end of the pin, causing complete separation of the north chain at this point. (34, 70, 94)

4. With respect to the brittle fracture in eyebar No. 330, the laboratory work has shown that:

(a) The small crack which existed prior to the collapse was large enough to account for the brittle fracture in the special steel of which the eyebars were made at the stress level computed to exist at this location, without any additional dynamic effects. (47, 52, 95)

(b) This small crack probably initiated at a small corrosion pit. (32, 68, 95)

(c) The crack grew to critical size by the joint action of stress-corrosion cracking and corrosion-fatigue. The available evidence is not sufficient to permit a definite conclusion as to which mechanism was predominant. (37, 54, 68, 94, 95, 96)

5. The small size of the critical crack in eyebar No. 330, and its location on the inside surface of the hole, precluded its being found while the structure was intact, by the inspection techniques used, or by any other inspection technique available at this time for use in the field on heavy structures, without disassembly of the joint. (7, 32, 46)

6. The examination of other fractures which might have contributed to the brittle fracture of eyebar No. 330 by producing shock waves in the eyebar chain has shown that, although some of these fractures occurred at points of additional pre-existent cracks in the structure, there is sufficient evidence to demonstrate that these fractures occurred after the process of collapse had begun. (39, 40, 42, 45, 94)

7. The effect of surface corrosion (primarily ordinary rusting) on the load carrying capacity of the structure was carefully assessed by a corrosion survey of all main members at the reassembly site. Although there was deep rusting of some secondary elements such as stay plates, lacing bars, and diaphragms, there is no indication that the net critical sections of main members were reduced in cross section to the point where they were inadequate to carry the intended loads or those imposed by the loading just prior to collapse. (22)

B. With Respect to the Elements Which Contributed to the Failure:

The failure of the Point Pleasant Bridge was a result of the convergence of several trends, each of which was common in engineering practice in the era in which it was designed, and the existence of a subtle form of time-dependent crack growth of which little was known at the time of its construction, namely:

1. The trend toward use of higher strength materials for steel structures. The steel in the eyebars was a heat treated, relatively high carbon steel (compared to ordinary structural carbon steel). (84, 118)

2. The use of higher allowable stresses when the confidence with which the applied loads was known was high, as is typical in a long span bridge where most of the load is due to its own weight. The allowable stress for the eyebars was set at 50,000 psi. or 67 percent of the elastic limit of 75 000 psi. specified for the material. Typically, 75 to 80 percent of the applied stress was due to the weight of the structure itself. (117)

3. The practice of not computing certain secondary stresses or local effects where these were produced by static loads, and where the range of stress due to traffic loads and other transient effects was small. This practice was particularly common for eyebars, where it was required that the fabricator demonstrate by actual tests that the areas of local high stress in the head of the eye did not control its load capacity (under static load). (89, 91, 92, 93, 119)

4. The growth of a small crack by the stress-corrosion mechanism had been known only in a few ferrous and non-ferrous metals of that era under severe exposure conditions, such as containers used in the chemical and food processing industry, riveted steam boilers, and machine parts subjected to various corrosive environments. The role of corrosive environments in accelerating the normal fatigue process was also seldom considered in normal outdoor environments. In the light of present day knowledge, the stress at the edge of the hole in the eyebars was too high for a material subject to crack growth by either of these mechanisms without special corrosion protection. (120)

5. There was a water collection pocket adjacent to a point of high stress, as there is in any eyebar construction, where there is sufficient clearance between the pin and the pinhole surface to permit entry of water. (95)

6. This point of high stress was not accessible for inspection. (7, 32, 46)

7. The use of only two eyebars per link in the eyebar chain. This made the total failure of the chain inevitable once the fracture occurred in eyebar No. 330. Had there been three or more eyebars per link, there would have been the possibility that the failure of one bar would not have led to disaster. (7)

C. With Respect to the Implications for the Safety of Other Bridges:

1. The relatively rare combination of all the factors cited above for the Point Pleasant Bridge makes the recurrence of this exact type of failure remote. The only other bridge in this country to combine all these factors is at St. Marys, West Virginia, and it has been closed since early in this investigation. (2)

2. There are, however, many other structures which possess one or more of these factors as features in their designs. It is not precisely known what the critical combinations may be for the initiation and growth of similar hidden defects to critical size. (120)

3. The current vigorous efforts to upgrade the quality of bridge inspection will certainly detect those structures where surface corrosion, impact damage and other visible or measurable defects impair their strength. Nevertheless, the possibility of small flaws in critical elements made of material susceptible to stress-corrosion, corrosion-fatigue and other time dependent flaw growth phenomena does exist. In some cases these materials also have limited fracture toughness, so that the critical flaw size is undetectable by present inspection devices and methodology. (82, 83, 120)

4. An acceleration of the existing program of improvement of bridge safety is needed, and should include efforts to:

(a) Identify those bridge building materials used over the past, as well as those presently in use, which are susceptible to slow flaw growth by any of the suspected mechanisms. (120)

(b) Investigate these same materials to determine critical flaw size under various stress levels. (120)

(c) Develop a new generation of inspection equipment for use under field conditions to detect critical or near critical flaws in heavy structures. It will also be necessary to devise analytical procedures by which the data on flaw growth rates, under various types of exposure, can be interpreted to identify critical locations which require such detailed inspection. One hundred percent inspection will probably prove impractical and extremely expensive. (7, 32, 46, 120)

~~(d) Develop adequate understanding of these problems to permit the incorporation of appropriate safeguards in the design and fabrication of future bridges and for the qualification of materials for these structures. (120)~~

(e) Devise techniques for repair, protection or salvage of bridges damaged by internal flaws. (120)

(f) Expand our knowledge of the loading history and life expectancy of bridges. (117, 118, 120)

D. With Respect to the Status of Bridge Inspection and Maintenance:

1. The intensive actions of the Department of Transportation to establish standards for the proper safety inspections of bridges, and training programs for bridge inspectors as required by the Federal-Aid-Highway Act of 1968, are positive steps to increase the safety of highway bridges in the Federal-Aid-System. (82, 83)

2. Over 70 percent of the approximate total of 563,500 highway bridges in the United States are not in the Federal-Aid-System, and 94 percent of the approximate number of 373,000 bridges on county secondary roads, rural roads, and city streets were built prior to 1935. These older structures, which are most subject to extensive repair or replacement, must be funded for by State or local governments which, in many instances, have limited funds for such remedial actions. (82, 83)

3. While it is expected that the new Federal standards for bridge inspections, programs for training of inspectors, the Guide, and the AASHO Manual for Maintenance Inspections will become known to many state and local authorities responsible for bridges not in the Federal-Aid System, there is no requirement that such authorities implement the intent of these documents. (82, 83)

4. The bridge safety requirements of the Federal-Aid-Highway Act of 1968 have created the situation wherein bridges in the Federal-Aid System are required to meet rigorous Federal standards for inspection and maintenance, while the majority of the bridges in the country are not subject to those standards, except as voluntarily adopted. (82, 83)

VI. CAUSE

The Safety Board finds that the cause of the bridge collapse was the cleavage fracture in the lower limb of the eye of eyebar 330 at joint C13N of the north eyebar suspension chain in the Ohio side span. The fracture was caused by the development of a critical size flaw over the 40-year life of the structure as the result of the joint action of stress corrosion and corrosion fatigue.

Contributing causes are:

1. In 1927, when the bridge was designed, the phenomena of stress corrosion and corrosion fatigue were not known to occur in the classes of bridge material used under conditions of exposure normally encountered in rural areas.
2. The location of the flaw was inaccessible to visual inspection.
3. The flaw could not have been detected by any inspection method known in the state of the art today without disassembly of the eyebar joint.

VII. RECOMMENDATIONS

The Safety Board recommends that:

1. The Secretary of Transportation expand existing research programs or institute new research programs to:
 - a. Identify bridge building materials susceptible to slow flaw growth by any of the suspected mechanisms;
 - b. Determine critical flaw size under various stress levels in bridge building materials;
 - c. Develop inspection equipment capable of detecting critical or near critical flaws in standing bridge structures;
 - d. Devise analytical procedures to identify critical locations in bridge structures which require detailed inspection;
 - e. Develop standards which incorporate appropriate safeguards in the design and fabrication of future bridges to ensure protection against failures of material such as occurred in the Point Pleasant Bridge;
 - f. Develop standards for the qualification of materials for future bridge structures, using the information disclosed in this investigation;
 - g. Devise techniques for repair, protection, or salvage of bridges damaged by internal flaws; and
 - h. Expand the knowledge of loading history and life expectancy of bridges.

2. The Secretary of Transportation explore the alternatives for action to assure mandatory application of the bridge safety requirements of the 1968 Federal-Aid-Highway Act to all highway bridges in the United States, since the majority of older bridges in the country are not in the Federal-Aid-Highway System and these bridges are most susceptible to extensive repair or replacement; including such alternative courses of

action as urging the adoption by the States of mandatory standards, or the enactment of Federal legislation applicable to all highway bridges.

3. The Secretary of Transportation consider the advisability of proposing a program of Federal aid to ensure the adequate repair of all bridges not in the Federal-Aid-System.

BY THE NATIONAL TRANSPORTATION SAFETY BOARD:

/s/ JOHN H. REED
Chairman

/s/ OSCAR M. LAUREL
Member

/s/ FRANCIS H. McADAMS
Member

/s/ LOUIS M. THAYER
Member

/s/ ISABEL A. BURGESS
Member

Adopted: December 16, 1970

VIII. REFERENCES

1. Scheffey, C. F.; "Interim Report, Structural Analysis and Tests Working Group," dated September 1968, Point Pleasant Bridge Investigation, National Transportation Safety Board file SS-H-2, Washington, D.C.
2. O'Connell, Joseph J., et. al.; "Collapse of U.S. 35 Highway Bridge, Point Pleasant, West Virginia, December 15, 1967," National Transportation Safety Board Report SS-H-2, dated October 4, 1968, Washington, D.C.
3. Wilkes, W. J.; "Interim Report, Bridge Design Review and History Working Group," National Transportation Safety Board file SS-H-2, Point Pleasant Bridge Investigation, Washington, D.C.
4. Schmieg, A. L.; "Report of Chairman, Witness Working Group," Point Pleasant Bridge Investigation, National Transportation Safety Board file SS-H-2, Washington, D.C.
5. Transcript of Public Hearing, "Investigation of the Collapse of the U.S. 35 Highway Bridge at Point Pleasant, West Virginia, December 15, 1967," held on May 7-10, 1968. Charleston, West Virginia; National Transportation Safety Board, Washington, D.C.
6. Wilkes, W. J.; "Final Report of Chairman, Bridge Design Review and History Working Group," Point Pleasant Bridge Investigation, National Transportation Safety Board, Washington, D.C.
7. Wiles, E. G.; "Reassembly of Point Pleasant Bridge - Documentation of Structural Damage and Identification of Laboratory Specimens," Staff Report, Office of Research and Development, U.S. Bureau of Public Roads, Washington, D.C.
8. Hechtman, R. A.; "Preliminary Examination of Significant Fractures in the Wreckage of the Point Pleasant Bridge on the Ohio Shore," R. A. Hechtman & Associates Report to U.S. Bureau of Public Roads, dated February 19, 1968.
9. Hechtman, R. A.; "Further Examination of the Wreckage of the Ohio Side Span of the Point Pleasant Suspension Bridge," R. A. Hechtman & Associates Report to the U.S. Bureau of Public Roads, dated April 30, 1968.

10. Hechtman, R. A.; "Examination of Fractures in Towers and in Floor System and Trusses Adjacent to Ohio Tower of Point Pleasant Bridge," R. A. Hechtman & Associates Report to U.S. Bureau of Public Roads, dated August 28, 1968.
11. Hechtman, R. A.; "Plan for Cataloging Significant Fractures East of Ohio Tower in Point Pleasant Bridge," R. A. Hechtman & Associates Report to U.S. Bureau of Public Roads, dated September 12, 1968.
12. Hechtman, R. A.; "Further Examination and Cataloging of Fractures in Wreckage of Point Pleasant Bridge," R. A. Hechtman & Associates Report to U.S. Bureau of Public Roads, dated November 8, 1968.
13. Hechtman, R. A.; "Laboratory Test Program for Structural Steels of Point Pleasant Bridge," R. A. Hechtman & Associates Report to U.S. Bureau of Public Roads, dated January 20, 1969.
14. Hechtman, R. A.; "Investigation of Wreckage of Ohio Tower and Adjacent Suspension System for Evidence of Mode of Collapse," R. A. Hechtman & Associates Report to U.S. Bureau of Public Roads, dated September 9, 1969.
15. Masters, F. M. Jr., Bellanca, L. C. and Soong, T. Y.; "Corrosion Survey of the Silver Bridge," Report by Modjeski and Masters, No. 1663, dated September 23, 1969, to the State Road Commission of West Virginia.
16. Varney, R. F. and Viner, J. G.; "The Dynamic Response of the Eyebars Chain Suspension Bridge Over the Ohio River at St. Marys, West Virginia," Staff Report, Office of Research and Development, U.S. Bureau of Public Roads, dated June 1970.
17. Bennett, J. A.; "Metallurgical Examination and Mechanical Tests of Material from the Point Pleasant, West Virginia Bridge - Part 1," National Bureau of Standards Report No. 9981 to U.S. Bureau of Public Roads, dated February 14, 1969.
18. Bennett, J. A. and Meyerson, M. R.; "Metallurgical Examination and Mechanical Tests of Material from the Point Pleasant, West Virginia Bridge - Part 2," National Bureau of Standards Report No. 9981 to U.S. Bureau of Public Roads, dated July 31, 1969.

19. Ballard, D. B. and Yakowitz, H.; "Mechanisms Leading to the Failure of the Point Pleasant, West Virginia Bridge - Part 3," National Bureau of Standards Report No. 9981 to U.S. Bureau of Public Roads, dated September 17, 1969.
20. Feinberg, I. J.; "Metallurgical Examination and Mechanical Tests of Material from the Point Pleasant, West Virginia Bridge - Part 4," National Bureau of Standards Report No. 9981 to the U.S. Bureau of Public Roads, dated June 1, 1970.
21. Feinberg, I. J.; "Metallurgical Examination and Mechanical Tests of Material from the Point Pleasant, West Virginia Bridge - Part 5," National Bureau of Standards Report No. 9981 to the U.S. Bureau of Public Roads, dated June 10, 1970.
22. Feinberg, I. J.; "Examination of Fractures in the L12-L13 Lower Chord Member of the Point Pleasant, West Virginia Bridge," National Bureau of Standards Report 312.01/07 to the U.S. Bureau of Public Roads, dated June 10, 1970.
23. Feinberg, I. J.; "Examination of the Fractured Rivets in the Bearing Box of Joint U13N of the Point Pleasant, West Virginia Bridge," National Bureau of Standards Report, Part 7, to the U.S. Bureau of Public Roads, dated July 3, 1970.
24. Mindlin, H. et. al.; "Inspection and Evaluation of Two Steels from the Silver Bridge," Battelle Memorial Institute Columbus Laboratories report to the U.S. Bureau of Public Roads dated May 1970. Participating authors: Feddersen, C and Malik, K. - Structural Materials; Ireland, D. - Materials and Environmental Engr.; Berry, W. and Lane, W. C. - Corrosion Research; Meister, R. and Flox, R. - Materials Joining Engr.; Groeneveld, T. - Ferrous Metallurgy; and Crites, N. and Mesloh, R. - Applied Soil Mechanics.
25. Phelps, E. H.; "Examination of Point Pleasant Bridge Eyebars," Applied Research Laboratory, U. S. Steel Corp., Report dated May 18, 1970, with Appendices by Bomback, J. L. and Mann, W. L.
26. Nishanian, J.; "Fatigue Characteristics of Steel Used in the Eyebars of the Point Pleasant Bridge," Staff Report, Office of Research and Development, U.S. Bureau of Public Roads, dated June 5, 1970.

27. Scheffey, C. F., Cayes, L. R., and Boyer, C.; "Model Tests of Modes of Failure, Joint C13N of Eyebar Chain, Point Pleasant Bridge Investigation," Staff Report, Office of Research and Development, U.S. Bureau of Public Roads, dated June 9, 1970.
28. Starkey, W. L.; "The Possible Role of Mechanical Fretting in the Collapse of the Silver Bridge," Report by Professor W. L. Starkey of Ohio State University to the U.S. Bureau of Public Roads, April 17, 1968.
29. Starkey, W. L.; "Fretting-fatigue Characteristics of 1060 Steel Specimens Taken from the Silver Bridge at Point Pleasant, West Virginia," Report by Professor W. L. Starkey of the Ohio State University to U.S. Bureau of Public Roads, dated February 28, 1969.
30. Slutter, R. G.; "Silver Bridge Eyebar Test: Stress Concentration Factors," Letter Report, Lehigh University to Modjeski & Masters, dated July 9, 1969.
31. Slutter, R. G.; "Silver Bridge Eyebar Tests, Stress Concentration Factors," Letter Report, Lehigh University to Modjeski & Masters, dated August 6, 1969.
32. Bleich, Fredrich; "Theorie und Berechnung des eis. Brucken," Springer, Berlin, (1924) p. 256.
33. Coker, E. G.; "Photoelasticity," Journal Franklin Institute, (1925).
34. Takemura, K. and Hosakawa, Y.; "Reports, Acro. Institute," Tokyo, Vol. 18, (1926), p. 128.
35. Lutz, J. G.; "Field Notes, Point Pleasant Bridge Investigation," Installments 1, 2 and 3 by J. E. Greiner Company, submitted to S.A.&T. Working Group, January-February 1968.
36. Gough, H. J. and Sopwith, D. G.; "Some Comparative Corrosion-Fatigue Tests Employing Two Types of Stressing Action," Jor. Iron & Steel Institute, No. 1 (1933).
37. Ludwick, P.; "Notch and Corrosive Endurance Strength," Metallwirthschaft, Vol. 10, September (1931).
38. Fry, A.; Krupp Monatshefte, Vol. 7:185, (1926).
39. Ruttman, W.; Technische Mitteilungen Krupp, Vol. 4:25 (1936).

TABLE 1

**Summary of Fracture Toughness Data
Point Pleasant Bridge Eyebar Material**

<u>Type of Specimen</u>	<u>Number</u>	<u>Test Temperature, °F.</u>	<u>Critical Stress Intensity Factor, K_{Ic}, ksi$\sqrt{\text{in.}}$</u>	
			<u>Range</u>	<u>Average</u>
Notch bend	2	70	46.50-53.61	50.06
Notch bend	3	0	28.27-35.90	32.39
Surface flaw	3	70	47.90-50.9	50.2
Surface flaw	3	32	43.2 -50.8	46.4
Surface flaw	3	0	33.4 -41.8	38.0

TABLE 2

Summary of Chemical Analysis of A7-24 Type Steel
From Pt. Pleasant Bridge by Several Laboratories

Laboratory	Sample Sources	Composition, %									
		C	Mn	P	S	Si	Cu	Ni	Cr	Mo	Al
U. S. Steel	(1) Plate from Chain Bent Post, 1/2 inch thick	0.02	0.58	0.011	0.032	0.10	0.019	0.010	0.015	0.007	
Nat'l. Bureau of Standards	(1) Web from Chain Bent Post, 5/8 inch thick	0.29	0.71	0.018	0.029	<0.10		<0.10	<0.01	<0.01	<0.01
	(2) Gusset Plate U7N, 3/4 inch thick	0.22	0.40	0.013	0.017	<0.10		<0.10	<0.10	<0.10	<0.01

ASTM Specifications for A7-24 Steel
<0.05 <0.06

TABLE 3

**Summary of Mechanical Properties for A7-24 Type Steel
From Pt. Pleasant Bridge**

<u>Laboratory</u>	<u>Source of Sample</u>	<u>Yield Point</u> ksi.	<u>Yield Strength</u> 0.2% Offset ksi.	<u>Tensile Strength</u> ksi.	<u>Elongation, %</u> 1" 2"	<u>Reduction</u> Area %
National Bureau of Standards	3/4 inch Av.	31.2	31.5	59.6	37	64
	gusset U7N (Longitudinal)					
	Min.	29.8	30.1	59.0	36	63
	(Transverse)Av.	28.9	30.0	59.4	37	59
	Min.	29.2	29.5	59.2	36	58
U. S. Steel	5/8 inch Web, Chain Bent Post (Transverse)Av.	36.5	37.3	68.0	32	55
	Min.	35.5	36.2	67.4	30	54
U. S. Steel	1/2 inch Av. Plate, Chain Bent Post		35.5	63.2	33.0	66.5
	Min.		34.7	63.0	33.0	65.9
<u>Comparison Values</u> University of Wisconsin, 1927 ¹ .	Various Plates and Shapes, A7-24, 1/2 inch to 3/4 inch thick					
	Av.	35.8		64.2	28.0 (8 Inches)	
	Min.	27.6		52.2	13.2 (8 Inches)	

1. From M. O. Withey, "Tests of Specimens Cut from Different Portions of Structural Steel Shapes," presented June 1928, annual meeting of the American Society for Testing Materials.

TABLE 3 CONTINUED

<u>Comparison Values</u>						
<u>Laboratory</u>	<u>Source of Sample</u>	<u>Yield Point</u> ksi.	<u>Yield Strength</u> 0.2% Offset ksi.	<u>Tensile Strength</u> ksi.	<u>Elongation, %</u> 1" 2"	<u>Reduction Area</u> %
ASTM	A7-24 Specifications (Longitudinal Spec.) Min.	30.0		55.0-65.0	2 min.	

TABLE 4

**Fracture Toughness of A7-24 Steel, Point Pleasant Bridge
As Measured by Charpy Tests**

<u>Laboratory</u>	<u>Source of Sample</u>	<u>15 foot pound Transition Temperature, °F.</u>
U. S. Steel	1/2 inch Plate, Chain Bent Post, Longitudinal	55
National Bureau of Standards	5/8 inch Web, Chain Bent Post, Longitudinal; 3/4 inch Gusset, U7N Longitudinal Transverse	74 80 92
Battelle Memorial Institute	1/2 inch Plate, Chain Bent Post, Longitudinal	36

TABLE 5

Summary of Chemical Analysis of Eyebar Steel
From Point Pleasant Bridge

<u>Laboratory</u>	<u>Sample Identification</u>	<u>C</u>	<u>Mn</u>	<u>S</u>	<u>P</u>	<u>Si</u>	<u>Cu, Ni, Cr, V, Mo</u>
National Bureau of Standards	C9 head of C9-C11NN-C9	0.62	0.63	0.03	0.024	0.16	0.05
	C11 head of C11-C13NN-C0	0.61	0.66	0.03	0.028	0.14	0.05
	C13 head of C11-C13NN-C3*	0.58	0.64	0.03	0.025	0.13	0.05
	C13 head of C11-C13NS-C4	<u>0.60</u>	<u>0.65</u>	<u>0.03</u>	<u>0.028</u>	<u>0.14</u>	0.05
	Av.	0.60	0.65	0.03	0.026	0.14	
U. S. Steel	C9 head of C9-C11NN-C9	0.62	0.72	0.03	0.022	0.19	0.04
	C11 head of C11-C13NN-C0	0.61	0.66	0.035	0.023	0.15	(V not checked)
	C13 head of C11-C13NN-C3*	<u>0.57</u>	<u>0.64</u>	<u>0.029</u>	<u>0.023</u>	<u>0.15</u>	0.0?
	Av.	0.60	0.67	0.03	0.023	0.16	
American Bridge Company, (Six Sample Bars, 1927)	Av.	0.59	0.66	0.030	0.041	0.145	
	Min.	0.55	0.64	0.021	0.036	0.112	

*Samples from broken head of eyebar No. 330.

TABLE 6

Summary of Mechanical Properties of Eyebar Steel
From Point Pleasant Bridge

<u>Laboratory/Specimen Source</u>	<u>Yield Strength 0.2% Offset ksi.</u>	<u>Tensile Strength ksi.</u>	<u>Elongation, % 1"</u>	<u>Reduction Area, %</u>
Nat'l. Bureau of Standards				
C0, C9 Outer Layer	86.1	121.3	21	52
Inner Layer	71.2	117.7	22	48
Estimate for Bar*	81.0	120.0	21	50
C3 Outer Layer	85.4	120.9	19	52
Inner Layer	69.2	114.2	21	51
Estimate for Bar*	80.0	119.0	20	51
U. S. Steel Laboratory				
C9 Outer Layer	86.0	121.7	18	51.8
Inner Layer	69.8	116.2	20	50.6
C0 Outer Layer	85.6	120.2	18	54.3
Inner Layer	71.4	118.6	19	49.7
C3 Outer Layer	84.5	119.1	20	52
Inner Layer	68.0	117.7	21	51

TABLE 6 CONTINUED

<u>Laboratory/Specimen Source</u>	<u>Yield Strength 0.2% Offset ksi.</u>	<u>Tensile Strength ksi.</u>	<u>Elongation, % 1"</u>	<u>Reduction Area, %</u>
Battelle Memorial Laboratory (Control tests of material used for sustained load experiments on material from surface layers, eyebar No. 330)	87.5	110.4	20	
Bureau of Public Roads (Control tests of material used for fatigue experiments, specimens extend through thickness)	79.0	116.0	21	

*Estimate for bar computed as weighted average of one inner layer and two outer layers.

Notes for Table 6

C9 is from the C9 head of eyebar C9-C11NN

C0 is from the C11 head of eyebar C11-C13NN (Eyebar No. 330)

C3 is from the C13 head of eyebar C11-C13NN (Eyebar No. 330)

C4 is from the C13 head of eyebar C11-C13NS (Eyebar No. 33)

TABLE 7

<u>Eyebar Position</u>	<u>Area</u>	<u>Live Load Tension</u>	<u>Live Load Compression</u>	<u>Range of Load</u>	<u>Maximum Range of Unit Stress psi. Edge of Hole Concentration</u>	<u>Nominal</u>
U ₀ U ₁	43.5	541		541	34,500	12,450
U ₁ U ₃	48.0	753	-312	1065	61,500	22,200
U ₃ U ₅	51.0	857	-346	1203	65,500	23,600
U ₅ U ₇	51.0	848	-423	1271	69,200	25,000
U ₇ U ₉	45.0	562		562	34,800	12,500
C ₉ C ₁₁	46.5	571		571	34,000	12,300
C ₁₁ C ₁₃	46.5	582		582	34,800	12,500
C ₁₃ C ₁₅	48.0	592		594	34,400	12,400

APPENDIX A

EXCERPTS FROM REPORT OF E. G. WILES ON REASSEMBLY
SITE WORK, SPECIMEN IDENTIFICATION, AND
FRACTURE CATALOGUE

APPENDIX A

NOTES

- 1 All measurements of fracture locations to nearest foot.
- 2 Samples prefixed with "H" are those selected by R. A. Hechtman and shipped to NBS. Samples prefixed "HH" are those selected by R. A. Hechtman and shipped to BPR.

NOTATION

- FC - Flame Cut
- CL - Cleavage
- SH - Shear
- CS - Cleavage and Shear
- ⑤ Positive Match Point
- BPR ○ Shipped to BPR (1st ship)
- BPR ○ Shipped to BPR (2nd ship)
- NBS △ Shipped to NBS
- USS □ Shipped to USS
- BTL ○ Shipped to BATTELLE

MISCELLANEOUS SAMPLES

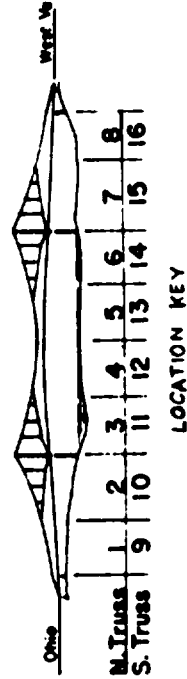
- Samples selected and shipped to Fritz Engineering Laboratory by Modjeski & Masters
1. Eyebars 25'-4" ± c.c. pin holes, yellow paint number 11 with original 1 1/2" diameter pin assembled in one end.
 2. Eyebars 25'-4" ± c.c. pin holes, yellow paint number 10, also numbered MM36
 3. 2 pins 1 1/2" diameter, 1'-1 1/2" long with 4" ring on each.
 4. Pin 1 1/2" diameter, 1'-5 1/2" long with 3" ring
 5. Pin 1 1/2" diameter, 1'-5 7/8" long, no ring

MISCELLANEOUS SAMPLES

- Gusset Plate U3 S BPR ○ HH2
- Gusset Plate U3 S S.E. BPR ○ HH3
- Upper end of chain bent post
- L0 U0 N. side Ohio end NBS △
- Short section of 2 eyebars
- B ± and 15' ± long NBS △
- Three pins, all the same length that would fit in joint C13
- Two pins include hanger plate NBS △
- Eyebars 51'-4 3/4" c.c. pin holes, numbered MM32, NBS △
- Eyebars 51'-4 3/4" c.c. pin holes, numbered M31, NBS △
- Eyebars 51'-4 3/4" c.c. pin holes, numbered 50, MM15 NBS △
- Eyebars 44'-4 3/4" c.c. pin holes, numbered MM10, NBS △
- Retainer cap and bolt BPR ○ HH4, unidentified

MISCELLANEOUS SAMPLES

- Eyebars heads from Ohio shore wreckage
- From eyebars designated as MM11, BTL ○
- From eyebars designated as #3, BTL ○ & BTL ○
- From eyebars designated as #5, BTL ○ & BTL ○
- From eyebars designated as #7, BTL ○ & BTL ○
- From eyebars designated as MM14, BTL ○
- From eyebars designated as MM7, BTL ○
- From eyebars designated as MM18, BTL ○



TRUSS AND EYEBAR REASSEMBLY WITH
FRACTURE NOTES AND SAMPLE LOCATIONS
Appendix A

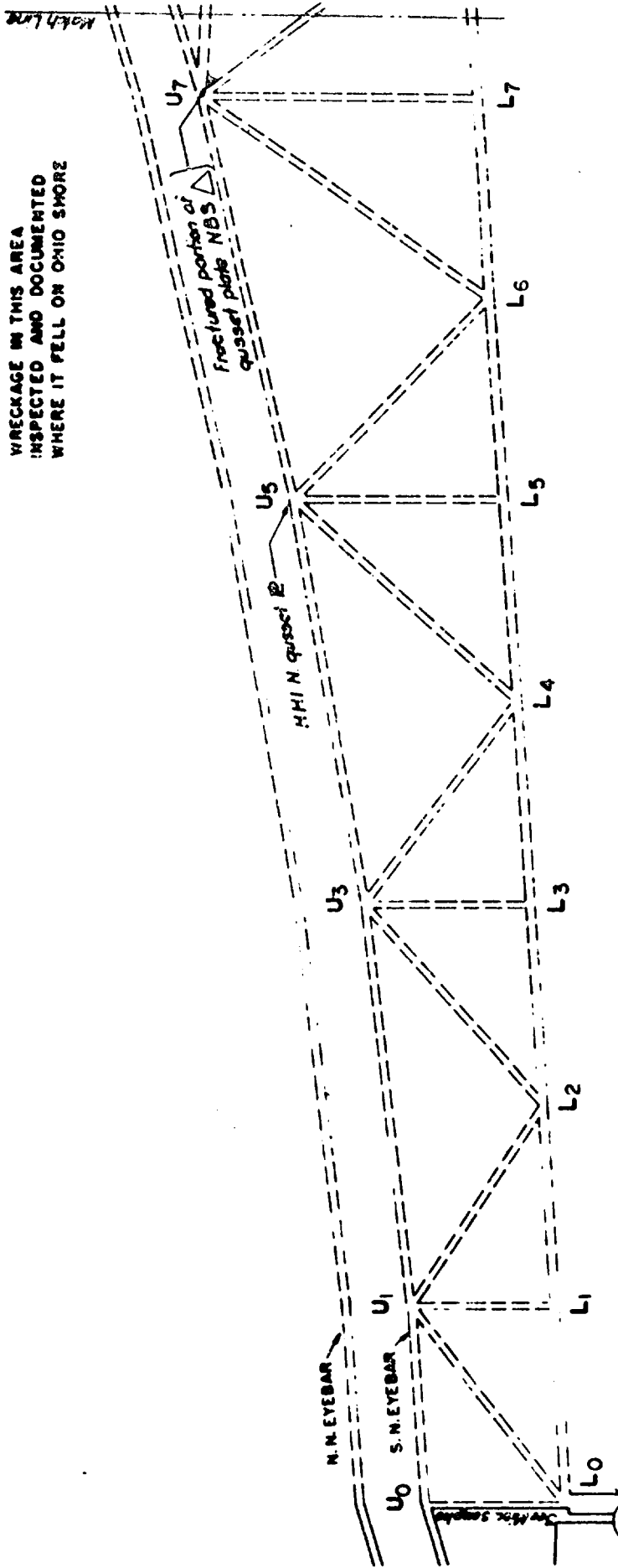
APPENDIX A

DR. 2



NORTH TRUSS
LOCATION KEY

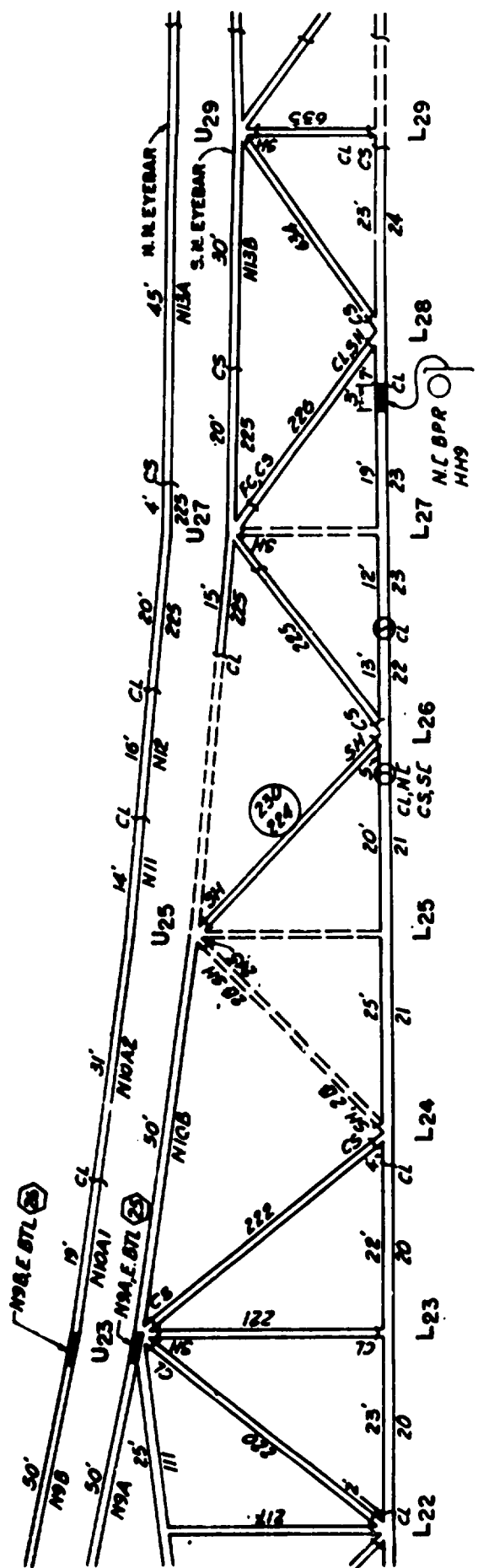
WRECKAGE IN THIS AREA
INSPECTED AND DOCUMENTED
WHERE IT FELL ON OHIO SHORE



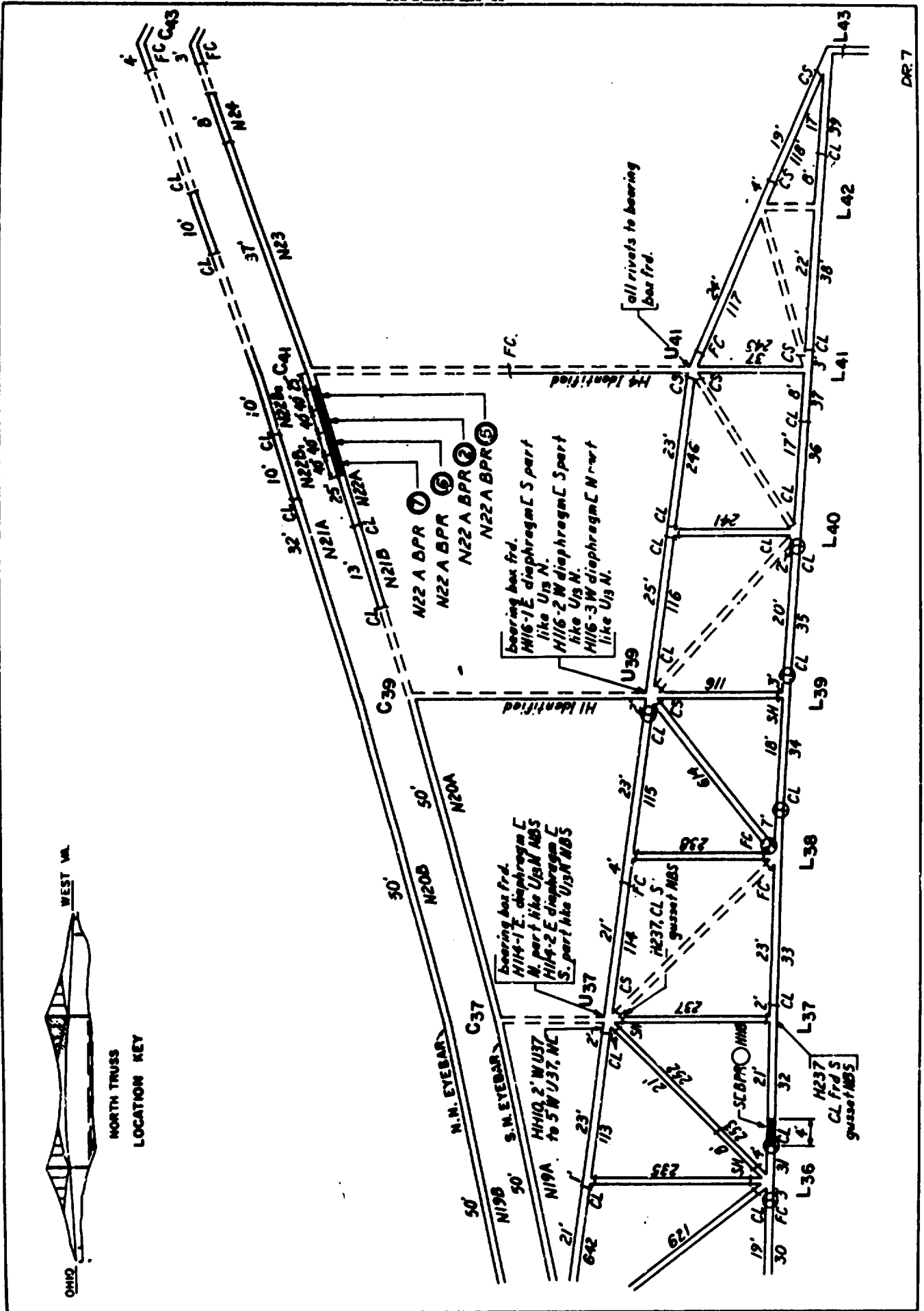
APPENDIX A



NORTH TRUSS
LOCATION KEY



APPENDIX A

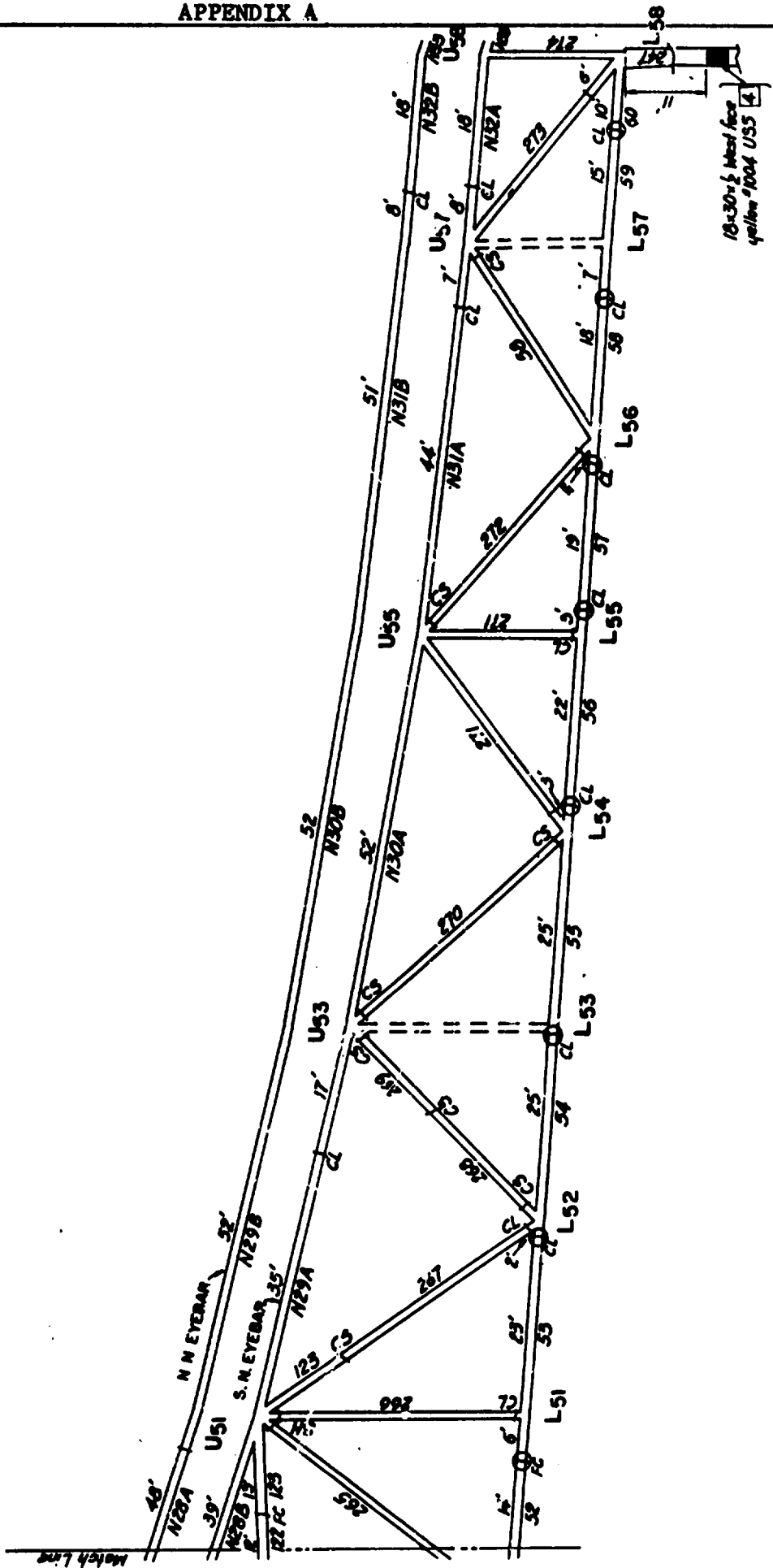


DR.7

APPENDIX A



NORTH TRUSS
LOCATION KEY



APPENDIX A

DR. 10

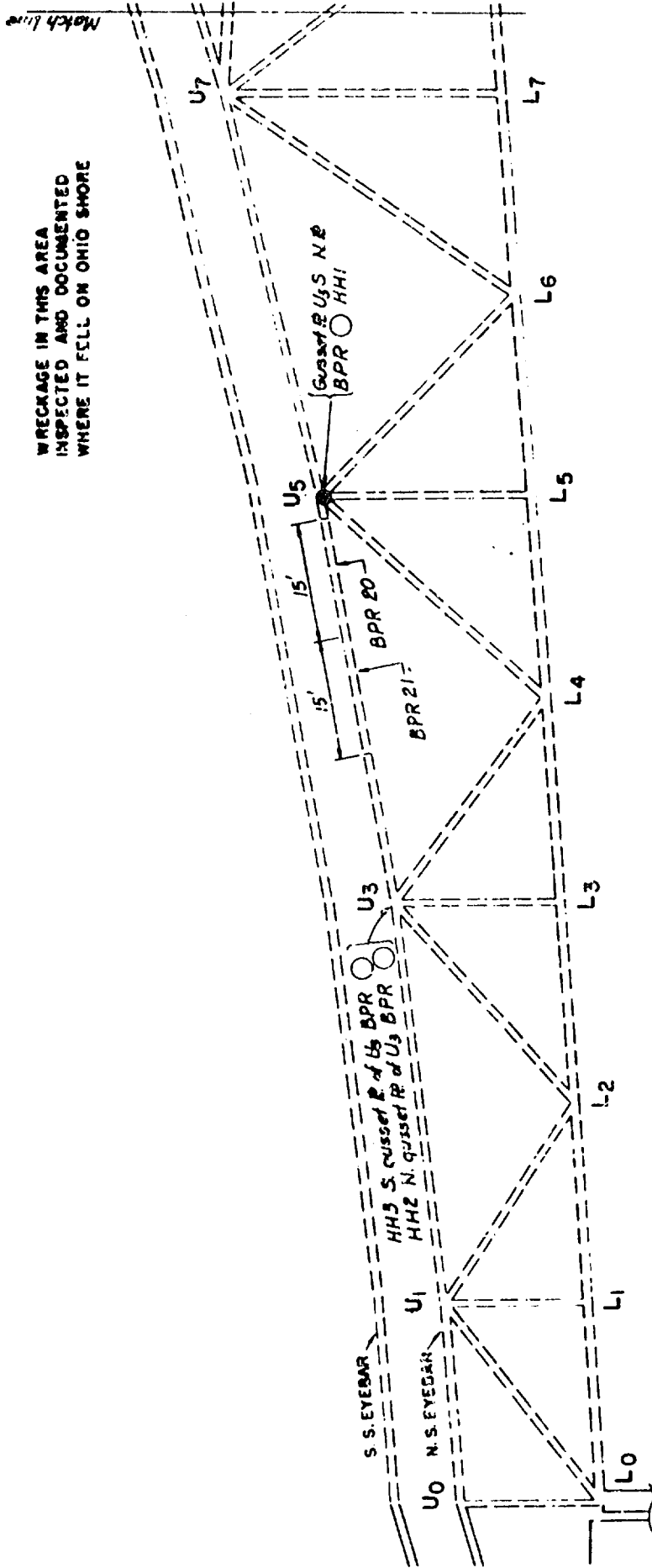
WRECKAGE IN THIS AREA
INSPECTED AND DOCUMENTED
WHERE IT FELL ON OHIO SHORE



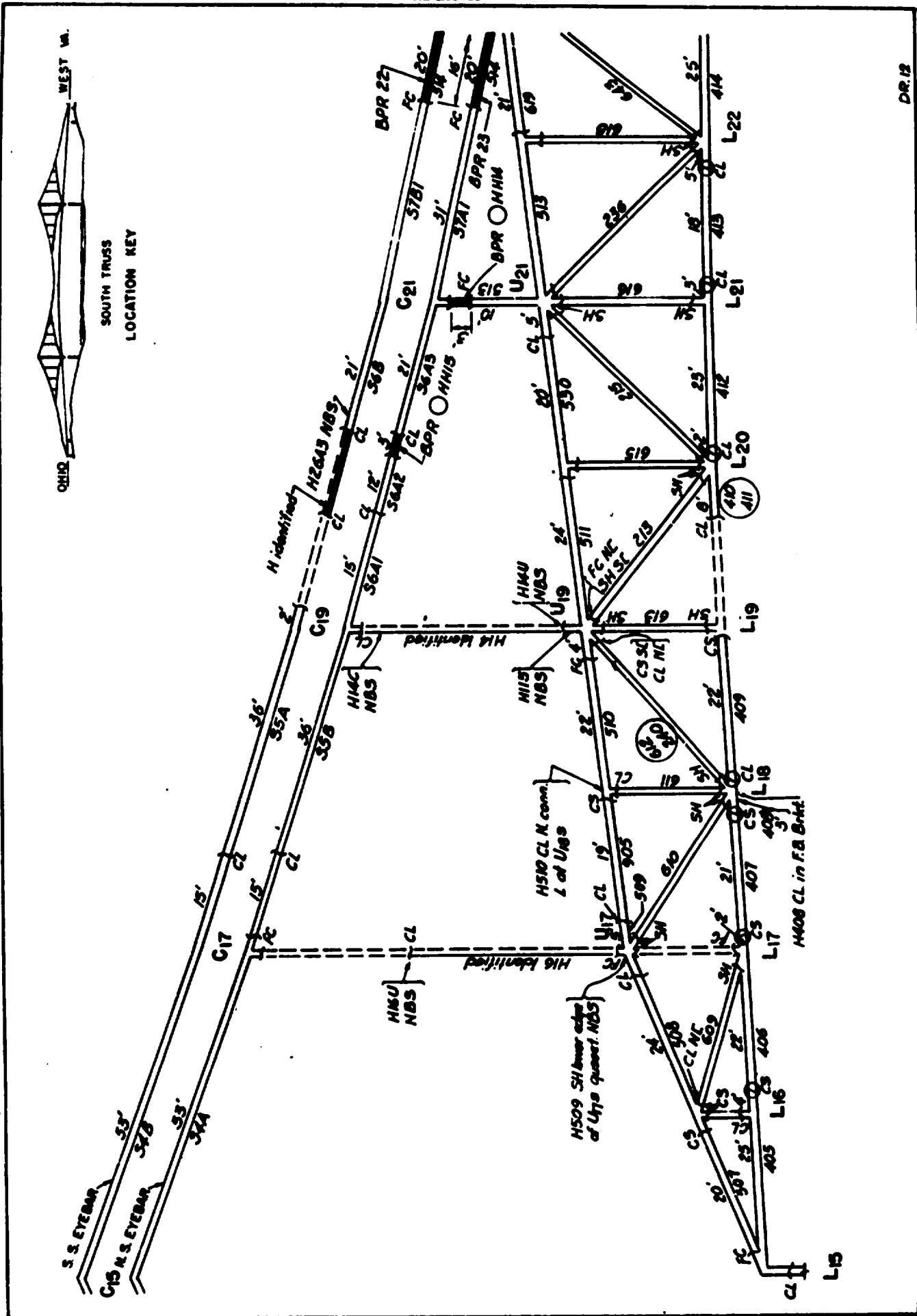
OHIO

WEST

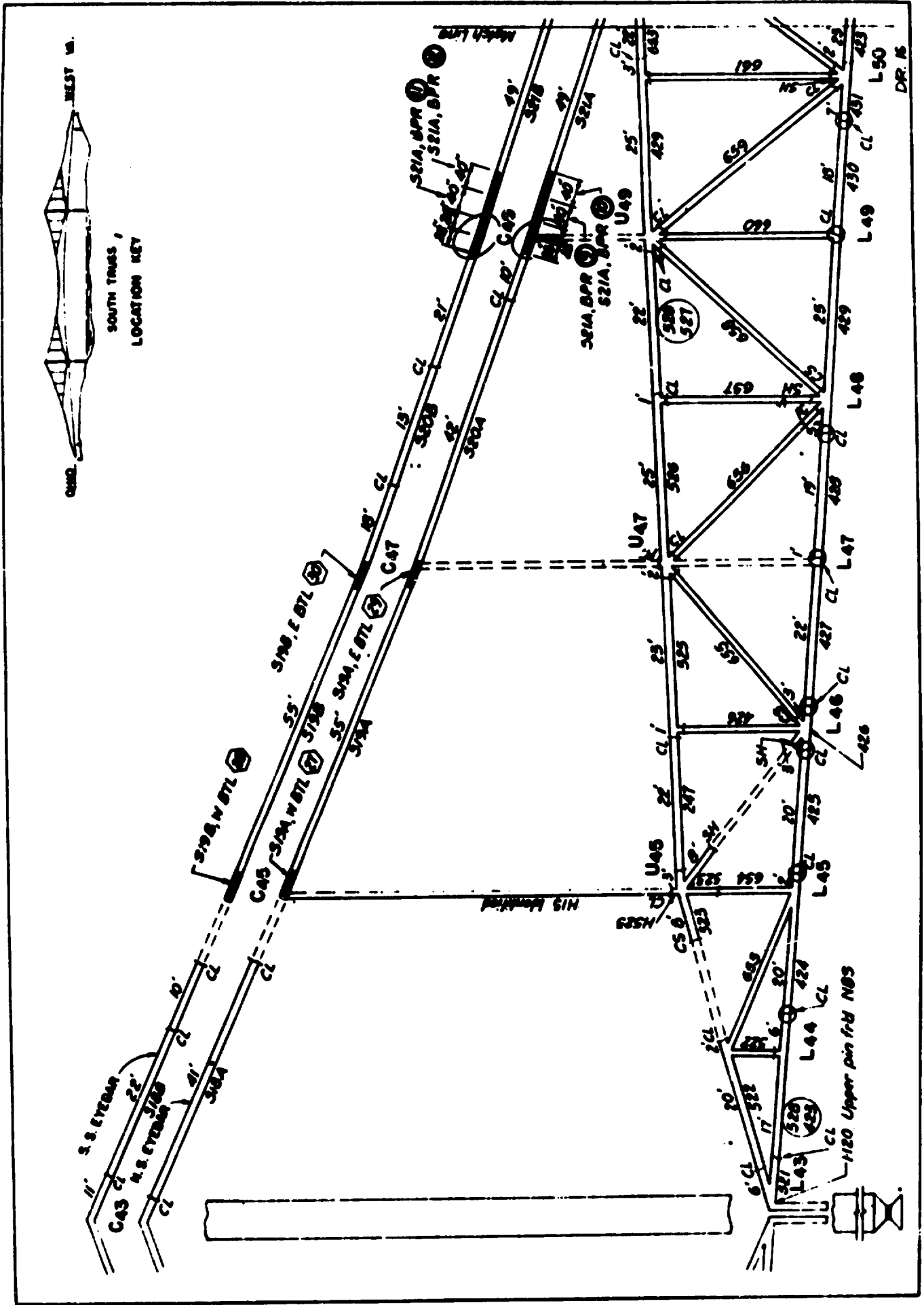
SOUTH TRUSS
LOCATION KEY



APPENDIX A



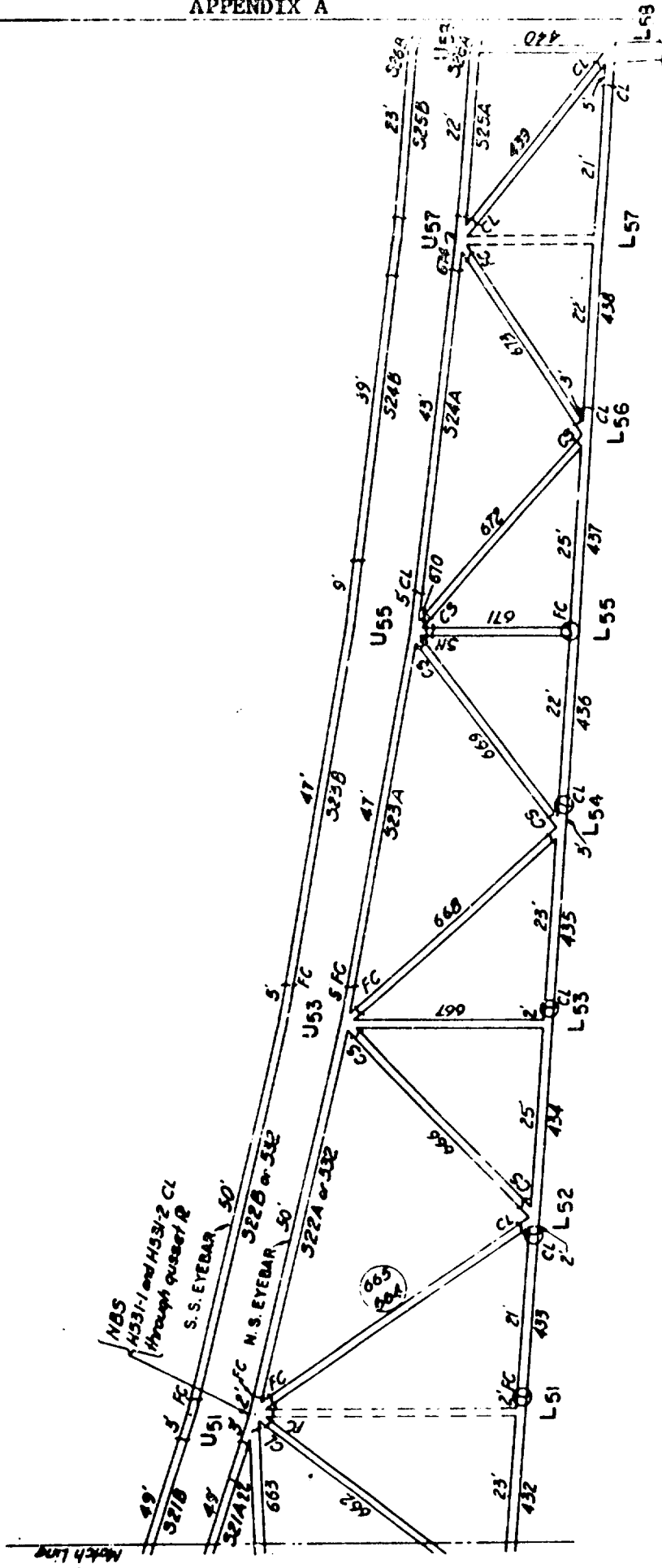
APPENDIX A



APPENDIX A



SOUTH TRUSS
LOCATION KEY



APPENDIX B

LABORATORY DATA ON PROPERTIES OF EYEBAR STEEL
AND A7-24 STEEL FROM POINT PLEASANT BRIDGE

APPENDIX B
 NATIONAL BUREAU OF STANDARDS TEST RESULTS

Table A1. Hardness Test Results,
 Eye CO, Segment 1.

Distance from south face		Vickers hardness number			
		Spec. A	Spec. D	Spec. F	Spec. H
0.5 mm	0.02 in.	245	238	233	210
1.0	.04	251	245	243	240
1.5	.06	253	245	251	243
2.5	.10	262	253	254	249
3.5	.14	264	251	251	249
4.5	.18	260	253	253	256
8.5	.33	258	256	254	258
12.5	.49	258	254	247	254
15.5	.61	251	253	249	253
22.5	.89			242	

Distanc e from north face		Vickers hardness number			
		Spec. C	Spec. E	Spec. G	Spec. J
0.5 mm	0.02 in.	232	216	212	213
1.0	.04	242	227	230	227
1.5	.06	243	233	235	235
2.5	.10	245	238	243	243
3.5	.14	251	242	245	242
4.5	.18	254	254	242	253
8.5	.33	258	254	253	254
12.5	.49	253	256	249	254
15.5	.61	249	249	251	253
22.5	.89			236	254

APPENDIX B
NATIONAL BUREAU OF STANDARDS TEST RESULTS

Table A1. (Cont.) Hardness Test Results,
Eye CO, Segment 1.

Distance from hole		Vickers hardness number		
		Spec. A	Spec. B	Spec. C
0.5 mm	0.02 mm	262	253	266
1.0	.04	264	254	262
1.5	.06	266	249	260
2.0	.08	262		258
2.5	.10	260	260	
3.0	.12	260		254
3.5	.14	258		262
4.0	.16	258		262
4.5	.18	262	251	258
8.5	.33		249	
15.5	.16		245	

Note: All measurements on specimens A and C were made approximately 4 mm (0.16 in.) from the face of the bar.

APPENDIX B

NATIONAL BUREAU OF STANDARDS TEST RESULTS

Table A2. Hardness Tests Results,
Eye C9, Segment 1.

Distance from south face*		Vickers hardness number			
		Spec. A	Spec. D	Spec. F	Spec. H
0.5 mm	0.02 in.	260	243	258	230
1.0	.04	256	247	262	243
1.5	.06	256	249	268	242
2.5	.14	254	262	260	264
4.5	.18	264	245	262	25P
8.5	.33		247	251	251
12.5	.49		242	242	247
15.5	.61		233	240	
22.5	.89		232	235	

* See text

Distance from north face		Vickers hardness number			
		Spec. C	Spec. E	Spec. G	Spec. J
0.5 mm	0.02 in.	247	235	236	216
1.0	.04	245	242	247	240
1.5	.06	254	253	251	245
2.5	.10	260	264	254	247
3.5	.14	270	266	258	254
4.5	.18	266	266	266	260
8.5	.33	260	260	258	254
12.5	.49	247	251	249	254
15.5	.61	242	243	247	256
22.5	.89		236	242	

APPENDIX B

NATIONAL BUREAU OF STANDARDS TEST RESULTS

Table A2. (Cont.) Hardness Test Results,
Eye C9, Segment 1.

Distance from hole		Vickers hardness number		
		Spec. A	Spec. B	Spec. C
0.5 mm	0.02 in.	256	238	270
1.0	.04	254	236	268
1.5	.06	253	236	274
2.0	.08	258		270
2.5	.10	256	240	268
3.0	.12	254		274
3.5	.14	253	236	266
4.0	.16	251		268
4.5	.18	254	233	266
8.5	.33		232	
15.5	.61		235	

Note: All measurements on specimens A and C were made approximately 2.5 mm (0.10 in.) from the face of the bar.

APPENDIX B

NATIONAL BUREAU OF STANDARDS TEST RESULTS

Table A3. Hardness Test Results,
Eye C3, Segment O

Specimen A - Plane 0.11 in. from south face

Distance from hole		Vickers hardness numbers			
1.0 mm	0.04 in.	258	260		
3	.12	256	256		
5	.20	260	256		
7	.28	262	270		
9	.35	266	266		
11	.43	266	268		
13	.51	268	268		

Specimen B - Plane 0.6 in. from south face

Distance from hole		Vickers hardness numbers			
1.0 mm	0.04 in.	230			
2	.08	232	247	245	245
3	.12	227	238		
4	.16	230	236		
5	.20	227	232		
6	.24	228	230		
7	.28	232	235		
8	.31	235	232		
9	.35	232			
10	.39	228			
11	.43	232			
12	.47	233			

APPENDIX B

NATIONAL BUREAU OF STANDARDS TEST RESULTS

Table A3. (Cont.) Hardness Test Results,
Eye C3, Segment O

<u>Specimen I - Plane 0.8 in. from south face</u>			
Distance from hole		Vickers hardness number	
1.0 mm	0.04 in.	247	251
3	.12	238	236
5	.20	240	238
7	.28	240	236
9	.35	233	235
11	.43	235	233

<u>Specimens II and III - Planes parallel to faces</u>			
Distance from fracture		Vickers hardness numbers	
		II-close to north face	III-1/4 in. from north face
1.0 mm	0.04 in.	232	249
2	.08	230	247
3	.12	232	247
4	.16	230	249
5	.20	233	251
6	.24	235	251
7	.28	236	
8	.31	232	
9	.35	228	

<u>Specimen IV - Plane 5 in. from hole surface</u>			
Distance from north face		Vickers hardness numbers	
0.5 mm	0.02 in.	209	
1	.04	233	
2	.08	251	
3	.12	251	
4	.16	251	
5	.20	251	

APPENDIX B
NATIONAL BUREAU OF STANDARDS TEST RESULTS

Table A3. (Cont.) Hardness Test Results,
Eye C3, Segment O

Specimen V, Plane 0.6 in. from hole surface

Distance from south face		Vickers hardness numbers
0.5 mm	0.02 in.	221
1	.04	233
2	.08	247
3	.12	254
4	.16	256
5	.20	258
6	.24	256
7	.28	256
8	.31	253
9	.35	249
10	.43	247
11	.43	247
12	.47	243
13	.51	240
14	.55	242
15	.59	242
16	.63	235
17	.67	238
18	.71	235

APPENDIX B

NATIONAL BUREAU OF STANDARDS TEST RESULTS

Table A4. Hardness Test Results,
Eye C3, Segment 1

Distance from south face		Vickers hardness number			
		Spec. 1	Spec. 3	Spec. 5	Spec. 7
0.5 mm	0.02 in.	221	240	245	236
1	.04	236	242	240	243
3	.12	247	254	251	254
5	.20	254	253	258	247
7	.28	254	245	264	245
9	.35	243	243	258	245
11	.43	240	240	254	245
13	.51	243	242	247	225
15	.59	238	233	249	243
17	.67	240	236	247	243
19	.75	236	233	245	242
21	.83	235	236	242	235
23	.91	230	228	240	228
25	.98	228	233	236	236
27	1.06	230	233	236	238

Distance from north face*					
16	.63	230	235	247	245
14	.55	235	233	243	242
12	.47	240	236	245	242
10	.39	243	243	251	254
8	.31	243	243	245	249
6	.24	251	249	245	253
4	.16	251	247	245	254
3	.12	247	240	243	
2	.08	247	247	249	249
1	.04	251	247		

* See text

APPENDIX B
NATIONAL BUREAU OF STANDARDS TEST RESULTS

Table A5. Hardness Test Results,
Eye C4

Distance from south face		Vickers hardness numbers	Distance from hole		Vickers hardness numbers
0.5 mm	0.02 in.	210	0.5 mm	.02 in.	251
1.0	.04	221	1.0	.04	251
1.5	.06	229	1.5	.06	249
2.0	.08	232	2.0	.08	246
2.5	.10	234	2.5	.10	254
3.0	.12	234	3.5	.14	244
3.5	.14	239	4.5	.18	249
4.0	.16	241	5.5	.22	254
4.5	.18	246	6.5	.26	246
5.0	.20	239	7.5	.30	249
5.5	.22	254	8.5	.33	246
6.0	.24	251	9.0	.35	251
6.5	.26	251			
7.0	.28	254			
7.5	.30	244			
8.0	.31	246			
8.5	.33	241			
9.0	.35	254			
9.5	.37	254			
10.0	.39	251			

The above measurements
were made 0.4 in. from
the south face.

APPENDIX B

NATIONAL BUREAU OF STANDARDS TEST RESULTS

Table A6. Tension Tests,
Specimens and Conditions

Specimen No.	Outer Layers	Center Layer	Static Strain Rate	100 ksi per Minute
2	x		x	
6	x			x
10	x		x	
14	x			x
<hr/>				
17		x	x	
21		x	x	
25		x	x	
29		x	x	
<hr/>				
32	x		x	
36	x			x
40	x		x	
44	x			x

APPENDIX B
NATIONAL BUREAU OF STANDARDS TEST RESULTS

Table A7. Tension Test Results,
Eye CO, Segment 2

Specimen No.	Yield Strength	Tensile Strength	Elongation	Reduction of Area
2	89.5 ksi	120.3 ksi	20%	55%
6	90.0	123.2	20	52
10	88.0	119.9	22	52
14	86.6	122.0	24	53
17	73.6	120.1	22	49
21	72.4	119.5	21	47
25	71.6	119.4	22	48
29	72.5	119.7	22	51
32	88.1	122.4	21	51
36	87.9	123.9	20	51
40	87.2	122.4	21	54
44	85.5	123.5	20	54

APPENDIX B
NATIONAL BUREAU OF STANDARDS TEST RESULTS

Table A8. Tension Test Results,
Eye CO, Segment 3

Specimen No.	Yield Strength	Tensile Strength	Elongation	Reduction of Area
2	85.7 ksi	120.0 ksi	22%	51%
6	86.8	122.2	19	53
10	83.3	118.1	21	49
14	82.2	120.5	20	51
17	72.1	117.4	23	50
21	72.5	119.0	20	46
25	71.2	117.8	21	47
29	72.0	118.1	21	48
32	86.9	123.0	21	50
36	86.6	123.3	22	53
40	84.9	120.9	21	52
44	82.1	121.8	20	49

APPENDIX B

NATIONAL BUREAU OF STANDARDS TEST RESULTS

Table A9. Tension Test Results,
Eye C9, Segment 5

Specimen No.	Yield Strength	Tensile Strength	Elongation	Reduction of Area
2	83.7 ksi	118.6 ksi	21%	50%
6	84.2	120.3	21	52
10	87.4	117.9	22	54
14	86.2	121.7	21	54
17	68.1	112.5	22	51
21	66.3	112.0	24	51
25	67.8	114.7	22	51
29	74.3	121.6	22	50
32	87.6	121.5	21	48
36	85.6	122.0	21	52
40	84.7	119.2	21	53
44	86.3	122.6	22	54

APPENDIX B

NATIONAL BUREAU OF STANDARDS TEST RESULTS

Table A10. Tension Test Results,
Eye C3, Segment 2

Specimen No.	Yield Strength	Tensile Strength	Elongation	Reduction of Area
2	83.4 ksi	117.7 ksi	19%	53%
6	86.2	120.5	19	51
10	86.4	121.6	19	52
14	85.7	123.9	18	51
17	67.8	111.4	22	52
25	70.6	117.1	20	50

APPENDIX B
 NATIONAL BUREAU OF STANDARDS TEST RESULTS

Table All. Charpy V-notch Impact Test Results
 Eye CO, Segment 2

		Test Temperature, F								
		32	75	125	165	190	212	230	250	
1	03	26	01	08	09	13	04	05	15	
2	3	2.5	5	5	8	10.5	15	20	24	
3	10	-	20	15	20	20	35	40	55	
4	2	-	6	4	7	9	8	18	23	
1	07	33	28	27	12	16	23	24	20	
2	3	2	2	4	10	9	16	20	23.5	
3	5	0	5	10	15	15	25	35	50	
4	2	0	0	3	9	8	14	20	22	
1	11	37	38	31	30	35	42	43	39	
2	2.5	2	2.5	4.5	5.5	8.5	12	21.5	24	
3	10	0	5	5	15	20	30	40	50	
4	1	0	1	3	5	7	11	17	22	
1	18	41			34					
2	2	4			6					
3	5	0			15					
4	0	1			6					
1	22									
2	2									
3	0									
4	0									

Code

1. Specimen no.
2. Fracture energy, ft-lb
3. Percent shear
4. Lateral expansion, 10^{-3} in.

APPENDIX B

NATIONAL BUREAU OF STANDARDS TEST RESULTS.

Table A12. Charpy V-notch Impact Test Results
Eye CO, Segment 3

			Test Temperature, F						
32			75	125	165	190	212	230	250
1	03	26	09	12	13	15	05	08	01
2	2	2	2.5	4	5.5	13	14.5	20.5	23
3	0	0	5	5	15	15	15	35	55
4	0	0	1	2	5	12	13	20	22
1	07	33	28	23	16	20	24	27	19
2	2	2	2	4	10	8	15	20	24.5
3	0	0	0	5	15	20	35	45	60
4	0	1	0	4	9	8	15	18	23
1	11	37	34	42	30	39	43	45	38
2	2	4	3	4	5	7.5	12	15	21.5
3	0	0	5	10	15	25	20	35	35
4	0	1	1	3	5	8	11	14	20
1	18	41			35				
2	2.5	2			9.5				
3	0	0			15				
4	1	1			6				
1	22								
2	2								
3	0								
4	0								

Code

1. Specimen no.
2. Fracture energy, ft-lb
3. Percent shear
4. Lateral expansion, 10^{-3} in.

APPENDIX B

NATIONAL BUREAU OF STANDARDS TEST RESULTS

Table A13. Charpy V-notch Impact Test Results
Eye C9, Segment 5

		Test Temperature, F							
		32	75	125	165	190	212	230	250
1	03	26	08	13	09	05	01	12	04
2	2	2	3	5.5	8	10	9.5	23.5	25.5
3	5	0	10	10	20	25	30	40	45
4	1	0	1	4	6	11	9	22	23
1	07	33	20	27	28	24	19	30	23
2	2.5	3.5	3	3	-	10	13	17	33.5
3	5	10	5	5	15	20	30	25	70
4	1	2	1	6	4	10	13	15	30
1	11	37	39	35	31	43	38	34	42
2	2.5	2.5	5	5.5	7	10	12.5	20.5	26
3	5	5	10	25	20	20	35	40	60
4	1	1	4	4	6	9	11	19	22
1	18	41			45				
2	2.5	3.5			6.5				
3	0	10			20				
4	0	3			6				
1	22								
1	2								
3	0								
4	1								

Code

1. Specimen no.
2. Fracture energy, ft-lb
3. Percent shear
4. Lateral expansion, 10^{-3} in.

APPENDIX B

NATIONAL BUREAU OF STANDARDS TEST RESULTS

Table A14. Charpy V-notch Impact Test Results
Eye C3, Segment 2

		Test Temperature, F					
		32	120	180	212	230	250
1	01	04	07	03	05	08	
2	3.5	5	10.5	19	23.5	30	
3	10	15	25	30	45	60	
4	2	3	9	16	19	25	
1		15	13	09	11	12	
2		8	9.5	14	13.5	27	
3		15	25	30	40	55	
4		5	8	11	12	22	
1	18	16	24	26	27	19	
2	2	4.5	8.5	13	18	32.5	
3	0	5	15	25	35	70	
4	0	3	8	12	16	30	

Code

1. Specimen no.
2. Fracture energy, ft-lb
3. Percent shear
4. Lateral expansion, 10^{-3} in.

APPENDIX B

NATIONAL BUREAU OF STANDARDS TEST RESULTS

Table A15. Drop Weight Test Results

Specimens 5/8" x 2" x 6", welded and notched
Machine - 60 lb, anvil clearance 0.075 in.,
height of drop 5 ft.

Specimen Number	Test Temperature	Break	No Break
965	210 F		x
971	190		x
972	170		x
966	75	x	
061	100	x	
066	130	x	

Point Pleasant Bridge
 USSteel Results
 February 11, 1969
 Revised: February 26, 1969

APPENDIX B

U. S. STEEL LABORATORY DATA

Composition (C9 and C0)

C9 is C9 head of C9-C11 NN
 C0 is C11 head of C11-C13NN(330)

	<u>C</u>	<u>Mn</u>	<u>P</u>	<u>S</u>	<u>Si</u>	<u>Cu</u>	<u>Ni</u>	<u>Cr</u>	<u>Mo</u>	<u>N</u>
C9	0.62	0.72	0.022	0.030	0.19	0.038	0.008	0.014	0.007	0.004
C0	0.61	0.66	0.023	0.035	0.15	0.015	0.010	0.014	0.008	0.005

APPENDIX B

U. S. STEEL LABORATORY DATA

Point Pleasant Bridge
U. S. Steel Results
February 14, 1969

Tensile Properties (C9)
(Standard 0.252" Diameter Specimens)

Segment (S ¹)	Specimen No. (2)	Strain Rate to Yield	Yield Strength at 0.2% Offset, ksi	Tensile Strength, ksi	Elongation in 1 Inch, %	Reduction of Area, %
Layer A ³⁾	6	Normal ⁵⁾	85.2	120.7	19.0	51.8
	14	"	85.2	125.8	18.0	51.8
	36	"	86.5	121.3	17.0	52.8
	44	"	88.9	126.3	18.0	53.8
Layer A	2	Static	78.7	118.7	19.0	51.3
	10	"	81.2	118.7	19.0	50.2
Center	17	"	61.5	111.3	20.0	50.5
	21	"	68.1	112.7	20.0	50.8
	25	"	67.6	116.3	20.0	50.5
	29	"	78.7	124.8	19.0	50.8
	32	"	83.5	120.8	17.0	49.0
40	"	83.0	121.3	19.0	53.9	
Layer B	6	Normal	86.2	120.7	18.0	52.4
	14	"	80.1	121.2	16.0	43.2
	36	"	86.7	121.2	17.0	52.4
	44	"	89.2	123.7	16.0	46.2
Layer A	2	Static	80.7	119.7	19.0	53.0
	10	"	78.5	119.3	19.0	52.4
Center	17	"	66.6	113.7	20.0	49.6
	21	"	67.2	115.2	19.0	48.5
	25	"	70.1	118.3	19.0	50.0
	29	"	79.0	122.8	16.0	40.0
Layer B	32	"	85.0	121.8	18.0	51.2
	40	"	84.8	122.2	18.0	51.4

- NOTES: 1) See Sketch C of Laboratory Specimen Plan.
 2) See Sketch D of Laboratory Specimen Plan.
 3) Layer A is adjacent to ground surface.
 4) Layer B is on opposite side where 0.05 inch was removed to dress up surface.
 5) Approximately 80 ksi/min.

United States Steel Corporation
 U. S. Steel Research
 February 14, 1963

U. S. STEEL LABORATORY DATA

Sample Properties (CO)

<u>Segment S51)</u>	<u>Specimen No. 2)</u>	<u>Strain Rate to Yield</u>	<u>Yield Strength at 0.2% Offset, ksi</u>	<u>Tensile Strength, ksi</u>	<u>Elongation in 1 Inch, %</u>	<u>Reduction of Area, %</u>
Layer A ⁶⁾	6	Normal ⁵⁾	87.5	119.8	18.0	54.4
Layer B ⁶⁾	14	"	83.5	118.3	18.0	54.4
	36	"	86.5	121.8	18.0	52.0
	44	"	83.5	119.6	18.5	55.5
Layer A	2	Static	88.5	120.3	18.0	52.4
	10	"	83.5	118.8	19.0	56.0
Center	17	"	71.6	119.3	19.0	47.6
	21	"	--	118.6	19.0	48.0
	25	"	69.6	118.7	19.0	43.6
	29	"	74.1	117.6	19.0	54.4
Layer B	32	"	86.7	122.7	18.0	50.6
	40	"	83.7	120.2	20.0	54.5

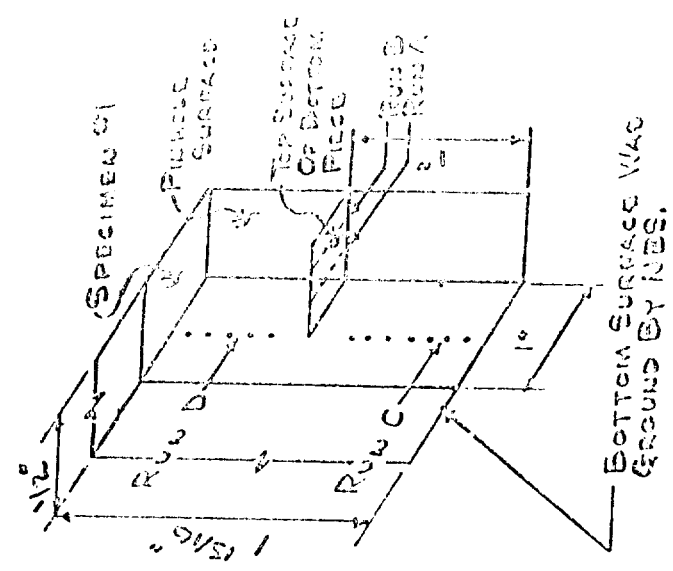
6) Layers A and B are adjacent to opposite surfaces, and 0.05 inch was removed to dress up surfaces.

1944
 U. S. STEEL LABORATORY
 PITTSBURGH, PA. 15205
 REVISION 100, 80, 1958

Hardness Tests (05)
Segment 801 Specimen A28

(Readings are Vickers hardness (DPH), Approximate Rockwell C conversion hardness values as determined from Wilson Conversion Chart are also shown).

Distance ³⁾ From Edge, in.	Run A		Run B		Run C		Run D	
	DPH	Rc	DPH	Rc	DPH	Rc	DPH	Rc
0.015	257	24.0	249	23.0	257	24.0	251	23.0
0.065	257	24.0	249	23.0	262	25.0	260	24.5
0.115	260	24.5	265	25.0	268	25.5	260	27.0
0.165	260	24.5	260	24.5	277	27.0	265	23.0
0.215	249	23.0	245	22.0	274	26.5	260	27.0
0.265	249	23.0	246	22.0	262	25.0	260	27.0
0.315	234	20.0	234	20.0	263	25.5	269	30.0
0.365	244	21.5	249	23.0	271	26.5	277	27.0
0.415	254	23.5	249	23.0	254	23.5	271	26.0
0.465	251	23.0	260	24.5	257	24.0	265	23.0
0.515	251	23.0	257	24.0	251	23.0	271	26.0
0.565	249	23.0	249	23.0	246	22.0	260	25.5
0.615					251	23.0	254	23.5
0.665					260	24.5	254	23.5
0.715					254	23.5	257	24.0
0.765					260	24.5	265	25.0
0.815					257	24.0		
0.865					254	23.5		
0.915			257	24.0				
0.965			260	24.5				



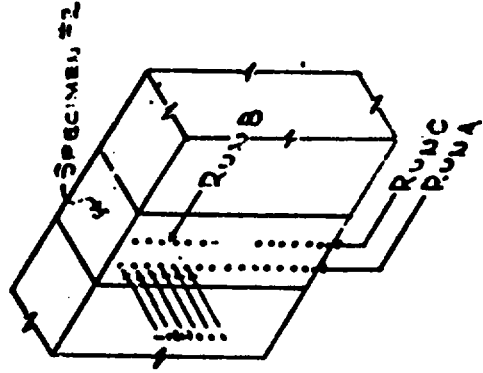
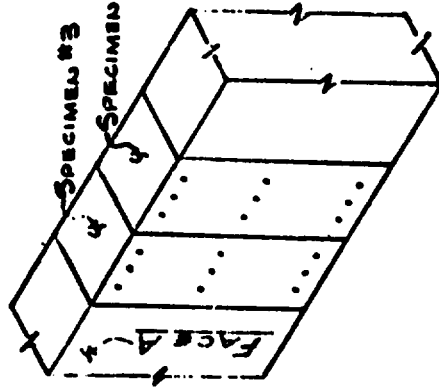
- Notes: 1) See Sketch C of Laboratory Specimen Plan.
 2) See Sketch B of Laboratory Specimen Plan.
 3) First reading was 0.01/0.02 inch from edge for various runs (average of 0.015 inch). Subsequent readings were spaced 0.05 inch apart.

Point Pleasant Bridge
 U. S. Steel Results
 February 14, 1969
 Revised: Feb. 26, 1969

Hardness Tests (C9)
Segment 801) Specimens 1-6

Specimen 2)	Hardness Near One Surface R _c		Hardness at Center R _B						Hardness Near Other Surface R _c					
	1	2	3	4	5	6	7	8	9	10	11	12	13	14
1	24, 24, 23	24, 24, 23	20.5	20.0	19.0	17.5	18.5	20.0	21.0	21.0	22.0	23.0	23, 23, 23	23, 23, 23
3	23, 23, 23	24, 24, 23.5	22.0	22.0	21.0	20.0	20.0	20.0	20.5	21.5	22.0	22.5	22, 23, 23	22, 23, 23
4	24, 24, 23.5	23, 22, 22.5	22.0	22.0	21.0	20.0	20.0	20.0	20.5	21.5	22.0	22.5	22.5, 22.5, 22.5	22.5, 22.5, 22.5
5	23, 22, 22.5	22.5, 23, 22.5	22.0	22.0	21.0	20.0	20.0	20.0	20.5	21.5	22.0	22.5	23.5, 23.5, 23.5	23.5, 23.5, 23.5
6	22.5, 23, 23	22.5, 23, 23	22.0	22.0	21.0	20.0	20.0	20.0	20.5	21.5	22.0	22.5	22.5, 23, 23	22.5, 23, 23

EXAMPLES



Rockwell C Hardness Across Cross-Section

Specimen	1	2	3	4	5	6	7	8	9	10	11	12	13	14
2 Run A	24.5	23.5	22.0	20.5	20.0	19.0	17.5	18.5	20.0	21.0	22.0	23.0	24.5	
5 Run A	24.0	23.5	22.0	21.5	21.0	21.0	20.0	20.0	20.5	21.5	22.0	22.5	23.5	22.5

Distance From Surface, in.

Specimen	Hardness	.025	.050	.075	.100	.125	.150	.175	.200	.225	.250	.275	.300
2 Run B	DPH	265	262	263	274	268	280	280	280	280	280	27	27
	R _c (3)	25	25	26	25.5	25.5	27	27	27	27	27	27	27
Run C	DPH	271	289	289	293	286	289	283	283	283	283	283	286
	R _c (3)	26	28.5	28.5	29	28	28.5	28	28	28	28	28	28
5 Run B	DPH	260	265	277	277	274	277	286	303	293	289	280	286
	R _c (3)	24.5	25	27	27	26.5	27	28	30	29	28.5	27	28
5 Run C	DPH	296	271	283	283	277	293	280	280	289	280	289	289
	R _c (3)	29	26	28	28	27	29	27	27	27	27	27	28.5

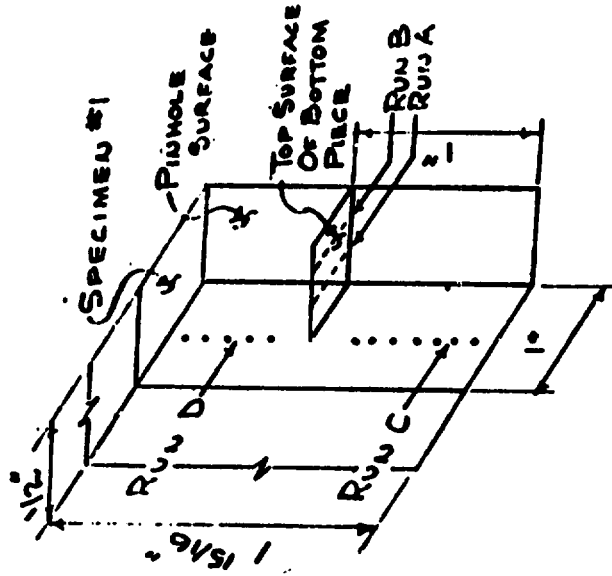
Notes: 1) See Sketch C of Laboratory Specimen Plan.
 2) See Sketch B of Laboratory Specimen Plan.
 3) Converted from LPH using Wilson Conversion Chart.

Point Pleasant Bridge
 U. S. Steel Results
 February 14, 1969
 Revised: Feb. 26, 1969

Hardness Tests (CO)
 Segment SO1) Specimen #12)

(Readings are Vickers hardness (DPH). Approximate Rockwell C conversion hardness values as determined from Wilson Conversion Chart are also shown).

Distance From Surface, in.	Run A		Run B		Run C		Run D	
	DPH	Rc	DPH	Rc	DPH	Rc	DPH	Rc
0.01	277	27.0	268	25.5	262	25.0	244	21.5
0.06	289	28.5	277	27.0	274	26.5	257	24.0
0.11	286	28.0	274	26.5	274	26.5	280	27.0
0.16	280	27.0	274	26.5	283	28.0	286	28.0
0.21	283	28.0	277	27.0	274	26.5	286	28.0
0.26	274	26.5	268	25.5	257	24.0	283	28.0
0.31	280	27.0	283	28.0	289	28.5	268	25.5
0.36	271	26.0	277	27.0	260	24.5	280	27.0
0.41	-	-	265	25.5	268	25.5	260	24.5
0.46	280	27.0	280	27.0	274	26.5	271	26.0
0.51	268	25.5	268	25.5	271	26.0	262	25.0
0.56	-	-	-	-	299	30.0	244	21.5
0.61	-	-	-	-	271	26.0	257	24.0
0.66	-	-	-	-	280	27.0	266	25.5
0.71	-	-	-	-	280	27.0	274	26.5
0.76	-	-	-	-	260	24.5	271	26.0
0.81	-	-	-	-	257	24.0	-	-
0.86	-	-	-	-	293	29.0	-	-
0.91	-	-	-	-	274	26.5	-	-



Notes: 1) See Sketch C of Laboratory Specimen Plan.
 2) See Sketch B of Laboratory Specimen Plan.

Young Picassent Bridge
 USTeel Results
 February 11, 1969
 Revised: February 26, 1969

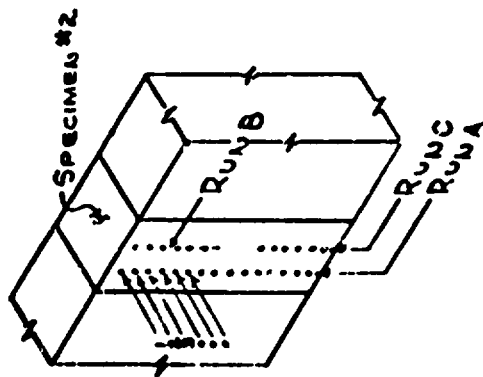
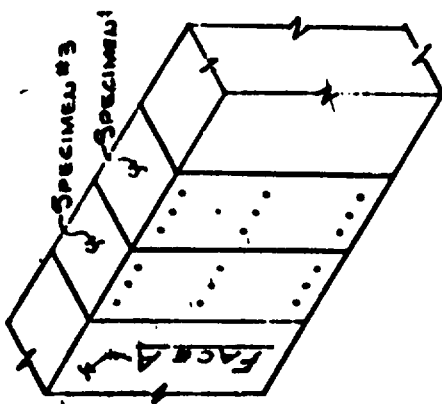
V-Notch Charpy Impact Properties (C9 and C0)

Segments 2 and 3 from C9 (C9 head of C9-C11NN)
 Segment 5 from C0 (C11 head of C11-C13NN, bar 330)
 See sketches C and D: 6/10/68 Lab Specimen Plan

Specimen No.	Test Temperature, F																							
	32			70			120			212			250			300								
	Layer A	Center	Layer B	A	Cent.	B	A	Cent.	B	A	Cent.	B	A	Cent.	B	A	Cent.	B						
3	7	11	18	22	26	33	37	41	12	28	34	9	24	35	4	19	42	8	23	39	5	20	38	
Code 2																								
ft-lb	3.5	3.0	3.5	2.0	1.5	2.0	2.0	2.5	2.5	5	2	2	7	4	4	12	16	11	24	30	22	32	43	28
% Shear	10	10	10	2	2	2	5	5	15	2	2	20	5	5	35	35	25	25	55	65	45	80	98	75
Lat Exp, mils	6	5	6	1	0	1	2	3	4	6	0	2	9	6	2	13	21	14	25	31	23	34	43	34
Rock C	22.0	22.0	22.5	19.0	19.5	20.0	21.5	21.0	21.5	23.0	23.0	24.0	22.5	20.0	21.5	21.0	23.0	23.0	22.5	19.0	21.0	22.0	19.0	21.5
Code 3																								
ft-lb	2.0	1.5	2.0	2.0	1.5	2.0	2.0	2.5	2.5	2	2	3	5	5	3	10	9	12	22	25	16	30	40	22
% Shear	2	2	2	2	2	2	5	5	2	2	2	5	10	5	2	23	15	20	50	55	45	80	95	75
Lat Exp, mils	1	2	2	2	2	2	2	2	4	1	1	2	6	4	3	19	14	17	22	21	18	32	39	35
Rock C	23.0	22.5	23.0	18.5	19.5	19.0	20.0	20.5	21.5	23.0	20.0	21.5	22.0	20.5	21.0	23.0	22.0	22.0	24.0	20.0	21.0	22.0	20.0	21.0
Code 5																								
ft-lb	5.0	1.0	3.5	2.0	2.0	2.0	2.5	2.0	2.0	7	3	4	3	6	11	8	8	21	24	24	25	34	36	36
% Shear	15	10	10	2	2	2	5	5	10	10	2	5	5	2	15	20	20	40	45	45	55	80	90	85
Lat Exp, mils	9	6	6	1	1	1	2	2	1	8	2	1	6	2	8	14	16	28	27	24	25	35	35	36
Rock C	20.5	20.0	21.0	19.0	21.0	20.0	23.0	22.5	21.0	21.0	21.5	22.5	22.5	20.5	22.0	22.5	21.0	21.0	23.0	21.0	23.0	23.5	22.0	21.5

Point Pleasant Bridge
 U. S. Steel Results
 February 14, 1969
 Revised: Feb. 26, 1969

EXAMPLE



Hardness Tests (00)
Segment 801) Specimens 1-6

Specimen 2)	Rockwell C						Hardness at Center		Hardness Near Other Surface						
	1	2	3	4	5	6	7	8	9	10	11	12	13	14	15
1															
3															
4															
5															
7															
6															

Specimen	Rockwell C Hardness Across Cross-Section														
	1	2	3	4	5	6	7	8	9	10	11	12	13	14	15
Run A	22.0	23.5	23.0	22.0	21.5	21.0	20.5	21.0	22.0	23.0	23.5	23.5	24.0	22.0	
Run A	22.0	23.0	22.0	22.0	22.0	21.5	20.5	20.5	21.0	21.5	22.0	22.5	22.5	23.5	23.0

Specimen	Hardness	Distance From Surface, in.														
		.025	.050	.075	.100	.125	.150	.175	.200	.225	.250	.275	.300			
Run B	DPH R _C 3)	262	260	262	268	283	283	280	249	286	296	289	286			
Run C	DPH R _C 3)	254	274	260	277	271	293	293	293	277	286	286	286			
Run E	DPH R _C 3)	257	246	246	262	277	260	257	280	277	265	280	274			
Run C	DPH R _C 3)	251	260	274	280	283	262	265	268	283	268	268	268			

- otes: 1) See Sketch C of Laboratory Specimen Plan.
 2) See Sketch B of Laboratory Specimen Plan.
 3) Converted from DPH using Wilson Conversion Chart.

APPENDIX B

U. S. STEEL LABORATORY DATA

Point Pleasant Bridge
U. S. Steel Results
February 10, 1969

Composition and Properties
of 1/2-Inch-Thick Plate From Chain Bent Post
L58 - U58 North

(Mechanical tests oriented with axis from top to bottom of post)

Composition									
C	Mn	P	S	Si	Cu	Ni	Cr	Mo	N
0.20	0.58	0.011	0.032	0.10	0.019	0.01	0.015	0.007	0.006

Tensile Properties

Diameter, in.	Yield Strength, ksi	0.2% Offset ksi	Tensile Strength, ksi		Elongation, %	Reduction of Area, %
			1"	2"		
0.440	36.8	63.0	63.0	32.0	67.3	67.3
0.437	34.7	63.0	63.0	35.0	65.9	65.9
0.252	35.3	63.9	63.9	33.0	66.0	66.0
0.252	35.3	63.1	63.1	33.0	66.9	66.9

V-Notch Charpy Tests

	Test Temperature, F			
	32	50	70	90
Pt-Lb	7.8	13,10,13	19,28,36	67,61
Percent shear	15,15	30,25,30	35,50,45	70,65
Lateral Expansion, mils	10,11	19,17,20	26,37,42	70,63
Rockwell B	72.5	71,74,75	73.5,70.5,76	72.5,74
				75,71
				74.5,73.5

Johns Hancock Bridge
 U. S. Steel Results
 May 21, 1969

U. S. STEEL LABORATORY DATA

Composition (C3)
 C3 is the C13 head of C11-C13MN (Bar 330)
 (Segment S4)

<u>C</u>	<u>Mn</u>	<u>P</u>	<u>S</u>	<u>Si</u>	<u>Cu</u>	<u>Ni</u>	<u>Cr</u>	<u>Mo</u>	<u>V</u>	<u>Al</u> Total	<u>N</u>
0.57	3.64	0.023	0.029	0.15	0.012	0.010	0.016	0.012	<0.005	0.004	0.004

Tensile Properties (C3)
 (Standard 0.252" Diameter Specimens)

Segment S2 ¹⁾	Specimen No. 2)	Strain Rate to Yield	Yield Strength at 0.2% Offset, ksi	Tensile Strength, ksi	Elongation in 1 Inch, %	Reduction of Area, %
Layer B ³⁾	36	Normal ⁴⁾	84.0	118.5	20.0	52.4
	44	"	80.1	120.8	20.0	51.8
Center	21	Static	65.6	114.7	21.0	51.3
	29	"	70.5	120.8	20.0	50.0
Layer B	32	"	82.3	117.9	20.0	52.0
	40	"	83.5	119.2	20.0	51.8

- NOTES: 1) See Sketch A of Laboratory Specimen Plan
 2) See Sketch D of Laboratory Specimen Plan
 3) Layer B is adjacent to original unground surface.
 4) Approximately 80 ksi/min.

Point Pleasant Bridge
 U. S. Steel Reinforce
 May 21, 1969

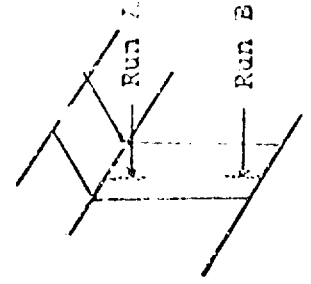
Hardness Tests (C3)
 Segment 811, Specimens 2,4,6,8

Specimen ²⁾	Hardness Near		Hardness at Center		Hardness Near		Examples
	Ground Surface, R _C	R _C	R _C	R _B	Other Surface, R _C	R _C	
2	22.5, 22.5, 22.5	18.5, 19.5, 20.0	98.5, 98.5, 98.5		23.5, 24.0, 24.0		
4	22.0, 22.5, 23.0	20.5, 20.5, 20.0			23.5, 23.5, 24.5		
6	23.5, 25.5, 24.5	20.5, 21.5, 21.5			24.5, 23.0, 23.5		
8	23.5, 24.5, 23.5	23.0, 24.0, 24.0			23.5, 24.0, 23.0		

Hardness Survey, Specimen 4

Location	Hardness	Distance From Surface, in.											
		0.025	0.050	0.075	0.100	0.125	0.150	0.175	0.200	0.225	0.250	0.275	
Run A	DPH	251	254	254	251	251	260	251	265	265	262	262	254
	R _C ³⁾	23	23	23	23	23	25.5	23	25	25	25	25	23
Run B	DPH	249	251	257	251	265	260	260	277	262	262	262	262
	R _C ³⁾	23	23	24	23	25	24.5	24.5	27	25	25	25	25

- NOTES: 1) See Sketch A of Laboratory Specimen Plan
 2) See Sketch B of Laboratory Specimen Plan
 3) Converted from DPH using Wilson Conversion Chart



U. S. Steel Research
 U. S. Steel Research
 May 21, 1969

V-Notch Charpy Impact Properties (C3)
Segment 2, see Sketches C and D,
Laboratory Specimen Plan

Specimen No.	Test Temperature, F					
	32	70	120	250		
2	41	38	20	42	50	43
2	2	3	4	5	28	28
2	5	3	10	15	55	50
Lateral Expansion, mils	1	3	5	6	30	26
Hardness, Rc	21.0	22.5	21.0	22.5	20.0	23.0
	21.0	22.5	21.0	23.0	23.0	23.0

APPENDIX
 U. S. STEEL LABORATORY DATA

Tension and Compression Tests in Eyebar-Shanks
 (Bars 330 and 33)

Spec. Bar Diam, Test Spec No. in. Dir. No.*	Tension				Tens. Str.,		Elong, %		Red. of Area, Spec		Compression Yield		0.2% Offset Static
	Yield, ksi	UYP	LYP	Static	ksi	1"	2"	%	No.	UYP	LYP	Yield	

As-Received

330	0.252	L	11	79.5	74.6	75.0	74.1	119.3	22.5	57.0				
"	"	"	12	79.1	78.7	78.9	76.1	121.3	22.5	57.5				
33	"	"	11			77.5	75.5	118.9	22.5	58.0				
"	"	"	12	78.9	78.5	78.5	76.9	120.3	22.5	59.9				
330	0.505	L	3	80.7	80.6	80.6	78.3				7	85.4	83.2	
"	"	"	4	81.8	81.1	81.4	79.3				8	84.0	82.5	
"	"	T	9			83.0	81.1							
"	"	"	10			81.0	78.8							
33	"	L	3			76.3	74.8				7	83.9	82.6	
"	"	"	4			80.9	78.6				8	87.1	86.2	
"	"	T	9			82.7	80.7							
"	"	"	10			83.3	81.8							

Stress-Relieved

330	0.505	L	1	82.0	79.8	120.7	19.5	55.2	5	83.9	83.0	83.0	80.6
"	"	"	2	80.6	78.6	119.3	20.5	54.2	6	83.4	82.4	87.4	83.4
33	"	"	1	79.7	78.1	118.5	20.0	57.0	5	87.9	85.0	85.1	82.9
"	"	"	2	82.0	79.5	119.9	20.0	56.0	6	87.1	85.9	85.9	83.5

* According to Laboratory Specimen Plan of 6/10/68, Sketch F.

NOTE: As indicated, upper and lower yield points were not always obtained. Also, specimens were not always pulled to failure.

APPENDIX B

U. S. STEEL LABORATORY DATA

Pt. Pleasant Bridge
U. S. Steel Results
August 8, 1969

SUMMARY OF TENSION AND COMPRESSION YIELD STRENGTHS*

(Bars 330 and 33)

<u>Bar No.</u>	<u>Longitudinal</u>					<u>Trans.</u>	
	<u>.252"</u>	<u>0.505" Diameter</u>				<u>As Rec'd.</u> <u>Tens.</u>	
	<u>Tens.</u>	<u>As-Received</u>		<u>Stress-Relieved</u>			
		<u>Tens.</u>	<u>Comp.</u>	<u>Tens.</u>	<u>Comp.</u>		
		0.2% Offset Yield Strength, ksi					
330	77.0	81.0	84.7	81.0	85.2	82.0	
33	78.0	78.6	85.5	80.9	85.5	83.0	
		Static Yield Strength, ksi					
330	75.1	78.8	82.9	79.2	82.0	80.0	
33	76.2	76.7	84.4	78.8	83.3	81.3	

*Refer to "Tension and Compression Tests in Eyebar Shanks (Bars 330 and 33)," U. S. Steel Results, July 28, 1969